


2023

Diversification of Ergot Alkaloid Biosynthesis in Natural and Engineered Fungi

Kyle Austin Davis

West Virginia University, ksdavis@mix.wvu.edu

Follow this and additional works at: <https://researchrepository.wvu.edu/etd>

 Part of the [Molecular Biology Commons](#)

Recommended Citation

Davis, Kyle Austin, "Diversification of Ergot Alkaloid Biosynthesis in Natural and Engineered Fungi" (2023). *Graduate Theses, Dissertations, and Problem Reports*. 12095.

<https://researchrepository.wvu.edu/etd/12095>

This Dissertation is protected by copyright and/or related rights. It has been brought to you by the The Research Repository @ WVU with permission from the rights-holder(s). You are free to use this Dissertation in any way that is permitted by the copyright and related rights legislation that applies to your use. For other uses you must obtain permission from the rights-holder(s) directly, unless additional rights are indicated by a Creative Commons license in the record and/ or on the work itself. This Dissertation has been accepted for inclusion in WVU Graduate Theses, Dissertations, and Problem Reports collection by an authorized administrator of The Research Repository @ WVU. For more information, please contact researchrepository@mail.wvu.edu.

Diversification of Ergot Alkaloid Biosynthesis in Natural and Engineered Fungi

Kyle A. Davis

Dissertation submitted to the Davis College of Agriculture, Natural Resources and Design at
West Virginia University in partial fulfillment of the requirements for the degree of

Doctor of Philosophy in
Genetics and Developmental Biology

Daniel Panaccione, Ph.D., Chair

Jennifer Hawkins, Ph.D.

Matthew Kasson, Ph.D.

Teiya Kijimoto, Ph.D.

Division of Plant and Soil Sciences

Morgantown, West Virginia

2023

Keywords: ergot alkaloids, genetic engineering, gene cluster, fungi, specialized metabolism

Copyright 2023 Kyle A. Davis

Abstract

Diversification of Ergot Alkaloid Biosynthesis in Natural and Engineered Fungi

Kyle A. Davis

Ergot alkaloids are a complex family of tryptophan-derived mycotoxins produced by a diverse range of fungi that occupy a wide variety of ecological niches including soil saprotrophs, plant endophytes, pathogens of plants or insects, and opportunistic pathogens of humans and other mammals. Ergot alkaloids are a similarly diverse family of chemicals that elicit a variety of pharmacological activities in animals due to their resemblance to neurotransmitters and high binding affinity for neurological receptors, including those that bind adrenaline, dopamine, and 5-hydroxytryptamine receptors. These structural similarities allow us to create medicines aimed at treating a range of neurological diseases and disorders including dementia, migraines, and Parkinson's. The genes encoding ergot alkaloid biosynthesis are found clustered together in the genomes of the different fungi that make them. The fungus *Metarhizium brunneum* produces lysergic acid α -hydroxyethylamide (LAH), an ecologically and pharmaceutically relevant compound, as its main ergot alkaloid and secretes most of this compound into the surrounding environment. The first objective of this study involved engineering *M. brunneum* to produce the dihydrogenated versions of its natural ergot alkaloids, that is dihydrolysergic acid (DHLA) and dihydroLAH. The results showed that the fungus can produce both products and was also found to secrete most of both compounds at levels comparable to their unsaturated counterparts. The fungus *Aspergillus leporis* is a soil saprotroph that has been previously shown to have evolved the capacity for LAH production independently of species in the Clavicipitaceae. Two partial, fragmented gene clusters encoding different clavine-type ergot alkaloid branches were discovered in separate areas of the *A. leporis* genome and formed the basis for a second study. Chemical analyses indicated that fumigaclavine A production is encoded by one of the fragmented gene clusters. Concentrations of fumigaclavine A peaked around 15 days, following a decrease in LAH levels. The other partial cluster encoded two enzymes necessary to complete production of rugulovasines A and B, but rare production in *A. leporis* indicated some unknown environmental stimuli required for their production. Expression of these two genes in an appropriate background of *M. brunneum* allowed for confirmation of their function. The fungus *Aspergillus fumigatus*, an opportunistic human pathogen, is a known producer of fumigaclavines, another branch of clavine ergot alkaloids, and a distant relative to *A. leporis*. Due to this relation, *A. fumigatus* was chosen as platform with which to study the activity and localization of a novel gene from *A. leporis*, named *easT*, that encodes a putative major facilitator superfamily transporter. The results indicate that the transporter encoded by *easT* localizes to discrete regions of fungal hyphae independent of mCherry-tagged peroxisomes and plays a role in transport of ergot alkaloids and/or their precursors. Collectively, the results presented here showcase different ways that ergot alkaloid production can be diversified in both natural and engineered fungal systems.

Table of Contents

Chapter 1: Introduction	1
<hr/>	
Chapter 2: Genetic Reprogramming of the Ergot Alkaloid Pathway of <i>Metarhizium brunneum</i>	12
<hr/>	
Abstract	12
Introduction	14
Results	17
Discussion	23
Materials and Methods	27
Acknowledgements	34
Figures and Tables	35
Chapter 3: Two satellite gene clusters enhance ergot alkaloid biosynthesis capacity of <i>Aspergillus leporis</i>	53
<hr/>	
Abstract	53
Introduction	55
Results	58
Discussion	65
Materials and Methods	69
Acknowledgements	78
Figures and Tables	79
Chapter 4: Localization of EasT, a novel ergot alkaloid transporter protein	108
<hr/>	
Abstract	108
Introduction	110
Results	113
Discussion	115
Materials and Methods	118
Acknowledgements	125
Figures and Tables	126
Chapter 5: Summary	142
<hr/>	
References	146
<hr/>	

Chapter 1

Introduction

Ergot alkaloid background/significance

Humans have been impacted both negatively and positively by fungal specialized metabolites, or mycotoxins, throughout history. Mycotoxin producing fungi have historically been detrimental, with the most impactful effect being contamination of grain crops that would lead to mass poisoning events. Many of these events occurred due to infection of crops by the ergot alkaloid-producing fungus *Claviceps purpurea* (Matossian 1989, Haarmann et al. 2009, Florea et al. 2017). Ergot alkaloids are a complex family of indole-derived mycotoxins produced by a diverse range of fungi belonging to the Eurotiales and Hypocreales (Wallwey and Li 2011, Florea et al. 2017, Tasker and Wipf 2021, Robinson and Panaccione 2015). These fungi occupy a wide variety of ecological niches including soil saprotrophs, plant endophytes, pathogens of plants or insects, and opportunistic pathogens of humans and other mammals (Schardl et al. 2006, Gerhards et al. 2014, Young et al. 2015, Leadmon et al. 2020, Panaccione 2023). Ergot alkaloids are a similarly diverse family of chemicals that elicit a variety of pharmacological activities in animals due to their resemblance to neurotransmitters and high binding affinity for neurological receptors, including those that bind adrenaline, dopamine, and 5-hydroxytryptamine receptors (Pertz and Eich 1999, Eich et al. 1985). The psychotropic and narcotic properties of ergot alkaloids have been utilized by humans throughout history (Schultes and Hofmann 1973, Hofmann 1980). Most ergot alkaloids, such as lysergic acid, possess vasoconstrictive properties while dihydrogenated ergot alkaloids, which are rare in nature, possess vasorelaxant properties. Semi-synthetic derivatives of both classes have also been developed as pharmaceuticals to treat a wide variety of neurological diseases and disorders (Iliff et al. 1977, Østergaard et al. 1981,

Schiff 2006). The next few paragraphs will be dedicated to describing the ergot alkaloid biosynthetic pathway and several of its branches that are important for understanding the research herein.

Ergot alkaloid biosynthesis: Early steps

Ergot alkaloid biosynthesis is encoded by a set of ergot alkaloid synthesis (*eas*) genes clustered together within a biosynthetic gene cluster (Tsai et al. 1995, Tudzynski et al. 1999, Coyle and Panaccione 2005, Unsöld and Li 2005, Schardl et al. 2013, Panaccione 2023). The pathway and all branch points discussed herein can be found in Figure 1. Five genes (*dmaW*, *easF*, *easE*, *easC*, and *easD*) are required for biosynthesis of chanoclavine-I aldehyde, the precursor to several other branches of the ergot alkaloid pathway. The first pathway step is carried out by 4- γ -dimethylallyltryptophan synthase encoded by *dmaW* which utilizes dimethylallylpyrophosphate to prenylate tryptophan at position 4 (Tsai et al. 1995), generating 4-dimethylallyltryptophan (DMAT). DMAT is then methylated at the primary amine by the methyltransferase encoded by *easF* (Rigbers and Li 2008) producing *N*-methyl-4-dimethylallyltryptophan. The oxidoreductase and catalase products of *easE* and *easC*, respectively, then carry out decarboxylative closure of third ergoline ring, generating the simplest clavine-type ergot alkaloid—chanoclavine-I (Lorenz et al. 2010, Goetz et al. 2011, Yao et al. 2021). The primary alcohol of chanoclavine-I is then oxidized to an aldehyde by FgaDH, the short-chain alcohol dehydrogenase product of *easD*, generating chanoclavine-I aldehyde (Wallwey et al. 2010a).

Ergot alkaloid biosynthesis: Branchpoint

Chanoclavine-I aldehyde serves as the major branchpoint to several other ergot alkaloid classes including lysergic acid amides and ergopeptines as well as their dihydrogenated forms.

The distinction between biosynthesis of saturated and unsaturated forms lysergic acid amides and ergopeptines depends upon whether the version of *easA* present within an organism's gene cluster encodes a reductase or isomerase allele (Cheng et al. 2010a, Cheng et al. 2010b, Coyle et al. 2010). In both cases, the product of *easA* catalyzes closure of the fourth (or D) ring of the ergoline ring system, generating an iminium ion. Subsequent reduction of the N6-C7 bond through the reductase encoded by *easG* completes ring closure (Wallwey et al. 2010b, Matuschek et al. 2011), generating either the agroclavine (via the product of the isomerase allele of *easA*) or festuclavine (via the reductase allele *easA*) (Coyle et al. 2010, Cheng et al. 2010b). Agroclavine serves as precursor to lysergic acid (LA), whereas festuclavine is the precursor to dihydrolysergic acid (DHLA). The isomerase allele, such as that found in the fungus *Epichloë festucae* (formerly called *Neotyphodium lolii*), encodes an enzyme that temporarily reduces the C8-C9 double bond of chanoclavine-I aldehyde to allow for isomerization before the C8-C9 double bond is restored. This isomerization brings the aldehyde and amine groups into proximity, facilitating ring closure. The reductase allele of *easA* found in *Neosartorya fumigata* (*Aspergillus fumigatus*) encodes an enzyme that fully reduces the double bond, allowing for rotation of the aldehyde functional group such that it can react with the secondary amine. In either case, the resulting iminium ion is subsequently reduced by the product of *easG* (Wallwey et al. 2010a, Matuschek et al. 2011). The P450 monooxygenase encoded by *cloA* can then catalyze a six-electron oxidation of the methyl groups of agroclavine and festuclavine to carboxylic acids, generating either lysergic acid (LA) or dihydrolysergic acid (DHLA), respectively (Haarmann et al. 2006, Robinson and Panaccione 2014). While versions of *cloA* from either side of the pathway carry out similar reactions, work by Bragg et al. (2017) and Arnold and Panaccione (2017) has shown that only versions of *cloA* from dihydroergot alkaloid

producers can accept festuclavine as substrate, indicating a degree of specialization among these species.

Ergot alkaloid biosynthesis: Ergopeptines

Ergopeptine biosynthesis relies on the combinatorial actions of nonribosomal peptide synthetases (NRPSs) which encode large, multidomain enzymes responsible for attaching short chains of amino acids to lysergic acid and dihydrolysergic acid. These NRPSs, known as lysergyl peptide synthetases (LPSs), are composed of two subunits formed by the enzymes LpsB and LpsA (Correia et al. 2003, Ortel and Keller 2009). The subunit LpsB (or Lps2) is responsible for binding to and activating LA/DHLA while LpsA, which contains three amino-acid specific modules, adds the tripeptide chain. Once the peptide chain is complete, the product is released from the NRPS while the second and third amino acids are cyclized, forming the piperizinedione ring of the ergopeptide lactam. A version of EasH is then responsible for hydroxylating the α -carbon of the amino acid adjacent to D-lysergic acid, driving cyclolization of the α -carbon with the terminal lactam carbonyl group generated by LPS1/LPS2 (Havemann et al. 2014). Production of lysergic acid amides, such as ergonovine and lysergic acid α -hydroxyethylamide (LAH), requires the NRPS combination of LpsB and LpsC (Ortel and Keller 2009; Davis et al. 2020). LAH synthesis also involves a Baeyer-Villiger monooxygenase encoded by *easO* (Steen et al. 2021). An α/β hydrolase fold protein encoded by *easP* contributes to, but is not required for, biosynthesis of LAH in the fungus *Metarhizium brunneum* (Britton et al. 2022).

Ergot alkaloid biosynthesis: Clavines

Clavines, like lysergic acid amides and ergopeptines, represent the third main class of ergot alkaloids and often comprise the pathway end products of species belonging to the Eurotiales. This group of ergot alkaloids includes cycloclavine, fumigaclavines, and

rugulovasines with chanoclavine-I aldehyde again serving as the main branch point.

Cycloclavine is a unique ergot alkaloid containing a cyclopropyl ring moiety originally isolated from seeds of the morning glory *Ipomoea hildebrandtii* (Stauffacher et al. 1969) (which were later shown to be symbiotic with an ergot alkaloid-producing species of *Periglandula* [Beaulieu et al. 2015]) and later the fungus *Aspergillus japonicus* (Furuta et al. 1982). Work by Jakubczyk and others has determined that cycloclavine production in *A. japonicus* is dependent upon a version of the EasH acting as a dioxygenase that acts in combination with the reductase version of EasA and EasG to catalyze formation of a cyclopropyl ring moiety attached to the clavine ring system (Jakubczyk et al. 2015, Jakubczyk et al. 2016). The version of EasH utilized by *A. japonicus* also displays a degree of promiscuity as it is capable of catalyzing asymmetric hydroxylation of other clavines such as elymoclavine and festuclavine (An et al. 2022). The combination of EasM, EasN, and EasL acting on festuclavine in the absence of a CloA allele is responsible for production of fumigaclavines A, B, and C in the opportunistic human pathogen *Aspergillus fumigatus* (synonym *Neosartorya fumigata*) (Unsöld and Li 2006, Liu et al. 2009, Bilovol and Panaccione 2016). Rugulovasines A and B are a pair of stereoisomeric pair of clavines originally isolated from several *Penicillium* species including *P. bifforme* (Abe et al. 1969, Dorner et al. 1980). Biosynthesis of rugulovasines is carried out by the aldehyde dehydrogenase EasQ together with a version of EasH with similar activity to the version from *A. japonicus* (Fabian et al. 2018).

Ergot alkaloid producing fungi

Ergot alkaloid-producing fungi belong to several different genera including *Claviceps*, *Metarhizium*, *Periglandula*, *Balansia* and *Epichloë* of the Order Hypocreales as well as *Penicillium* and *Aspergillus* of the Order Eurotiales (Wallwey and Li 2011, Robinson and

Panaccione 2015, Florea et al. 2017, Tasker and Wipf 2021, Panaccione 2023). These fungi occupy a diverse range of niches including soil saprophytes, mutualistic plant endophytes, plant pathogens, entomopathogens, and opportunistic mammalian pathogens (Gerhards et al. 2014, Schardl et al. 2006, Young et al. 2015, Leadmon et al. 2020, Panaccione 2023). Here I will introduce the three fungi that form the central focus of this research: *Metarhizium brunneum*, *Aspergillus leporis*, and *Aspergillus fumigatus*.

Metarhizium brunneum, a member of the Clavicipitaceae, is a natural producer of the LA amides LAH and ergonovine (also known as ergometrine) (Leadmon et al. 2020). This fungus is capable of both beneficially colonizing plant roots (Liao et al. 2014, Krell et al. 2018) and parasitizing a range of insect orders including Coleoptera, Thysanoptera, Hemiptera, Lepidoptera, Orthoptera, Blattodea, Hymenoptera, and Diptera (Russell et al. 2010, Castrillo et al. 2011, Dogan et al. 2017, Nishi and Sato 2017). Insect cadavers that result from fungal infection nearby colonized roots are thought to help provide nitrogen to the plant in exchange for carbon (Hu and Bidochka 2019). Several isolates of this species have been developed into biocontrol agents for different insects including weevils (Reddy et al. 2014), mites (Han et al. 2021), and ticks (Met52®; Novozymes). Previous work has shown that *Metarhizium brunneum* produces no detectable ergot alkaloids when colonizing plants and little in culture, but instead produces large quantities during insect infection (in this case the model lepidopteran *Galleria mellonella*; Leadmon et al. 2020).

Aspergillus leporis, a member of the Eurotiales, is an ergot alkaloid-producing species originally isolated from jackrabbit dung (States and Christensen 1966). Previous work found that the fungus produces relatively high concentrations of LAH during infection of *G. mellonella* and that LAH contributes to the pathogenic potential of the fungus (Jones et al. 2023). It was

previously determined that *A. leporis* evolved the tailoring enzymes needed to produce LA amides independently of species in the Order Hypocreales (Jones et al. 2021) and that it utilizes two ergot alkaloid clusters to do this. Both clusters contain the complete set of genes needed to synthesis LAH (minus one pseudogenized *easD* copy) including a novel NRPS-encoding gene, *lpsD*, that represents a potential fusion of the genes *lpsB* and *lpsC* (Jones et al. 2021, Fabian 2023).

Aspergillus fumigatus, a distant relative of *A. leporis*, is a common airborne saprotroph and opportunistic human pathogen known to cause disease in individuals with immunodeficiencies (Denning 1998). Previous work has determined that this fungus primarily produces its ergot alkaloids within, or on, its conidia at quantities >1% the total conidium mass (Panaccione and Coyle 2005). The exact role that ergot alkaloids play during human pathogenesis is still unknown, but ergot alkaloids (particularly fumigaclavine C) contribute to virulence of the fungus in an insect model of aspergillosis (Panaccione and Arnold 2017). Since no new ergot alkaloids were detected during host infection (Panaccione and Arnold 2017) the immunosuppressant activities of fumigaclavines associated with conidia may help in evasion of the host immune system during early stages of infection (Wu et al. 2005, Zhao et al. 2010, Li et al. 2013, Du et al. 2011). This species is very easily grown in overnight cultures which contrasts greatly with the more slow-growing *M. brunneum* and *A. leporis*, making it a powerful tool with which to study ergot alkaloid production.

Genetic manipulation of ergot alkaloid producing fungi allows us to study how these chemicals are made as well as the role(s) they might play for a specific fungus. Characterization of the different ergot alkaloid pathway branches has allowed us to engineer strains aimed at increased production of desired end products and/or production of rare end products in species

that are more easily cultivated. The engineering of fungi to further our understanding of the diversification of ergot alkaloid biosynthesis forms the basis for the investigations herein.

Research objectives:

1. To engineer strains of *Metarhizium brunneum* that produce and secrete pharmaceutically relevant and novel ergot alkaloids, including lysergic acid, dihydrolysergic acid (DHLA), and the novel compound dihydrolysergic acid α -hydroxyethylamide (dihydroLAH)
 - a. *Metarhizium* species produce and secrete high amounts of its ergot alkaloids, with LAH being the most predominant. By substituting the version of *easA* found in this fungus, while also including a specialized *cloA* allele, it should be feasible to engineer the fungus to produce dihydroergot alkaloids.
 - b. The use of CRISPR-Cas9 gene editing in *Metarhizium brunneum* has not been reported prior to this study and is utilized for knockout of *lpsB* aimed at DHLA production.
 - c. Additionally, this fungus should be capable of producing dihydroLAH (a hypothetical ergot alkaloid not found in nature) when its copy of *lpsB* is left intact.

2. To investigate the presence of two partial ergot alkaloid clusters encoding steps for production of fumigaclavines and rugulovasines in *Aspergillus leporis*
 - a. The presence of multiple, fragmented biosynthetic gene clusters encoding different branches of the ergot alkaloid pathway has not been observed in any

other species to date. The lack of duplication for earlier pathway steps indicates reliance on one or both previously characterized LAH pathways in this fungus.

3. To investigate localization and activity of a novel membrane-bound transporter found in *Aspergillus leporis* by fusion to cyan fluorescent protein (CFP) and overexpression in *Aspergillus fumigatus*

- a. No transporter for ergot alkaloid secretion or production has been characterized to date. *Aspergillus leporis* represents one member of a small group of *Aspergilli* which contain this gene in their ergot alkaloid gene cluster. The impact of this transporter on fumigaclavine production is unknown.

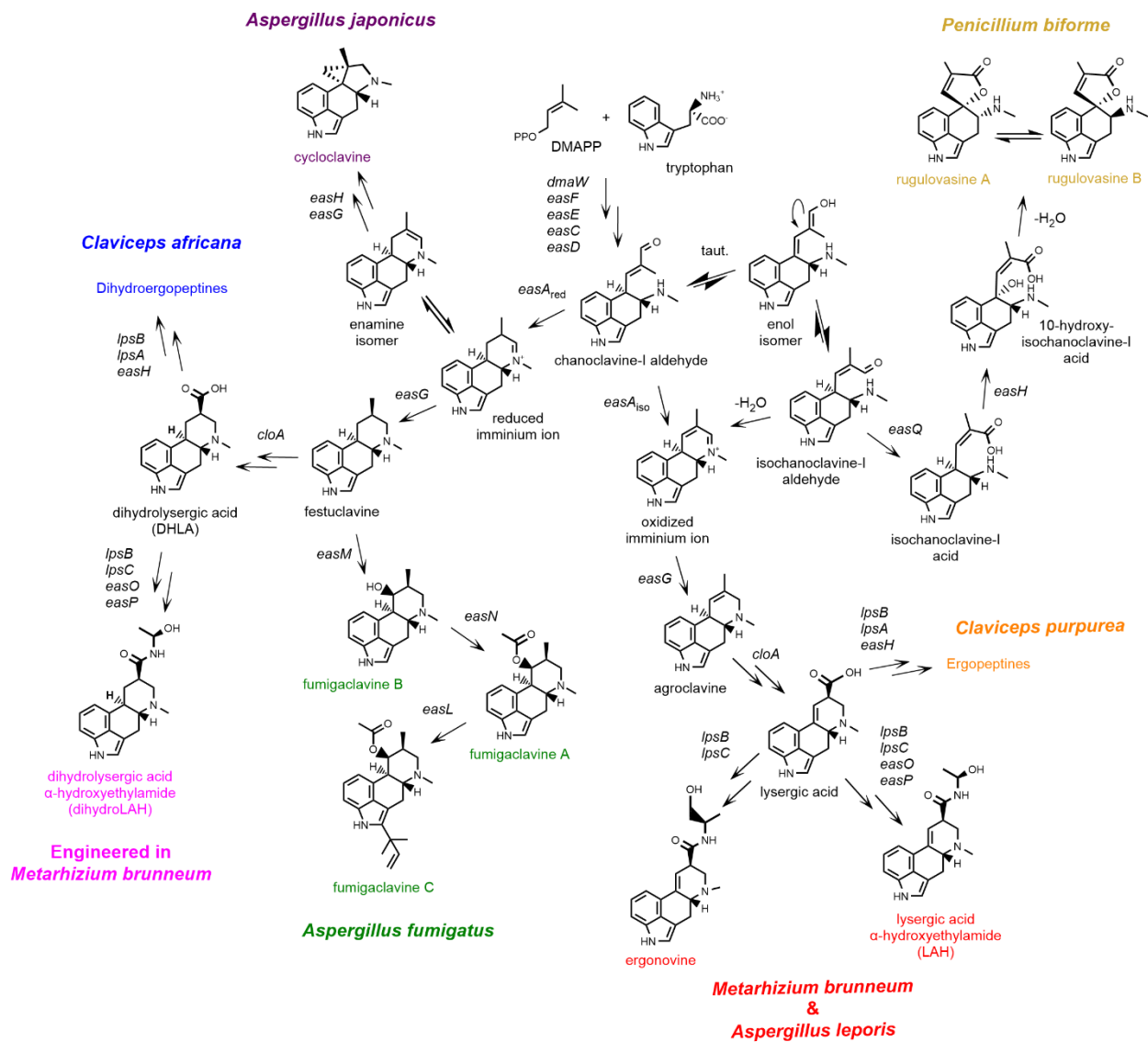


Figure 1. Pathways showing the enzymatic steps for the biosynthesis of different ergot alkaloids and example species that produce them. All branches begin with a set of five conserved genes (*dmaW*, *easF*, *easE*, *easC*, *easD*) and branch depending on the allele of *easA* present along with other tailoring *eas* genes. Pathways that utilize the isomerase *easA* allele include ergopeptines as are found in *C. purpurea* and several *Epichloë* species (Haarmann et al. 2009, Wallwey and Li 2011, Robinson and Panaccione 2015) (labeled in orange) and lysergic acid amides as are found in *M. brunneum* and *A. leporis* (Leadmon et al. 2020, Jones et al. 2021) (labeled in red). Pathways that instead utilize the reductase *easA* allele

include cycloclavine, which is found in *A. japonicus* (Furuta et al. 1982, Jakubczyk et al. 2015) (labeled in purple), fumigaclavines, which are found in *A. fumigatus* (Gerhards et al. 2014) (labeled in green), and dihydroergopeptines, which are rarer and found only in sorghum-infecting *Claviceps* species like *C. africana* and *C. sorghi* (Arnold and Panaccione 2017, Mantle and Waight 1968) (labeled in blue). Production of the rugulovasine A and B in *P. biforme* branches from the enol tautomer of chanoclavine-I aldehyde and involves the enzymes encoded by *easQ* and *easH* (Fabian et al. 2018) (labeled in gold). DihydroLAH is not found in nature and has only been engineered in *M. brunneum* (Davis et al. 2020) (labeled in pink). Double arrows indicate multiple enzymatic steps and equilibrium states are indicated by half-arrows. DMAPP, dimethylallylpyrophosphate; red, reductase; iso, isomerase; taut, tautomerization.

Chapter 2

Genetic Reprogramming of the Ergot Alkaloid Pathway of *Metarhizium brunneum*

Abstract

Ergot alkaloids are important fungal specialized metabolites that are used to make potent pharmaceuticals for neurological diseases and disorders. Lysergic acid (LA) and dihydrolysergic acid (DHLA) are desirable lead compounds for pharmaceutical semi-synthesis but are typically transient intermediates in the ergot alkaloid and dihydroergot alkaloid pathways. Previous work with *Neosartorya fumigata* demonstrated strategies to produce these compounds as pathway end products, but their percent yield (percentage of molecules in product, as opposed to precursor, state) was low. Moreover, ergot alkaloids in *N. fumigata* are typically retained in the fungus as opposed to being secreted. We used CRISPR-Cas9 and heterologous expression approaches to engineer these compounds in *Metarhizium brunneum*, representing an alternate expression host from a different lineage of fungi. The relative percent yields of LA (86.9%) and DHLA (72.8%) were much higher compared to those calculated here for previously engineered strains of *N. fumigata* (2.6% and 2.0%, respectively). Secretion of these alkaloids also was measured, with an average 98.4% of LA and 87.5% of DHLA being secreted into the growth medium; both values were significantly higher than those measured for the *N. fumigata* derivatives (both of which were less than 5.6% secreted). We used a similar approach to engineer a novel dihydroergot alkaloid in *M. brunneum* and, through high performance liquid chromatography-mass spectrometry analyses (LC-MS), provisionally identified it as the dihydrogenated form of lysergic acid α -hydroxyethylamide (LAH). The engineering of these strains provides a strategy

for producing novel and pharmaceutically important chemicals in a fungus more suitable for their production.

Introduction

Ergot alkaloids are a complex family of specialized metabolites produced by several species of fungi in the phylum Ascomycota. These alkaloids are historically known for causing massive poisoning events as a result of infection of grain crops by the fungus *Claviceps purpurea* (Florea et al. 2017, Haarmann et al. 2009). Some other ergot alkaloid-producing species are symbionts of plants, where the alkaloids deter insect and mammalian herbivores (Florea et al. 2017, Haarmann et al. 2009, Potter et al. 2008, Panaccione et al. 2006). The effects of these toxins are due to their structural similarity to, and high binding affinity for, several neurological receptors, including the adreno, dopamine, and 5-hydroxytryptamine receptors (Pertz and Eich 1999, Østergaard et al. 1981). Many natural ergot alkaloids are derivatives of lysergic acid (LA) and possess vasoconstrictive properties. Derivatives of dihydrolysergic acid (DHHLA), which are rare in nature, have been shown to possess vasorelaxant properties and are used to synthesize several ergot-alkaloid-derived pharmaceuticals (Østergaard et al. 1981, Iliff et al. 1977). Most ergot alkaloid-derived pharmaceuticals are semi-synthetics made by hydrolyzing naturally occurring ergot alkaloids to LA (sometimes reducing LA to DHHLA) and then synthesizing amide side chains (Liu and Jia 2017). Availability of fungi that produce LA or DHHLA as pathway end products, as opposed to transient intermediates, might facilitate pharmaceutical research and production.

The difference between LA and DHHLA is the presence of a double bond in the fourth formed and final ring (D ring) of ergoline nucleus (Fig. 1). Ergot alkaloid synthesis begins with a set of five genes (*dmaW*, *easF*, *easC*, *easE*, and *easD*), the products of which work together to prenylate tryptophan and convert it into a tricyclic intermediate, chanoclavine-I aldehyde (Florea et al. 2017, Haarmann et al. 2009, Robinson and Panaccione 2015, Wallwey and Li 2011). In the

next series of steps, closure of the D ring can result in either an unsaturated or saturated product, yielding agroclavine or festuclavine, respectively. Agroclavine serves as precursor to LA, whereas festuclavine is the precursor to DHLA. The path taken at this branchpoint is dependent on the allele of *easA* present in an organism (Wallwey and Li 2011, Cheng et al. 2010a, Cheng et al. 2010b, Wallwey et al. 2010b). The isomerase allele, such as that found in the fungus *Epichloë festucae* (formerly called *Neotyphodium lolii*), encodes an enzyme that temporarily reduces the C8-C9 double bond of chanoclavine-I aldehyde to allow for isomerization before the C8-C9 double bond is restored. This isomerization brings the aldehyde and amine groups into close proximity, facilitating ring closure. The reductase allele of *easA* found in *Neosartorya fumigata* (*Aspergillus fumigatus*) encodes an enzyme that fully reduces the double bond, allowing for rotation of the aldehyde functional group such that it can react with the secondary amine. In either case, the resulting iminium ion is subsequently reduced by the product of *easG* (Wallwey et al. 2010a, Matuschek et al. 2011).

During synthesis of LA and DHLA, the P450 monooxygenase product of *cloA* catalyzes a six-electron oxidation reaction, oxidizing the methyl groups of agroclavine and festuclavine to the corresponding carboxylic acids (Haarmann et al. 2006, Robinson and Panaccione 2014). Robinson and Panaccione (2014) showed that *N. fumigata* is capable of accumulating LA when the *cloA* allele from an *Epichloë* species is expressed in a mutant background that produces agroclavine, the substrate for CloA. A specialized allele of *cloA* from *Claviceps africana* or *C. gigantea* is needed in the synthesis of DHLA. Synthesis of DHLA in *N. fumigata* was achieved by expressing the *cloA* allele from *C. gigantea* (Bragg et al. 2017) or a synthetic version of the allele from *C. africana* (Arnold and Panaccione 2017) in a festuclavine-accumulating background; however, the percent yield of DHLA was poor, as approximately 2% of the

precursor festuclavine was converted to DHLA in engineered strains of *N. fumigata* (Bragg et al. 2017). The authors hypothesized that *N. fumigata* may have had issues with enzyme and substrate compartmentalization or with accumulating products of the reaction. Moreover, *N. fumigata* typically retains its ergot alkaloids in or on its conidia, with only very small quantities of ergot alkaloids found in its growth medium (Mulinti et al. 2014). This combination of substrate conversion and product retention issues raises doubts about the ability of *N. fumigata* to serve as an effective expression host for LA and DHLA derivatives. A fungus that naturally produces LA derivatives may be better suited to produce LA and its derivatives, or DHLA and its derivatives, as artificial end products. Moreover, a fungus that secretes these compounds, as opposed to retaining them, would facilitate alkaloid isolation and purification.

The fungus *Metarhizium brunneum*, a member of the Clavicipitaceae, beneficially colonizes plant roots (Hu and Bidochka 2019, Liao et al. 2014) and also acts as a generalist entomopathogen (Russell et al. 2010, Dogan et al. 2017, Castrillo et al. 2011). This species produces several LA amides, with its pathway culminating in production of lysergic acid α -hydroxyethylamide (LAH), along with much smaller quantities of ergonovine (also known as ergometrine) (Leadmon et al. 2020). Production of ergonovine occurs through the combination of the nonribosomal peptide synthetase products of *lpsB* and *lpsC*. The product of *lpsB* activates LA by adenylation and binds it as a thioester to prepare it for incorporation into LA amides (Correia et al. 2003, Ortel and Keller 2009). Knockout mutation of *lpsB* in *C. purpurea* resulted in the accumulation of LA (Correia et al. 2003). Formation of LAH has been hypothesized to require peptide synthetases encoded by *lpsB* and *lpsC* and to also involve the products of *easO* and *easP* (Florea et al. 2017, Robinson and Panaccione 2015, Schardl et al. 2013). *Metarhizium brunneum* also is noteworthy in that it secretes relatively large proportions of its ergot alkaloids

compared to other ergot alkaloid-producing fungi (Leadmon et al. 2020). As a producer of lysergic acid amides, *M. brunneum* contains the isomerase allele of *easA* and a functional copy of *lpsB*.

The studies described above have elucidated the roles of EasA, CloA, and LpsB, leading to strategies for producing LA and DHLA in different fungal backgrounds through introduction or modification of the genes encoding these enzymes. We hypothesized that engineering pathways for production of LA and DHLA in *M. brunneum*, which typically produces LA amides, would result in a higher conversion of substrate to the desired product than was observed in *N. fumigata* strains, which were engineered in a background that lacks capacity to make LA amides. We also hypothesized that since *M. brunneum* secretes the majority of its own LA amides (Leadmon et al. 2020), it would secrete the related but simpler molecules LA and DHLA when engineered as pathway end products. A final hypothesis tested in this present study was that *M. brunneum* could be modified to produce novel derivatives of DHLA, in particular a dihydrogenated form of LAH. Here, we show the generation of strains of *M. brunneum* capable of accumulating the pharmaceutically important ergot alkaloids LA and DHLA, as well as a novel dihydroergot alkaloid, and assess the percent yield and secretion of these compounds relative to these traits in previously engineered *N. fumigata* strains.

Results

Production and secretion of lysergic acid in *M. brunneum*.

Generation of a strain of *M. brunneum* capable of accumulating LA was achieved through an approach in which a single guide RNA (sgRNA) specific for *lpsB* was complexed with Cas9 (CRISPR associated protein 9) for transient expression in transformed protoplasts, resulting in

knockout of *lpsB*. The sgRNA:Cas9 complex was cotransformed along with a fragment of DNA containing the *bar* gene conferring resistance to phosphinothricin (Fig. 2). Sanger sequencing of the *lpsB* locus in the mutated strain revealed it to have recombined in such a way that after being cut by Cas9, two partial fragments of the *bar* construct amplicon used as the selectable marker were incorporated into the *lpsB* locus in the ensuing repair process (Fig. 3). Phosphinothricin resistance in the strain was provided by an additional, full copy of the *bar* amplicon integrated elsewhere in the genome as confirmed through further PCR and Sanger sequencing. The *lpsB* knockout strain was analyzed by high performance liquid chromatography (HPLC) with fluorescence detection and compared to wild-type *M. brunneum* and a strain of *N. fumigata* previously engineered to accumulate LA (Robinson and Panaccione 2014) as references (Fig. 4). The *lpsB* knockout strain lacked LAH; instead, it accumulated LA as the end-product of its ergot alkaloid pathway as evidenced by detection of peaks corresponding to LA at ~16 min, along with its stereoisomer at ~22 min.

Broth cultures of the *lpsB* knockout mutant were grown in triplicate and compared to similarly grown cultures of the *N. fumigata* strain previously engineered to accumulate LA (Robinson and Panaccione 2014). Alkaloid extracts prepared from the dried fungal mats were analyzed through HPLC with fluorescence detection and compared to extracts of their respective growth medium. Percent yield of LA was approximated by comparing relative peak areas of LA and its precursor agroclavine to standard curves prepared from ergot alkaloids with similar fluorophores. The *M. brunneum lpsB* knockout strain had a much higher percent yield compared to that observed in the LA-producing strain of *N. fumigata* ($P = 0.0002$) (Fig. 5A). The difference in percent yield between engineered *M. brunneum* and *N. fumigata* strains also is evident in the amount of the CloA substrate agroclavine accumulating in *N. fumigata* strain

relative to that of the *M. brunneum* strain in HPLC chromatograms (Fig. 4B; Table 2).

Comparison of the solid and liquid phase extracts also revealed the *M. brunneum lpsB* knockout strain secreted LA in a much higher proportion compared to the *N. fumigata* strain ($P < 0.0001$) (Fig. 5B).

Production and secretion of DHLA in *M. brunneum*.

Generation of a strain of *M. brunneum* producing DHLA was achieved through two successive transformations (Fig. 2). In the first transformation, the *easA* locus of wild-type *M. brunneum* was targeted for knockout in an approach similar to that described for the *lpsB* knockout. The resulting mutant recombined at the *easA* locus, incorporating a full copy of the *bar* construct selectable marker (Fig. 6) and disrupting the *easA* coding sequences. HPLC analysis of this strain indicated a lack of LAH and accumulation of chanoclavine-I, as observed previously in an *N. fumigata easA* knockout (Coyle et al. 2010) (Fig. 7).

In the second transformation, with the *easA* knockout strain as recipient, the *lpsB* locus was knocked out by the CRISPR-based strategy described above and, at the same time, the strain was augmented by the introduction of a construct containing two genes previously shown to be required for synthesis of DHLA. Fusion PCR was used to generate a dihydroergot alkaloid expression construct, which contained the *easA* allele from *N. fumigata* (to complement the *easA* knockout in the recipient but with an allele that produces the dihydroergot alkaloid substrate festuclavine) (Coyle et al. 2010) and a previously generated synthetic *cloA* allele based on the protein sequence found in *C. africana* (to oxidize festuclavine to DHLA) (Arnold 2017). The two genes were divergently transcribed under the control of a bidirectional *dmaW/easG* promoter from the *M. brunneum eas* cluster (Fig. 7). This ‘dihydro’ construct was introduced into the *easA* knockout strain of *M. brunneum* in pBChygro (Silar 1995), as a selectable marker, along with a

sgRNA:Cas9 complex targeting *lpsB* for knockout. Knockout of *lpsB* was assessed by a strategy similar to that used for the previously discussed knockouts (Fig. 6). The mutated locus incorporated a fragment of the pBChygro vector in the *lpsB* coding sequence. Resistance to hygromycin and expression of the dihydro construct was conferred by a full construct integrated elsewhere. Extracts of this strain were analyzed by HPLC and compared with extracts of wild-type *M. brunneum*, the *easA* knockout strain of *M. brunneum*, and a chemical standard for DHLA as references (Fig. 8). The mutant strain lacked LAH and did not accumulate detectable levels of chanoclavine-I. Instead, the mutant accumulated DHLA, as indicated by the presence of a peak that aligned with the standard at ~12 min.

Broth-based cultures of the mutant were grown in triplicate and compared to similarly grown cultures of a previously described strain of *N. fumigata* that accumulates DHLA (Bragg et al. 2017). Dried fungal mats were extracted and compared to extracts of their respective growth medium by HPLC with fluorescence detection, as described above for the LA accumulators. The DHLA-accumulating *M. brunneum* strain converted festuclavine substrate to DHLA to give a much higher percent yield than did the previously engineered strain of *N. fumigata* ($P = 0.0006$) (Fig. 9A; Table 2). The *M. brunneum* DHLA-accumulating strain also secreted DHLA in a very high proportion, whereas no DHLA was detectable in the spent culture fluids of the *N. fumigata* strain (Fig. 9B).

Production and secretion of a novel lysergic acid amide in *M. brunneum*.

The ability of *M. brunneum* to produce and secrete additional, novel dihydroergot alkaloids was demonstrated by substituting alleles at the *easA* locus (to produce the dihydroergot alkaloid intermediate festuclavine) and augmenting with a festuclavine-oxidizing allele of *cloA*.

The *easA* and *cloA* alleles were introduced via the previously described *easA/cloA* dihydro construct while targeting the *easA* locus of wild-type *M. brunneum* for knockout. The strategy was thus similar to that used above to generate the DHLA mutant, but in this case the recipient fungus retained a functional copy of *lpsB* such that the DHLA produced might be incorporated into amides of DHLA. The *easA* knockout strain incorporated a full copy of the expression construct as cloned into pBChygro (Fig. 10). HPLC analysis of this strain revealed a lack of peaks corresponding to the stereoisomers of LAH (Fig. 11A). Instead the engineered strain contained a novel peak eluting at ~37 min in the 272/372 nm fluorescence chromatogram, corresponding to a slightly shorter retention time relative to that of LAH, which was observed in the wild type and which fluoresces maximally with excitation at 310 nm and emission at 410 nm (Fig. 11B). The change in fluorescence properties is consistent with a shift from an unsaturated D ring typical of LA derivatives (fluorescing stronger at 310 nm/410 nm) to the saturated D ring of dihydroergot alkaloids (fluorescing more intensely at 272 nm/372 nm) (Panaccione et al. 2012).

Extracts of this strain were then compared further with those of the wild type through liquid chromatography-mass spectrometry (LC-MS) (Fig. 12). Parent ions of m/z 312.2 were found in the wild-type strain, with four peaks eluting at ~5.7 min to ~6.7 min. The observed m/z values of these four ions are consistent with those expected for the protonated ions of the four stereoisomers of LAH. These stereoisomers result from alternate stereochemistry at the site where the alanine derivative attaches to LA and from the keto-enol tautomerization that occurs at C8 of LA, where the amide side branch attaches from the ergoline ring system (Fig. 1) (Leadmon et al. 2020, Panaccione et al. 2012, Flieger et al. 1982). None of these LAH stereoisomer peaks were detected in the mutant strain; instead, the mutant accumulated parent ions of m/z 314.2,

which is consistent with the $[M + H]^+$ of the dihydrogenated form of LAH (dihydroLAH). The presence of two peaks (~5.6 min and at ~6.5 min) indicates the presence of stereoisomers, which would be expected from the chiral carbon at the attachment site of the alanine derived residue of dihydroLAH. Dihydrogenated ergot alkaloids lack the stereoisomers from the keto-enol tautomerization that occurs at C8 (Bragg et al. 2017, Arnold and Panaccione 2017, Panaccione et al. 2012, Mantle and Waight 1968).

Fragmentation analyses revealed a close relationship between the m/z 312.2 ions of wild-type *M. brunneum* and the m/z 314.2 ions of the engineered *M. brunneum* mutant (Fig. 12). Major ions of m/z 268 and m/z 294 were obtained from the m/z 312 ion. The m/z 268 ion corresponds to ergine, the simple amide of LA and spontaneous hydrolysis product of LAH, and the m/z 294 ion is consistent with $[LAH - H_2O]^+$. The fragmentation pattern of the m/z 314 ion aligned with that of LAH, but with each fragment two Daltons greater, consistent with the presence of a saturated D ring in the ergoline nucleus of the molecule. Collectively, the data strongly suggest that the novel metabolites accumulating in the engineered strain are stereoisomers of dihydroLAH, a compound not previously found in nature. Cultures of this mutant were grown similarly to those described for the previous strains, and the mean percent yield of the putative dihydroLAH (relative to DHLA as precursor) was calculated to be 16.9% (\pm 4.3% SE). A mean of 95.9% (\pm 0.61% SE) of the provisional dihydroLAH was secreted from the fungus into the growth medium.

Discussion

Our data show that *M. brunneum* can be engineered to accumulate LA and DHLA with higher percent yields than were calculated for strains of *N. fumigata* previously engineered to

produce these same ergot alkaloids (Robinson and Panaccione 2014, Bragg et al. 2017, Arnold and Panaccione 2017). Moreover, we have found that the natural ability of *M. brunneum* to secrete its own alkaloids (Leadmon et al. 2020) allows for these engineered strains to secrete the majority of each of these products. We also demonstrated that *M. brunneum* can be engineered to produce a novel derivative of DHLA, which evidence indicates is dihydroLAH, and that the fungus secretes almost the entire proportion of this product. The increased percent yields of products relative to those observed in *N. fumigata*, abundant secretion of LA, DHLA, and their derivatives, and amenability to engineering of novel compounds make *M. brunneum* an effective platform for ergot alkaloid research and, potentially, production.

Previous experiments have shown that *N. fumigata* can be engineered to accumulate LA through the expression of the isomerase allele of *easA* along with *cloA* in an appropriate mutant background (Robinson and Panaccione 2014). While conversion of agroclavine to LA was not measured in that previous study, the same strain was used in our experiments, and we observed yield of LA from agroclavine with a relatively low percentage. Our strain of *M. brunneum*, which normally produces derivatives of LA, had no difficulty accumulating LA as the terminal product of its pathway. The *M. brunneum* strain had a much higher percent yield compared to *N. fumigata*.

Additional previously published experiments have shown that *N. fumigata* can be engineered to produce DHLA when alleles of *cloA* from species that naturally produce this compound are introduced into a festuclavine-accumulating mutant (Bragg et al. 2017, Arnold and Panaccione 2017). Bragg et al. (2017) tested the allele from the maize ergot pathogen *C. gigantea* in an *N. fumigata* mutant and determined that conversion of festuclavine to DHLA was very low. A similar result was obtained when Arnold and Panaccione (2017) used a *cloA* allele

from *C. africana* that was codon-optimized for *N. fumigata*. The authors suspected that the low conversion could have been due to issues related to enzyme and substrate compartmentalization or accumulation of the reaction products. *Metarhizium brunneum* appeared to have no significant problem in converting substrate to end product, although the reasons for the difference in results between expression hosts have yet to be elucidated. Secretion was not tested in the previous studies, because *N. fumigata* typically retains its alkaloids (Mulinti et al. 2014); however, secretion from the relevant *N. fumigata* strain was tested here for comparison purposes and found to be low for LA and non-detectable for DHLA. In contrast, the engineered *M. brunneum* strain secreted the vast majority of its LA and DHLA.

Lps2 (also called LpsB), the product of *lpsB*, is required for the formation of ergopeptines (Correia et al. 2003, Ortel and Keller 2009, Riederer 1996) and ergonovine (Ortel and Keller 2009). A similar requirement of this enzyme in the biosynthesis of LAH was reasonable to hypothesize, but a direct role for LpsB in LAH biosynthesis had not been demonstrated until the present study. We showed that the presence of this gene is necessary not only for LAH, which was not detectable in the *lpsB* knockout, but also for production of its dihydrogenated form, which accumulated when the dihydro expression construct was introduced into the *easA* knockout but not when introduced into the *lpsB* knockout. Our data indicate LpsB from *M. brunneum* accepts DHLA as a substrate, but the relatively low rate of conversion of DHLA to provisional dihydroLAH (16.9%) may indicate a lower affinity for DHLA as substrate. This enzyme substrate combination was tested previously in *C. purpurea* by Riederer et al. (1996) who showed that LpsB (Lps2) of *C. purpurea* accepted DHLA with the same K_m with which it accepted LA. In our dihydroLAH example, however, the low relative percent yield may reflect

factors other than the affinity of LpsB for DHLA as substrate, because several activities downstream of LpsB are required for the conversion of DHLA into dihydroLAH.

The reasons why *M. brunneum* can produce LA and DHLA more efficiently than did *N. fumigata* is an area yet to be explored. The presence of transporter proteins allowing for easy movement of substrates and reaction products would be one potential explanation for the higher percent yield and secretion; however, no candidate alkaloid transporter genes have yet been identified in *M. brunneum*, and no genes in the *eas* cluster resemble transporter-encoding genes. Research on the biosynthesis of other fungal toxins has shown the importance of cellular compartmentalization and transport of pathway intermediates or end products between compartments (Roze et al. 2011, Menke et al. 2012, Kistler and Broz 2015). Compartmentalization and/or interaction of enzymes relative to one another may also be more conducive for product formation in *M. brunneum*, which naturally produces similar ergot alkaloids, as opposed to *N. fumigata*, which produces ergot alkaloids from a different branch of the pathway (Robinson and Panaccione 2015, Wallwey and Li 2011).

Although the *M. brunneum* strains more efficiently produced and secreted higher proportions of LA and DHLA compared to similarly engineered *N. fumigata* strains, the absolute quantities of ergot alkaloids the fungus produced in culture (Table 2) was low in comparison to the quantities observed when the fungus colonizes *Galleria mellonella* larvae (Leadmon et al. 2020). Culture conditions or genetic modifications that promote increased and more reliable yields of ergot alkaloids in culture would help make this fungus an excellent platform for ergot alkaloid modification and production. The great differences in accumulation of ergot alkaloids in insects compared to cultures (Leadmon et al. 2020) indicate strong regulation of the pathway. The *eas* clusters of *Metarhizium* species lack genes that would appear to encode transcription

factors; thus, genes controlling expression of *eas* genes may be encoded elsewhere in the genome. The increased accumulation of ergot alkaloids in insects also indicates a role for ergot alkaloids in fungus-insect interaction. The mutants generated in this present study may be helpful in assessing potential effects of different ergot alkaloids in fungus colonization of insects.

The use of hygromycin as a selectable marker for transformed *M. brunneum* strains was facilitated through the utilization of a very high concentration of the chemical. Previous literature (Bernier et al. 1989, Goettel et al. 1990) has mentioned the insensitivity of *Metarhizium* spp. to hygromycin as an impediment to using this compound as a selectable marker for transformation. Nonetheless, we tested concentrations from 200 µg/mL to 800 µg/mL and found a concentration of 600 µg/mL allowed for the formation of transformed colonies that were distinguishable from background growth when compared to growth observed on no-DNA control plates.

Overall, our work shows that *M. brunneum* has the potential to serve as a platform in which to produce pharmaceutically relevant ergot alkaloids and novel derivatives of these compounds. The approaches used here also may facilitate functional analysis of additional genes involved in LA amide synthesis, which is ongoing in our laboratory. Additional future work will focus on the identification of factors responsible for the higher percent yield and secretion observed in this fungus.

Materials and Methods

Growth and maintenance of fungi.

Cultures of wild-type *M. brunneum* (ARSEF 9354, United States Department of Agriculture-ARS Collection of Entomopathogenic Fungal Cultures, Ithaca, NY) and its

transformants were maintained on sucrose yeast-extract (SYE) agar medium (per liter: 20 g sucrose, 10 g yeast extract, 1 g of magnesium sulfate-heptahydrate, and 15 g agar). Cultures were grown at 30°C for at least seven days before testing for ergot alkaloids. Cultures of the previously engineered *N. fumigata* strains (Robinson and Panaccione 2014, Bragg et al. 2017) were maintained at 37°C on malt extract agar medium (per liter: 6.0 g malt extract, 1.8 g maltose, 6.0 g dextrose, 1.2 g yeast extract, and 15 g agar).

Design of CRISPR sgRNA and Cas9 complexing.

Single guide RNA (sgRNA) sequences targeting the *easA* (GenBank accession: [XM_014685465.1](#)) and *lpsB* (GenBank accession: [XM_014685466.1](#)) loci were chosen based on sequence recommendations for Cas9 cutting efficiency (Liu et al. 2016). A 20-nucleotide target sequence (underlined in the primers, listed below) was chosen for both genes and primers containing these were used for sgRNA synthesis, with TTCTAATACGACTCACTATAGGACAGGAAATAGACTCGGCGTTTTAGAGCTAGA used as the primer for *lpsB* sgRNA synthesis and TTCTAATACGACTCACTATAGGACAAGAAGCCAATCTTGCGTTTTAGAGCTAGA used for *easA*. Both primers were diluted to 1 µM before being included in sgRNA synthesis reactions involving the EnGen® sgRNA Synthesis Kit (New England Biolabs [NEB], Ipswich, MA). sgRNA products were cleaned using the Monarch® RNA Cleanup Kit (NEB). Quality of sgRNA was confirmed by SDS PAGE. Prior to fungal transformation, sgRNAs were diluted to 20 µM and complexed with EnGen® Spy Cas9 NLS (NEB) by combining 2 µL of sgRNA, 2 µL of Cas9 enzyme, 0.5 µL of 10X Buffer 3.1 (NEB), and 0.5 µL of nuclease-free water. The reaction

was incubated at room temperature for 30 minutes to allow for complexing before being moved to ice until needed.

Preparation of transformation constructs.

A synthetic version of the phosphinothricin N-acetyltransferase gene coding sequence (GenBank accession: MT350122), which confers resistance to bialaphos, was codon optimized for *M. anisopliae*, placed under the control of the GPDH promoter from *M. brunneum* ARSEF 3297 (nucleotides 1,625,569–1,626,574 in GenBank accession: [NW_014574712.1](#)), and purchased from Genscript (Piscataway, NJ) in a pUC57 construct. The promoter and coding portion of this construct, referred to as the *bar* construct or *bar* amplicon, were amplified through polymerase chain reaction (PCR). All PCRs were performed with Phusion Green Hot Start II High-Fidelity PCR Master Mix (Thermo Scientific, Waltham, MA) and followed a similar protocol with an initial denaturation at 98°C (15 s), annealing at a temperature specific to each primer as indicated in Table 1 (15 s), extension at 72°C (for the time interval specified in Table 1), and a final extension at 72°C for 60 s. PCRs were conducted in 20 µL containing 10 µL of PCR master mix (dNTPs, buffer, polymerase, and gel loading dye), primers at a final concentration of 0.5 µM each, and approximately 20-100 ng of template DNA. The optimized GPDH promoter-*bar* fusion construct was amplified with primer combination 1. A DNA Clean and Concentrator kit (Zymo Research, Irvine, CA) was used to purify the amplicon.

A construct for expressing the *N. fumigata easA* allele (Coyle et al. 2010) together with the synthetic, intron-free *C. africana cloA* allele (Arnold and Panaccione 2017) under the control of the bidirectional *easG/dmaW* promoter from *M. brunneum* (nucleotides 206,186—207,489 in GenBank accession: [NW_014574698.1](#)) was generated using a three-way fusion PCR. The

individual fragments were amplified using primer sets to include overlaps to allow for fusion, with both gene portions including roughly 150 bp of their native 3' untranslated region (3' UTR). The primers used in the final fusion PCR included recognition sites for *NotI* and *SalI* to allow for digestion and ligation into pBChygro (Silar 1995; Fungal Genetics Stock Center, Manhattan, KS). Genomic DNA was extracted from *N. fumigata* strain Af293 and wild-type *M. brunneum* samples according to the Gene Clean Spin protocol (MP Biomedicals, Solon, OH). These templates were used with primer combinations 2 and 3, respectively, to generate the *easA* and promoter fragments. Primer combination 4 was used together with a stock of the synthetic *cloA* allele plasmid (Arnold and Panaccione 2017). The fragments (consisting of 1543, 1345, and 1903 bp, respectively) were gel purified using a Zymoclean Gel DNA Recovery Kit (Zymo). Equimolar ratios of each fragment were then combined in a subsequent PCR reaction using primer combination 5. A DNA Clean and Concentrator kit (Zymo) was used to clean the fusion product before both it and pBChygro were subjected to double digestion. These fragments were then ligated following a cleanup step, and the final product, *A.f. easA-C.a. cloA*-pBChygro (referred to as the “dihydro construct”) was used in order to transform competent *Escherichia coli* (NovaBlue; Sigma-Aldrich, St. Louis, MO). Transformed cells were plated on LB medium (per liter: 10 g tryptone, 5 g yeast extract, 5 g NaCl, and 15 g agar) supplemented with chloramphenicol (25 µg/mL). Plasmid products were harvested and purified using a Zippy Plasmid Miniprep Kit (Zymo), and correct assembly was verified through double digestion with *NotI/SalI*.

Protoplast preparation and fungal transformation.

Protoplasts of *M. brunneum* were prepared as described previously for *N. fumigata* (Bilovol and Panaccione 2016). Protoplasts were then transformed with complexed sgRNA:Cas9 and selectable markers according to established methods (Coyle et al. 2010, Bilovol and Panaccione 2016). Our CRISPR-Cas9 approach differed from that employed by Chen et al. (2017) for the entomopathogenic fungus *Beauveria bassiana* in that we opted for transient expression of introduced, sgRNA-complexed Cas9 as opposed to stably transforming the gene encoding Cas9 into the fungus. Moreover, since our transformation reactions contained 50 million protoplasts, each containing variable numbers of nuclei, we co-transformed selectable marker genes along with sgRNA:Cas9 complexes to help identify colonies arising from protoplasts that took up introduced elements. In order to generate an *easA* knockout strain of *M. brunneum*, 5 μ L of complexed sgRNA:Cas9 targeting for *easA* was added together with 1 μ g of the optimized *bar* amplicon (in a maximum volume of 5 μ L). These transformants were plated in *bar* transformation medium (per liter: 310 g sucrose, 2.5 g ammonium nitrate, 1.7 g amino acid-free yeast nitrogen base, 1 g magnesium sulfate-heptahydrate, 0.5 g monobasic potassium phosphate, 0.5 g dibasic potassium phosphate, 0.5 g potassium chloride, 0.05 g chloramphenicol, and 7 g agarose) supplemented with phosphinothricin (Gold Biotechnology, St. Louis, MO) at 200 μ g/mL and incubated at 30°C. Upon surfacing, colonies were transferred to *bar* maintenance medium (per liter: 20 g sucrose, 2.5 g ammonium nitrate, 1.7 g amino acid-free yeast nitrogen base, 1 g magnesium sulfate-heptahydrate, 0.5 g monobasic potassium phosphate, 0.5 g dibasic potassium phosphate, 0.5 g potassium chloride, 0.05 g chloramphenicol, and 15 g agar) supplemented with phosphinothricin at 200 μ g/mL and incubated at 30°C to allow for further growth under selection. In order to generate a LA-accumulating strain of *M. brunneum*, the above protocol was repeated with the substitution of the sgRNA targeting *lpsB*.

To produce *M. brunneum* strains capable of producing DHLA and dihydroLAH, the wild-type and *easA* knockout strains were subjected to a slightly modified transformation. For a DHLA producer, the *easA* knockout strain was transformed with 5 μ L of complexed sgRNA:Cas9 targeting *lpsB* and 1 μ g of the dihydro expression construct (in a maximum volume of 5 μ L). Transformants were plated in TM102 medium (per liter: 310 g sucrose, 10 g malt extract, 10 g peptone, 2 g yeast extract, 1 g magnesium sulfate-heptahydrate, 0.5 g monobasic potassium phosphate, 0.5 g dibasic potassium phosphate, 0.5 g potassium chloride, 0.05 g chloramphenicol, and 15 g agar) supplemented with hygromycin (InvivoGen, San Diego, CA) at 600 μ g/mL and incubated at 30°C. To generate a dihydroLAH-producing strain, this protocol was repeated but with the wild-type *M. brunneum* strain and sgRNA targeting *easA*.

PCR and Sanger sequencing were used to assess recombination at the target loci. Genomic DNA was extracted from transformant lines (as described above) and primer combinations 7 and 8 were used in order to assess *easA* and *lpsB* loci, respectively. Primer set 5 was used to determine presence or absence of the dihydro expression construct. Upon failure to generate a product from those targeted at *easA* with the dihydro expression construct, we hypothesized that the entire ~11.4-kb construct had integrated, making amplification across the modified locus impractical. To amplify portions of the *easA* or *lpsB* loci and determine the orientation and extent of the dihydro expression construct integration, primer combinations 9 and 10 were tried together with primer combinations 11 and 12. PCR products were generated from primer combinations 9 and 10, due to the polarity of the inserted fragment. These fragments were cleaned, concentrated, and sequenced by Sanger technology at Eurofins Genomics (Louisville, KY).

HPLC and LC-MS analyses.

To obtain large quantities of ergot alkaloids for chemical analyses, *Galleria mellonella* larvae were inoculated as described previously (Leadmon et al. 2020, Panaccione and Arnold 2017) and incubated at room temperature for 7 days. Twenty microliters of each methanol-extracted sample were analyzed for ergot alkaloids by HPLC with fluorescence detection by methods described in detail previously (Panaccione et al. 2012). The column was a 150 × 4.6 mm i.d., 5- μ m particle size, Prodigy C18 (Phenomenex, Torrance, CA), and the mobile phase was a 55 min, binary, multilinear gradient of 5% acetonitrile to 75% acetonitrile in 50 mM aqueous ammonium acetate. Ergot alkaloids were detected with two serially connected fluorescence detectors, one set with excitation and emission wavelengths of 310 and 410 nm, respectively, to detect LA and its derivatives, and the other at 272 and 372 nm, to detect DHLA and its derivatives.

Extracts of wild-type *M. brunneum* and engineered *N. fumigata* strains (Robinson and Panaccione 2014, Bragg et al. 2017) served as chemical references for LA, DHLA, and LAH. A previously prepared DHLA standard (Arnold and Panaccione 2017) was also used as a reference at a concentration of 10 μ g/mL. For percent yield and secretion analyses, alkaloids were approximately quantified by comparing their peak areas to standard curves prepared from ergot alkaloids with identical fluorophores: dihydroergocristine (Sigma) for alkaloids fluorescing at 272 and 372 nm and ergotamine (Sigma) for alkaloids fluorescing at 310 and 410 nm. LC-MS analysis was conducted according to previously established methods (Ryan et al. 2015).

Percent yield and secretion.

In order to determine percent yield and secretion of individual alkaloids, 15 mL cultures of SYE broth were inoculated with 10^6 spores of each of the mutant strains of *M. brunneum*. *Neosartorya fumigata* strains that accumulate either LA (Robinson 2014) or DHLA (Bragg et al. 2017) were grown similarly, with the substitution of malt extract broth (promoting ergot alkaloid production in *N. fumigata*) as the medium. All cultures were grown in triplicate at room temperature and out of direct sunlight so as to prevent photochemical modification. After 10 days, fungal mats were separated from the remaining liquid via vacuum filtration through preweighed, 0.2- μ m nylon filters and were allowed to dry. Dried portions were weighed, while the volume of liquid portions of cultures were recorded. Alkaloids were extracted with methanol based on previously described methods (Leadmon et al. 2020). Percent yield was calculated as observed product relative to a theoretical yield wherein all observable precursor (e.g., agroclavine for LA) would have been converted to product (Table 2). Data from these analyses had variances that were normally distributed and so were analyzed by analysis of variance (ANOVA). In the case of DHLA, where no DHLA was detected in the broth of *N. fumigata* cultures, a Wilcoxon's rank sum test was used to compare treatments. All statistical analyses were performed with the JMP software package (SAS, Cary, NC).

Acknowledgements

This chapter has been published in Applied and Environmental Microbiology under the doi: [10.1128/AEM.01251-20](https://doi.org/10.1128/AEM.01251-20). I would like to acknowledge co-author Jessi Sampson for her

contribution in developing the phosphinothricin resistance construct for *M. brunneum* used extensively in this work.

This research was funded by NIH grant 2R15-GM114774-2, with additional support from USDA Hatch project NC1183. Experiments with lysergic acid-producing strains were conducted in accordance with licenses from the West Virginia Board of Pharmacy (TI0555042) and the U.S. Drug Enforcement Agency (RP0463353).

Figures and Tables

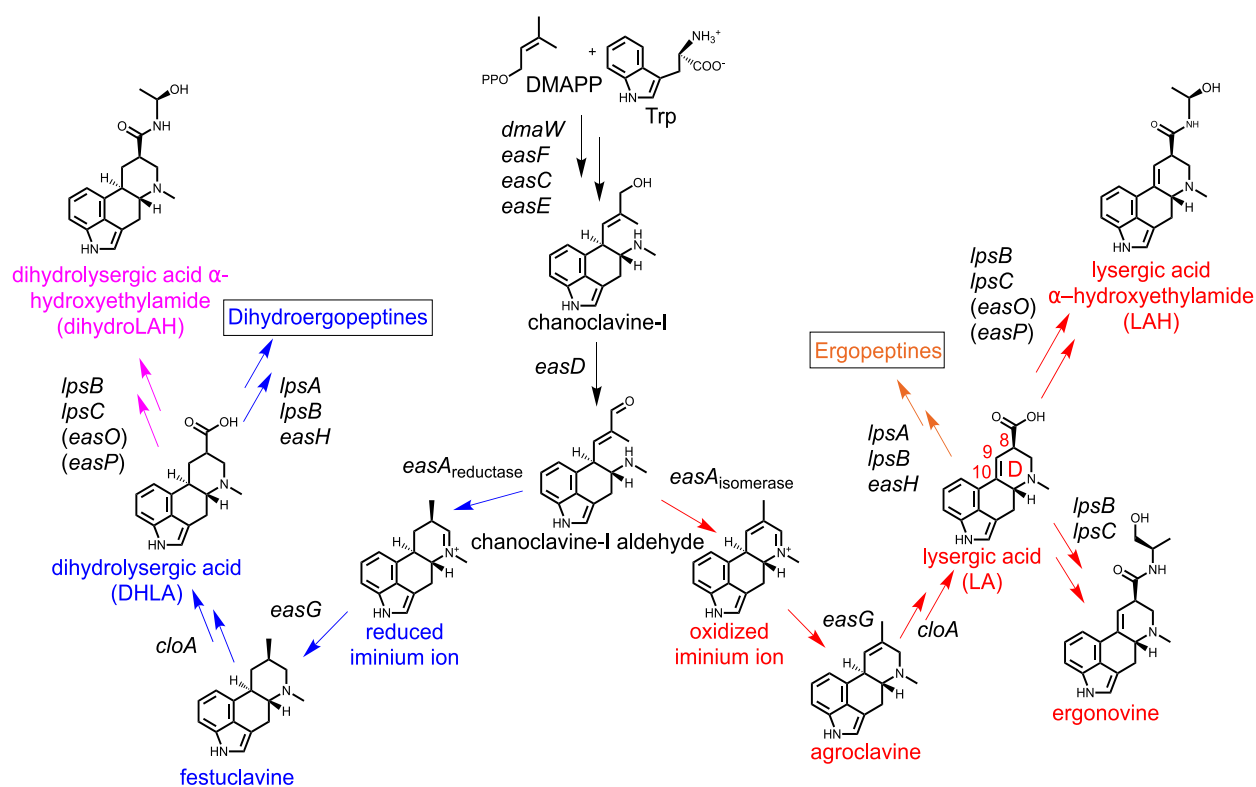


Fig 1. Pathways to the synthesis of lysergic acid amides and dihydrolysergic acid amides. Both pathways begin with the same core set of genes (*dmaW*, *easF*, *easE*, *easC*, *easD*) and branch at *easA* depending on the allele present in a species. The pathway branch to the right (with red labelling) leads to lysergic acid amides, as are found in *M. brunneum* (Leadmon et al. 2020), with a further branch to ergopeptines (labeled in orange), as found in *Claviceps purpurea* and several *Epichloë* species (Florea et al. 2017, Haarmann et al. 2009, Robinson and Panaccione 2015). Red font is used to mark the carbons present in the D ring of ergoline nucleus. The pathway branch to the left (with blue labelling) leads to dihydroergopeptines as found naturally in *C. africana* (Barrow et al. 1974) or in previously engineered strains of *N. fumigata* (Bragg et al. 2017, Arnold and Panaccione 2017). The dihydroergot alkaloid pathway features a further branch, shown in pink that occurs in no natural species but whose formation is a subject of this paper. Double arrows represent multiple enzymatic steps. Enzymes with hypothesized

roles are marked by parentheses. DMAPP, dimethylallylpyrophosphate. Trp, L-tryptophan; DMAPP, dimethylallylpyrophosphate.

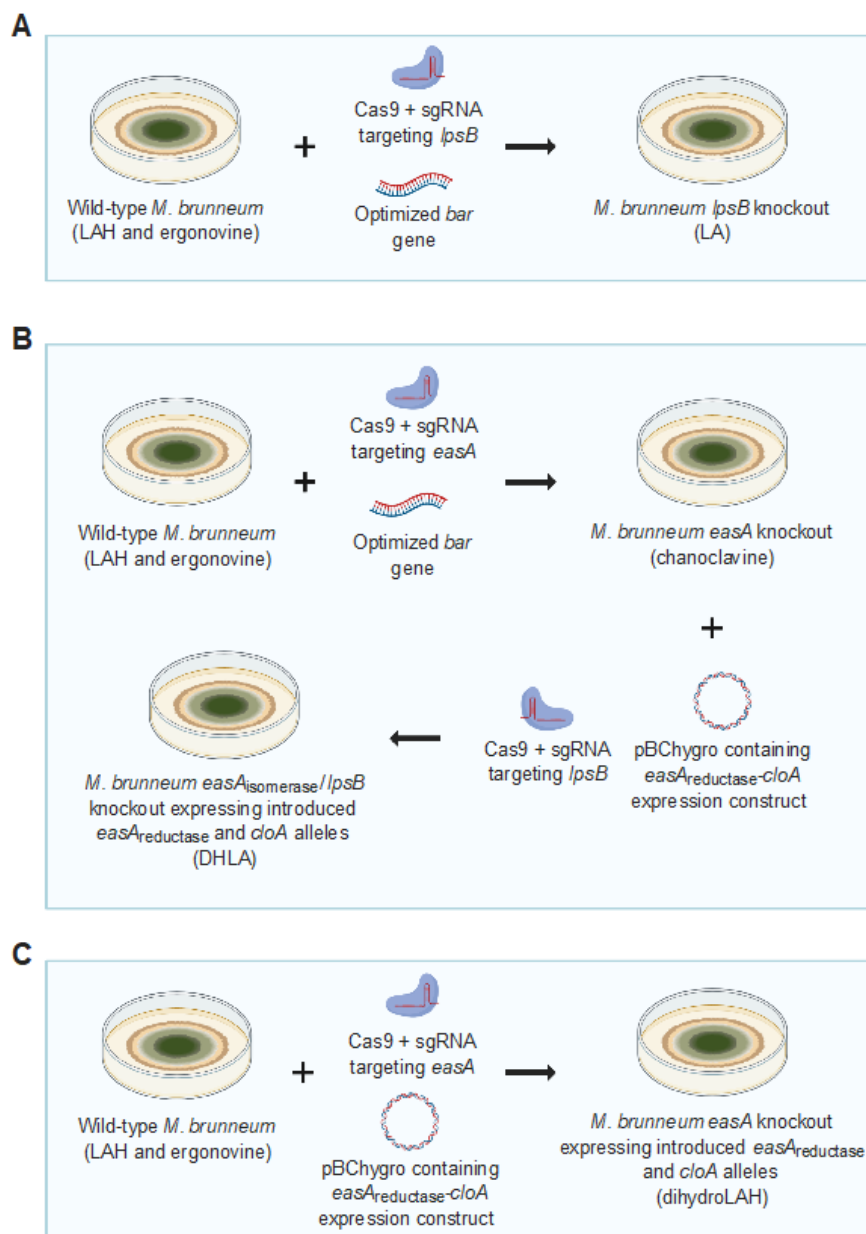


Fig 2. Strategies for engineering mutant strains of *M. brunneum*. Strains are listed with their terminal alkaloid product appearing in parentheses. (A) Strategy for engineering the LA-producing strain of *M. brunneum*. (B) Strategy for engineering the DHHLA-producing strain of *M. brunneum*. (C) Strategy for engineering the provisional dihydroLAH-producing strain of *M. brunneum*. LAH, lysergic acid α -hydroxyethylamide; LA, lysergic acid; DHHLA, dihydrolysergic acid; dihydroLAH, dihydrolysergic acid α -hydroxyethylamide. Created with BioRender.com.

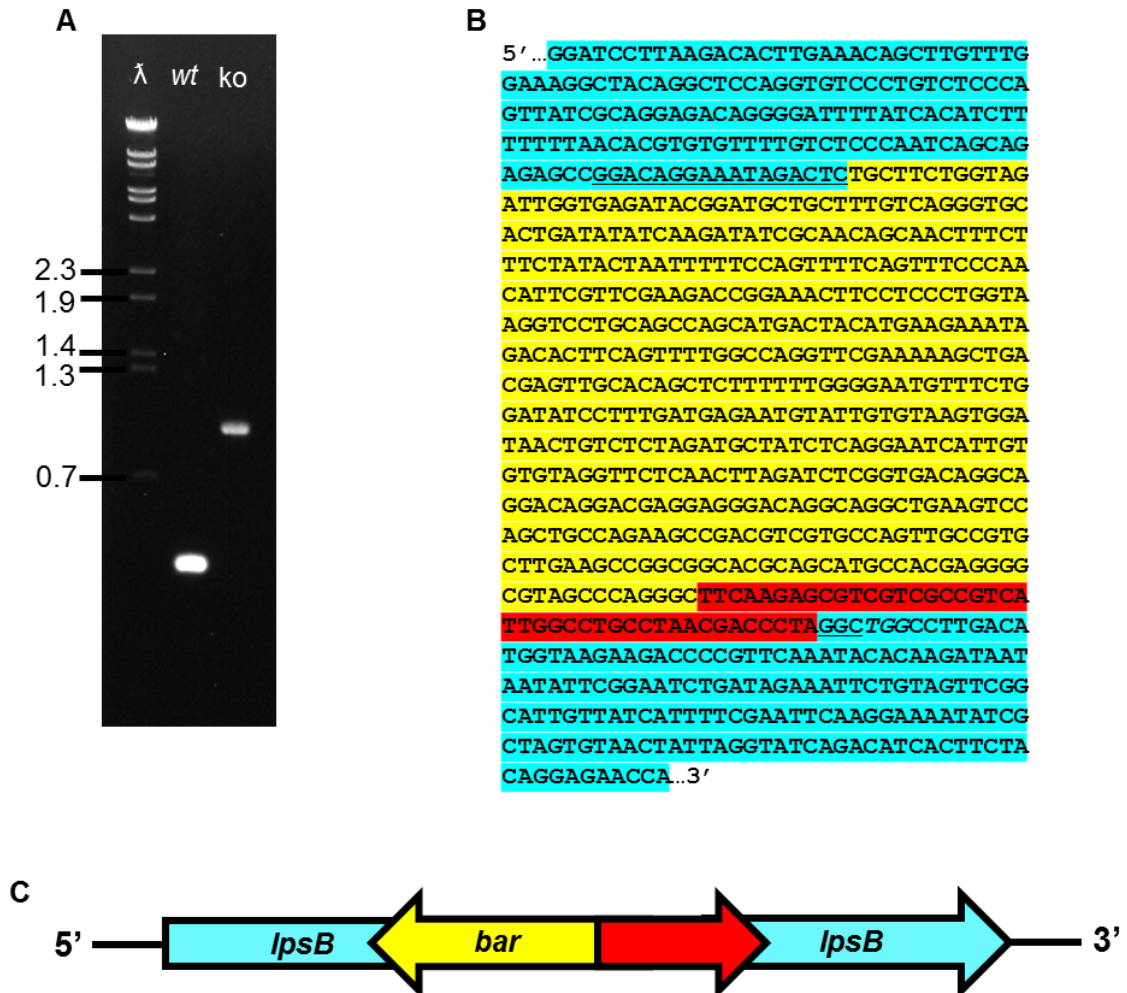


Fig 3. PCR analysis of *M. brunneum lpsB* locus following gene knockout. (A) PCR products from primer combination 7 (listed in Table 1) and genomic DNA isolated from wild type (wt) and *lpsB* knockout (ko) strains of *M. brunneum*. Sizes of relevant fragments from *Bst*EII-digested bacteriophage lambda DNA are indicated to the left. Gel was stained with ethidium bromide. (B) DNA sequence of *lpsB* locus after CRISPR mutagenesis. Blue highlight indicates sequences flanking the site of CRISPR-Cas9 recombination. Yellow highlight represents sequence fragment from optimized *bar* selectable marker. Red highlight represents another truncated fragment of *bar* marker present in the locus. Target sequence is underlined and protospacer-adjacent motif (PAM) is italicized. (C) Graphic displaying the orientation and components integrated into the cut sites for this mutant. Two partial fragments of the *M.b. bar* marker with different lengths and divergent orientations are shown to have integrated.

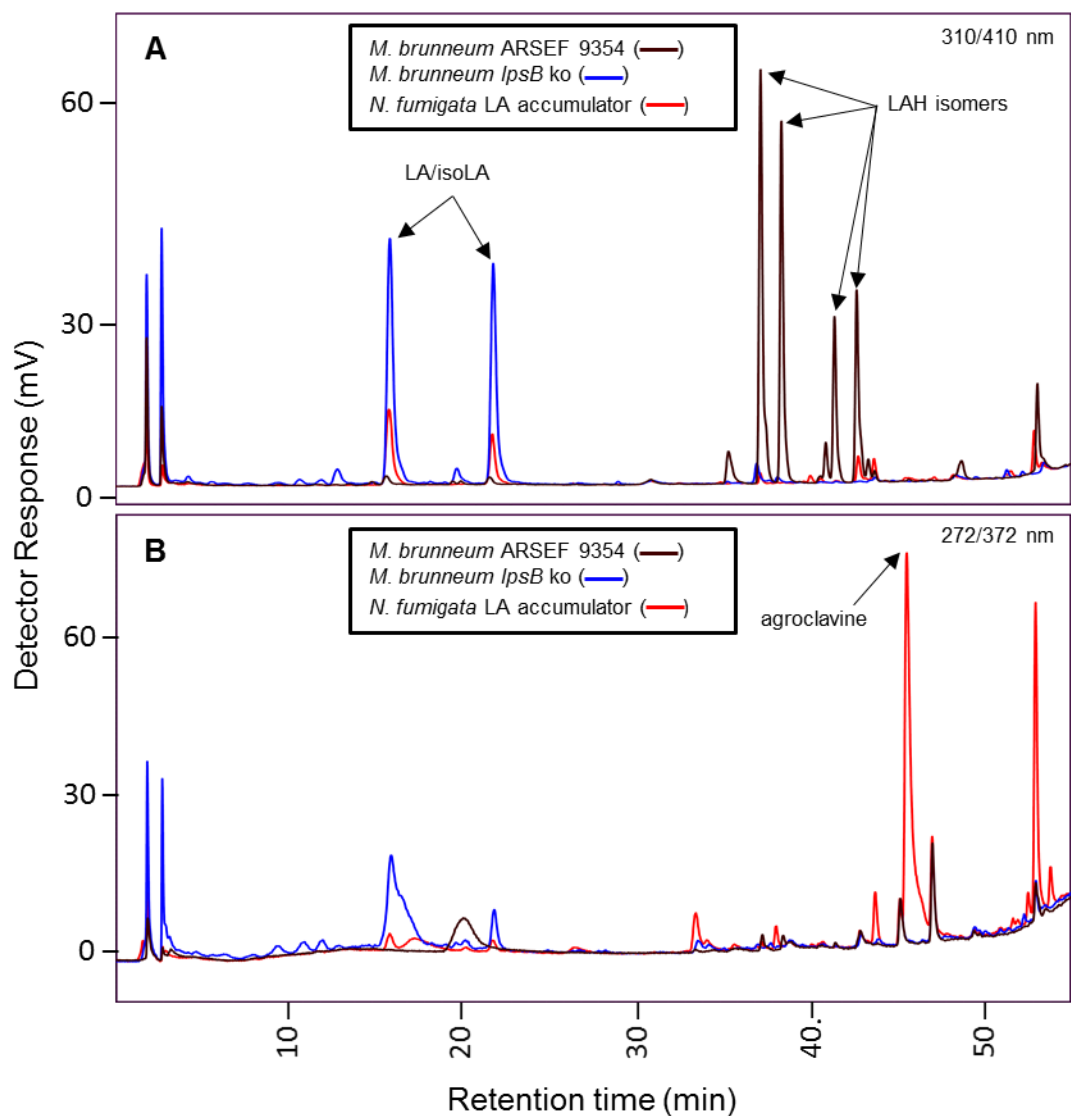


Fig 4. HPLC chromatograms of *lpsB* knockout of *M. brunneum* (*lpsB* ko) compared to wild-type *M. brunneum* and LA-accumulating strain of *N. fumigata*. Fluorescence was detected at (A) 410 nm after exciting at 310 nm and (B) at 372 nm after exciting at 272 nm. Peaks corresponding to characterized ergot alkaloids are indicated: LA/isoLA, lysergic acid/isolysergic acid; LAH, lysergic acid α -hydroxyethylamide.

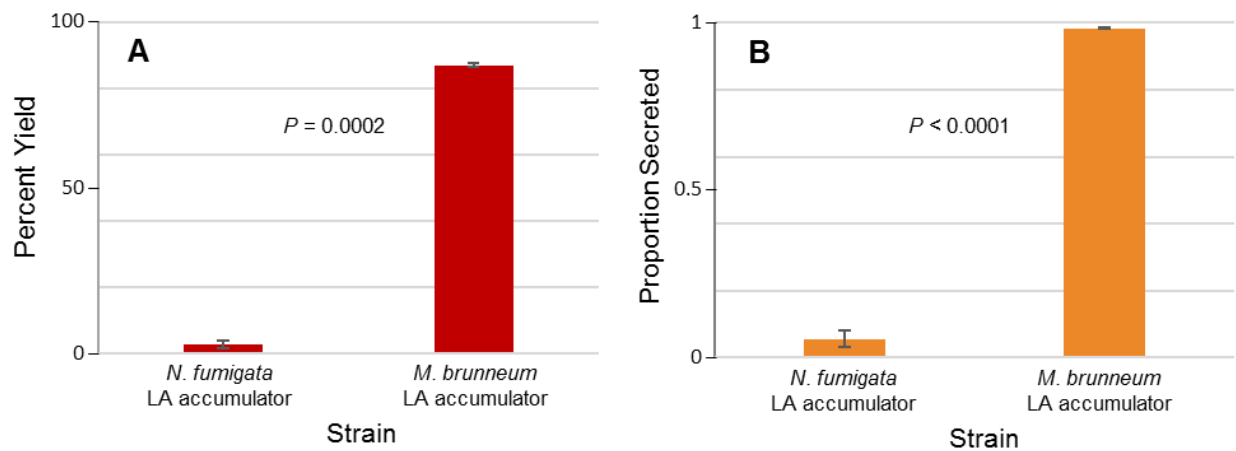


Fig 5. Percent yield and secretion of LA in *N. fumigata* mutant compared to *M. brunneum* mutant.

(A) Mean percent yield lysergic acid relative to precursor agroclavine between strains. (B) Mean proportion of lysergic acid secreted into growth medium by strains. Standard error of mean for both data sets is shown by the error bars. P values from analysis of variance (ANOVA) are shown between bars.

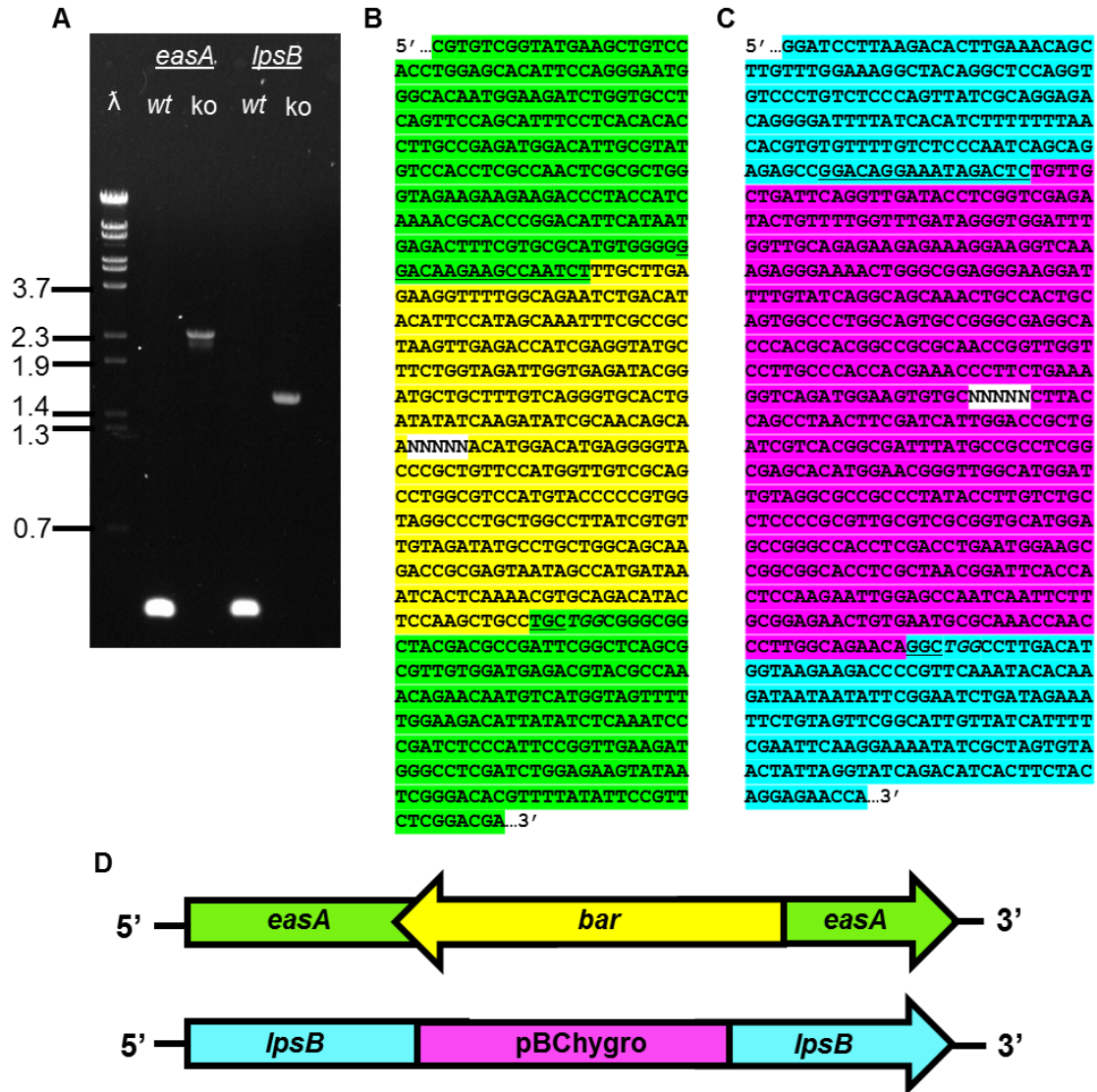


Fig 6. PCR analysis of *M. brunneum* *easA* and *lpsB* loci following gene knockout and transformation with *bar* marker and dihydro expression construct. (A) PCR products from primer combinations 7 or 8 (Table 1) and genomic DNA isolated from wild type (wt) and DHLA-producing (ko) strains of *M. brunneum*. Sizes of relevant fragments from *Bst*EII-digested bacteriophage lambda DNA are indicated to the left. Gel was stained with ethidium bromide. (B) DNA sequence of *easA* locus after CRISPR mutagenesis. Green highlight indicates sequences flanking the site of CRISPR-Cas9 recombination. Yellow highlight represents *bar* marker integrated in opposite orientation present in the locus. Target sequence is underlined, and protospacer-adjacent motif (PAM) is italicized. (C) DNA

sequence of *lpsB* locus after CRISPR mutagenesis concomitant with introduction of the dihydro construct. Blue highlight indicates sequences flanking the site of CRIPSR-Cas9 recombination. Pink highlight represents fragment from pBChygro portion of the dihydro expression construct with 612 nt omitted (represented by NNNNN) to simplify presentation. Target sequence is underlined, and protospacer-adjacent motif (PAM) is italicized. (D) Graphics displaying the orientation and components integrated into cut sites for both mutant loci.

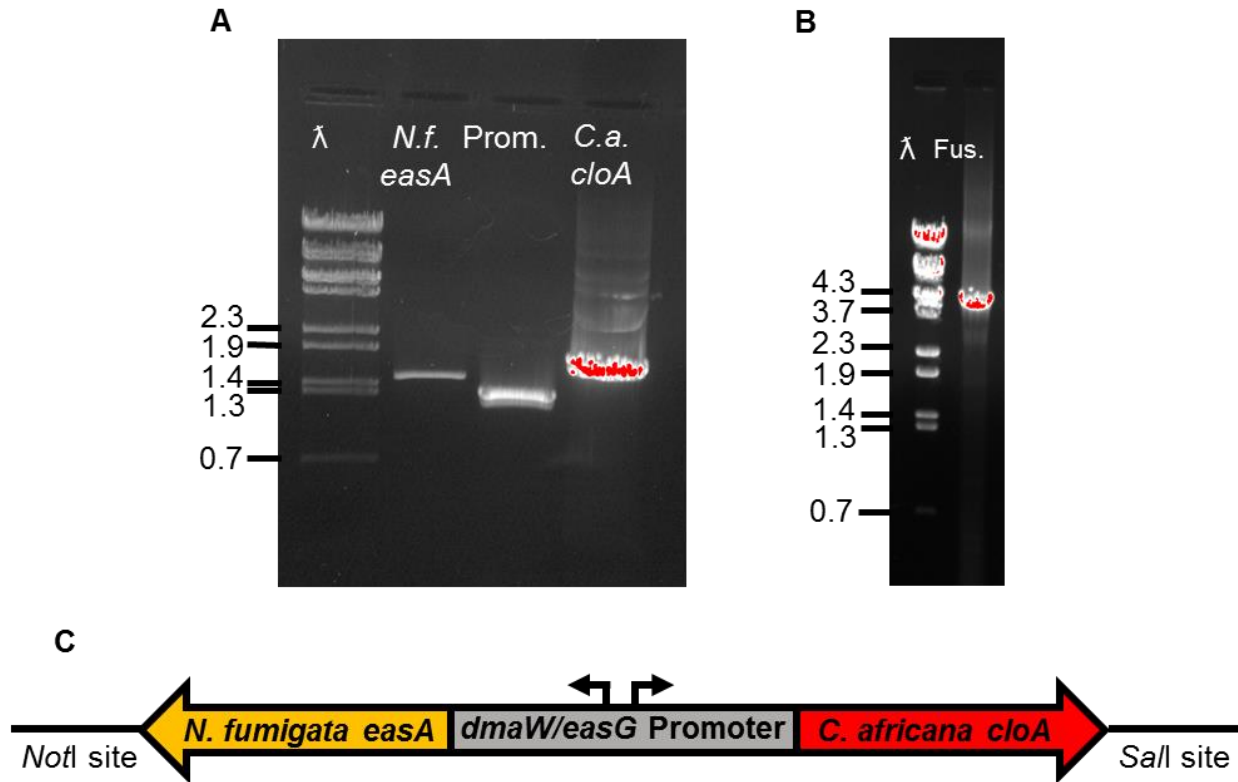


Fig 7. Construction of the dihydro expression construct prior to ligation into pBChygro. (A)

Products from primer combinations 2, 3, and 4 (Table 1) prior to fusion PCR. Sizes of relevant fragments from *Bst*EII-digested bacteriophage lambda DNA are indicated to the left of either gel. Gel was stained with ethidium bromide. Red tint indicates saturated pixels detected by imaging software. (B) Fusion product from PCR primer combination 5, prior to ligation into pBChygro. Fus., *easA*_{reductase}-promoter-*cloA* fusion product. (C) Graphic displaying the orientation and components of the dihydro expression construct.

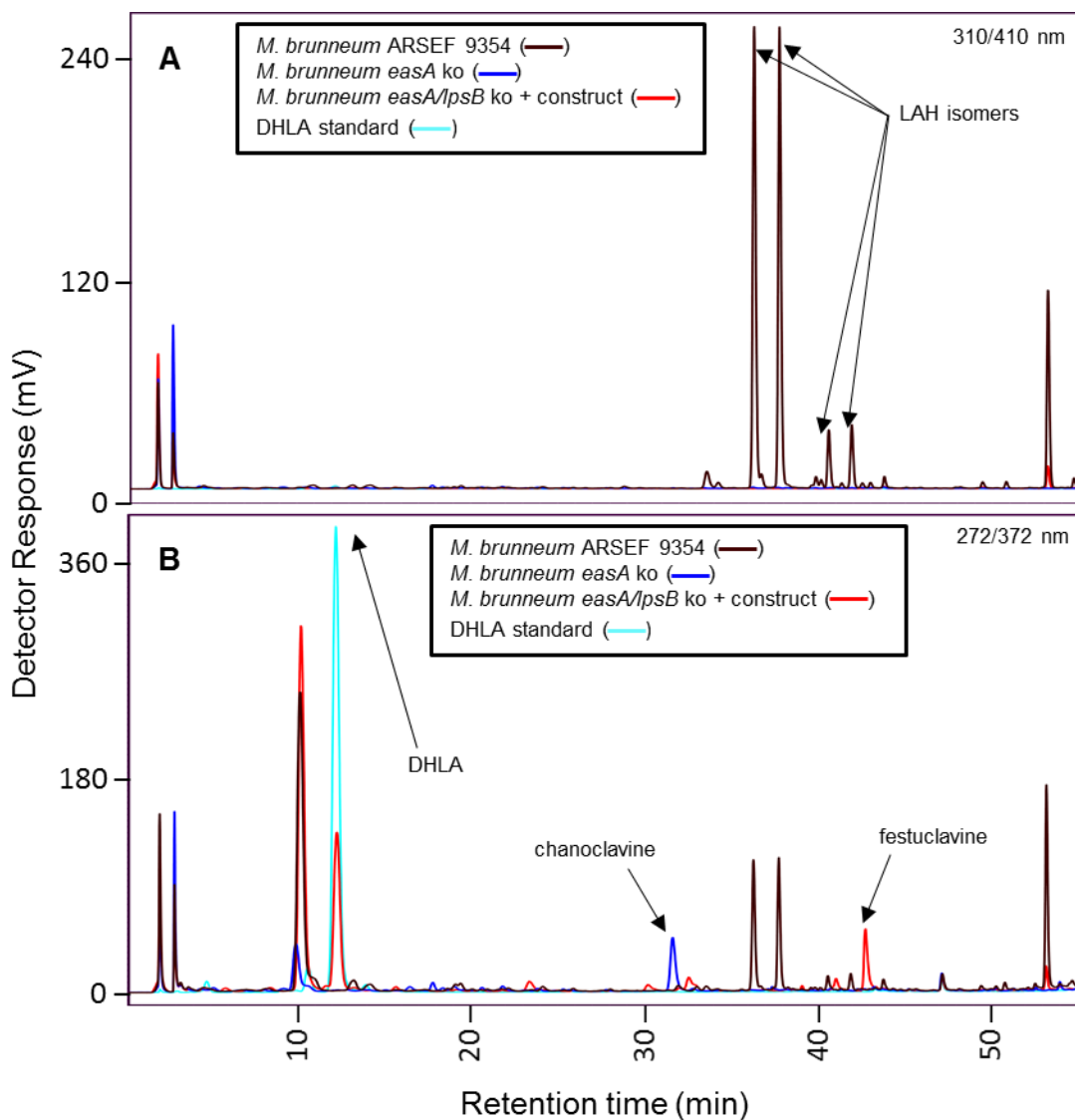


Fig 8. HPLC chromatograms of *M. brunneum* mutants compared to wild-type *M. brunneum*, DHLA-producing *N. fumigata* mutant, and DHLA standard. Fluorescence was detected at (A) 410 nm after exciting at 310 nm and (B) at 372 nm after exciting at 272 nm. LAH, lysergic acid α -hydroxyethylamide.

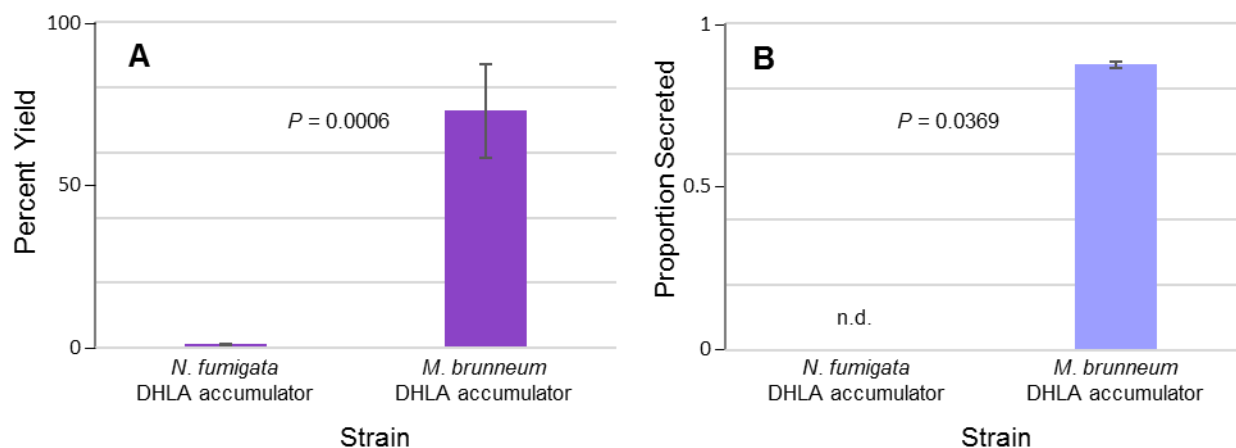


Fig 9. Percent yield and secretion of DHLA in *N. fumigata* mutant compared to *M. brunneum* mutant. (A) Mean percent yield DHLA relative to precursor festuclavine between strains. (B) Average proportion of DHLA secreted into growth medium by strains. Standard error of mean for both sets is shown by the error bars. P value from ANOVA is shown between bars in panel (A), whereas the P value for panel (B) was derived from a Wilcoxon rank-sum test because DHLA was not detected in *N. fumigata* culture filtrates. n.d., not detected.

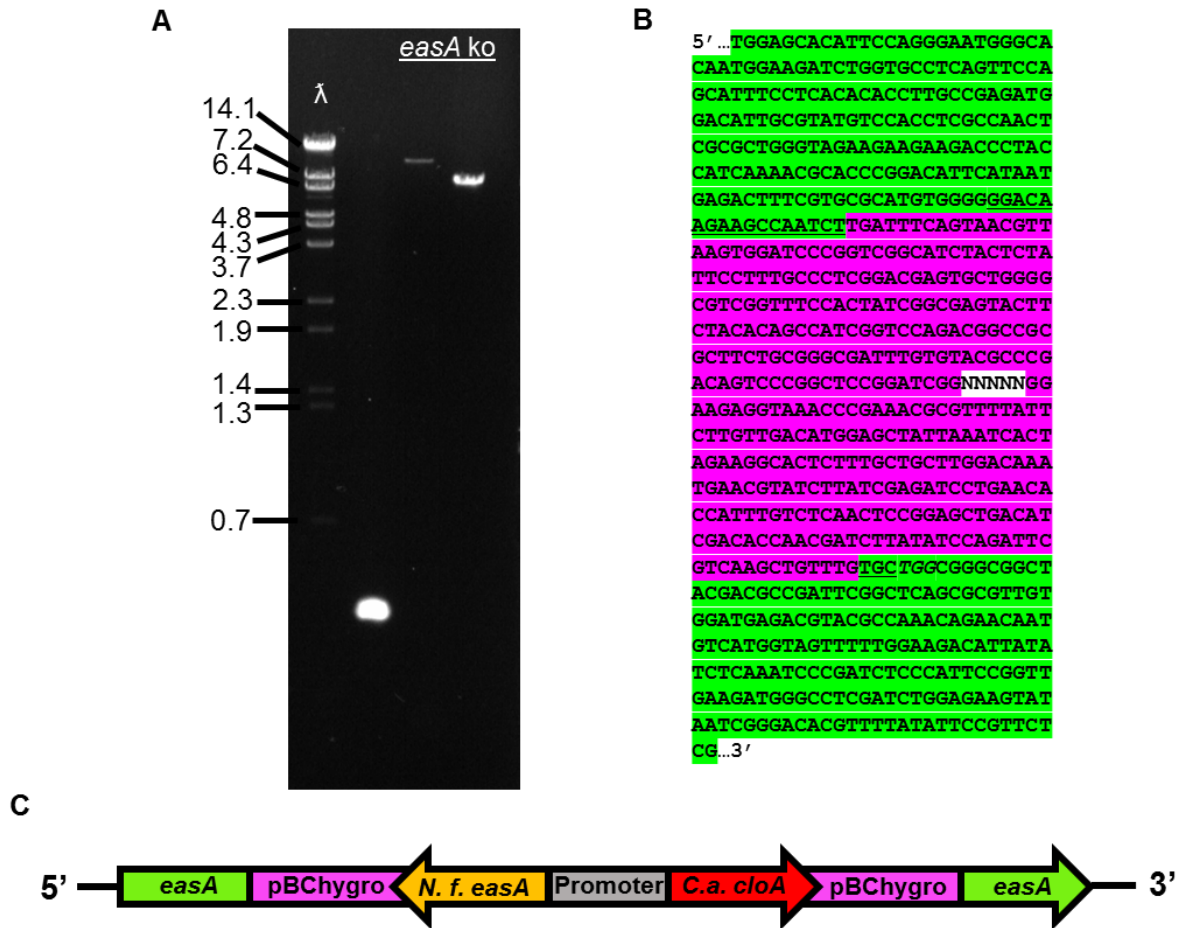


Fig 10. PCR analysis of *M. brunneum easA* locus following gene knockout and transformation with dihydro expression construct. (A) Products from primer combinations 8, 9, or 10 (Table 1) and genomic DNA isolated from wild type (wt) and dihydroLAH-producing strains (*easA ko*) of *M. brunneum*. Primer combination is listed in each lane below the corresponding strain. Sizes of relevant fragments from *Bst*EII-digested bacteriophage lambda DNA are indicated to the left. Gel was stained with ethidium bromide. (B) DNA sequence of *easA* locus after CRISPR mutagenesis concomitant with introduction of the dihydro construct. Green highlight indicates sequences flanking the site of CRISPR-Cas9 recombination. Pink highlight represents sequence from dihydro expression construct with 11,090 nt omitted (represented by NNNNN) to simplify presentation. Target sequence is underlined, and protospacer-adjacent motif (PAM) is italicized. (C) Graphic displaying the orientation and components integrated into cut sites for this mutant.

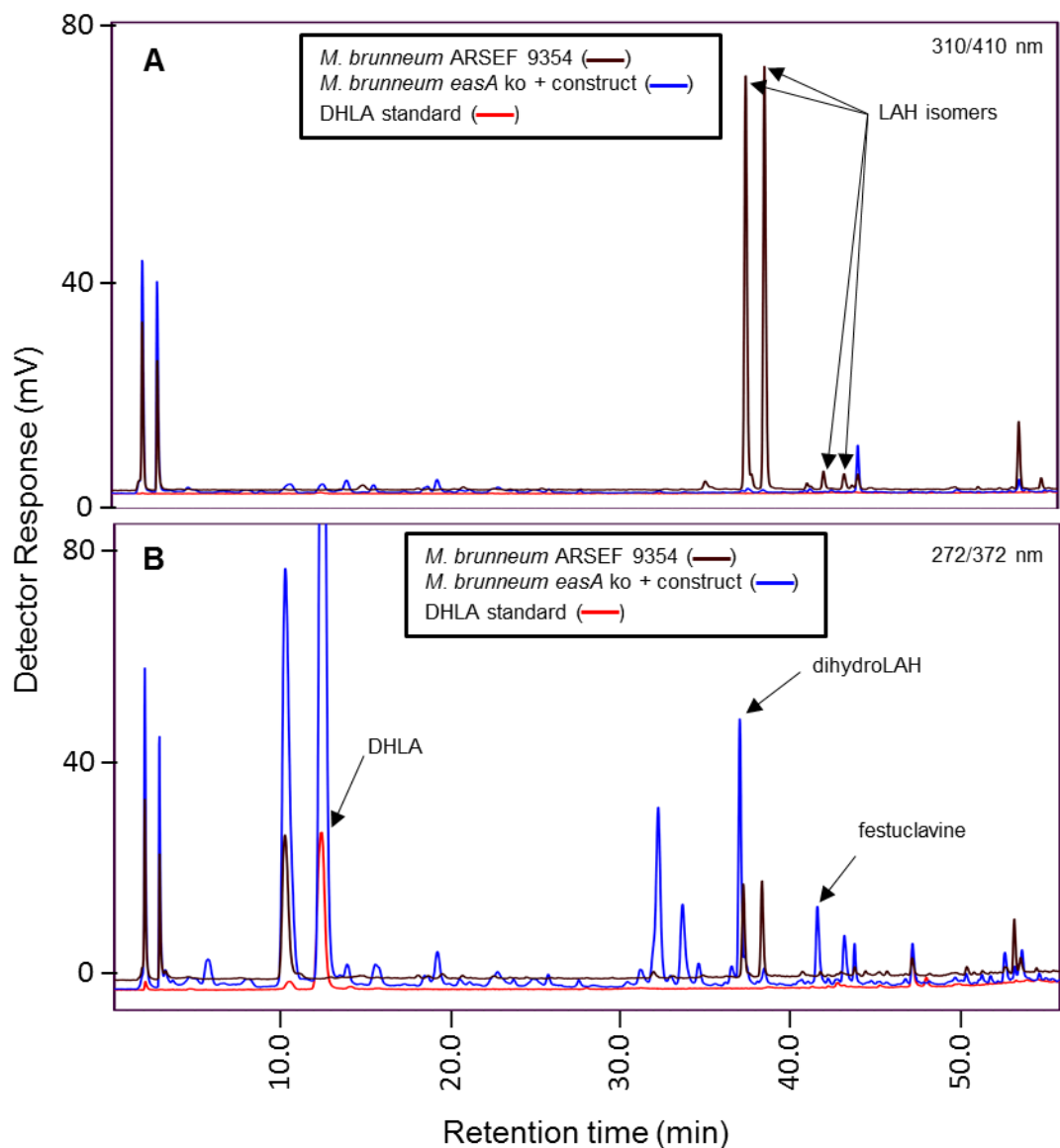


Fig 11. HPLC chromatograms of *M. brunneum* mutant with novel alkaloid compared to parental strains from which it was derived: wild-type *M. brunneum* and *easA* knockout (*easA ko*) of *M. brunneum*. Fluorescence was detected at (A) 410 nm after exciting at 310 nm and (B) at 372 nm after exciting at 272 nm. The wild-type (black line) peaks eluting just later than dihydroLAH correspond to the most abundant LAH isomers (marked in panel A) fluorescing under suboptimal excitation and emission wavelengths. A DHLA standard was also included. LAH, lysergic acid α -hydroxyethylamide; DHLA, dihydrolysergic acid; dihydroLAH, provisional dihydrolysergic acid α -hydroxyethylamide.

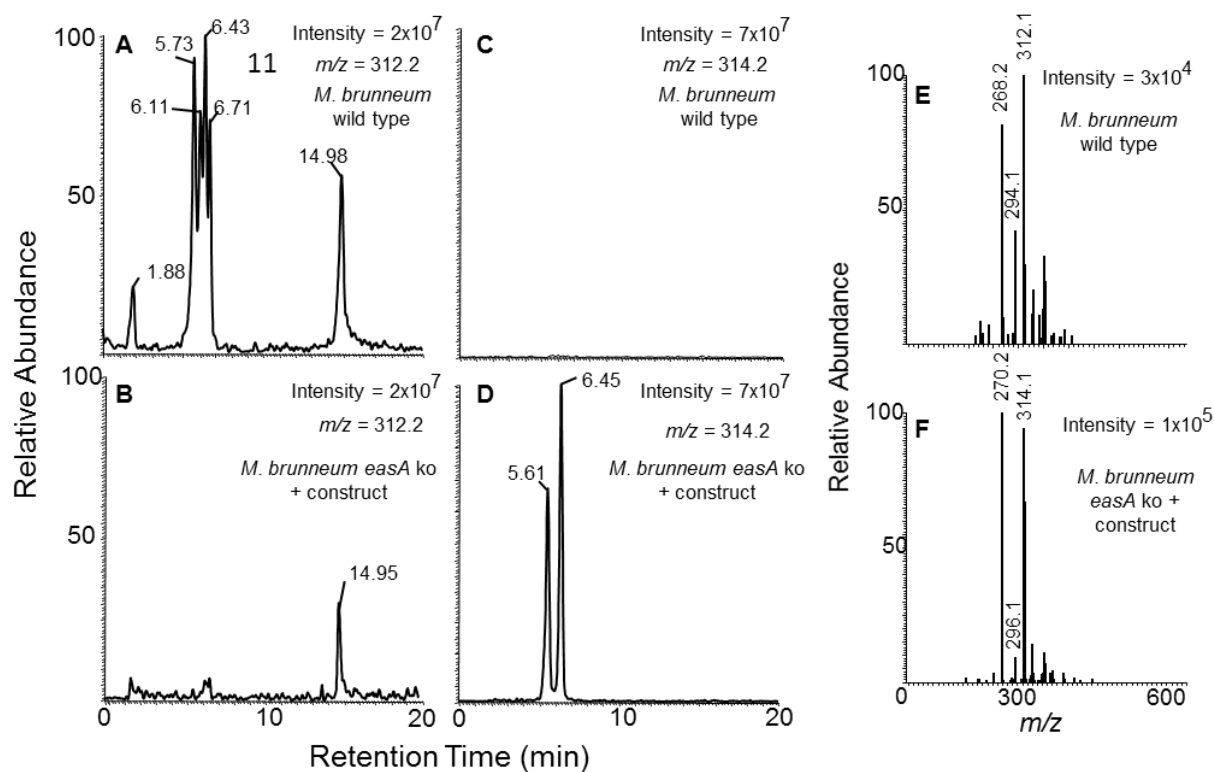


Fig 12. LC-MS analyses of *M. brunneum* mutant with novel alkaloid compared to wild-type *M. brunneum*. (A, C) Extracted ion chromatograms of wild-type *M. brunneum* analyzed at indicated m/z values compared to (B, D) the *easA* knockout strain expressing the dihydro expression construct. (E-F) Fragmentation spectra obtained from parent ions in panels A and D. Instrument resolution accurate to 0.1 Da.

Table 1. Primers and PCR Protocol Information

Primer pair	Primer sequences (5' to 3') ^a	Product (length in base pairs)	Annealing temperature (°C), Extension time
1	GGCAGCTTGGAGTATGTCTG + CCTTGCTTGAGAAGGTTTTGG	Optimized <i>bar</i> with GPDH promoter (1981 bp)	62, 60 s
2	CTCAGCGGCCGCGCACCATGTCAAGAAGTAGC + CCATCTCGGAAAAGAAAATGCGAGAAGAACCGTCCT	<i>N. fumigata easA</i> + overlap with <i>M. brunneum easG/dmaW</i> promoter (1543 bp)	62, 45 s
3	GAGGACGGTTCTTCTCGCATTTTTCTTTCCGAGATGG + GTACAGCCAAAGCTGAGACATCGTAAACCAGAGTATTATG	<i>M. brunneum easG/dmaW</i> promoter + overlaps for <i>N. fumigata easA</i> & synthetic <i>C. africana cloA</i> (1345 bp)	60, 45 s
4	CATAATACTCTGGTTTACGATGTCTCAGCTTTGGCTGTAC + CGTAGTCGACACAGCAAAGTCTGATAAGTG	Synthetic <i>C. africana cloA</i> + overlap with <i>M. brunneum easG/dmaW</i> promoter (1903 bp)	64, 60 s
5	CTCAGCGGCCGCGCACCATGTCAAGAAGTAGC + CGTAGTCGACACAGCAAAGTCTGATAAGTG	<i>N. fumigata easA</i> – <i>M. brunneum easG/dmaW</i> promoter – synthetic <i>C. africana cloA</i> fusion product (4713 bp)	70, 150 s

6	CCGCGCACCATGTCAAGAAG + CGAGGTCGACACAGCAAAGTC	<i>N. fumigata easA</i> – Promoter – <i>C. africana cloA</i> in pBChygro (4705 bp)	66, 150 s
7	GAGCAACAAGGAGCGTCAATG + GCTTATCGCTTGGCCAAGAG	<i>M. brunneum lpsB</i> internal sequence flanking CRISPR cut-site (425 bp) ^b	65, 30 s
8	GTCGGTATGAAGCTGTCCACC + GTATCCCTCGTCCGAGAACG	<i>M. brunneum easA</i> internal sequence flanking CRISPR cut-site (423 bp) ^b	65, 30 s
9	GTCGGTATGAAGCTGTCCACC + CGAGGTCGACACAGCAAAGTC	<i>N. fumigata easA</i> – <i>C. africana cloA</i> – pBChygro construct in <i>easA</i> cut-site (same orientation - 5' side) (variable bp)	65, 150 s
10	CCGCGCACCATGTCAAGAAG + GTATCCCTCGTCCGAGAACG	<i>N. fumigata easA</i> – <i>C. africana cloA</i> – pBChygro construct in <i>easA</i> cut-site (same orientation - 3' side) (variable bp)	64, 150 s
11	GTCGGTATGAAGCTGTCCACC + CCGCGCACCATGTCAAGAAG	<i>N. fumigata easA</i> – <i>C. africana cloA</i> – pBChygro construct in <i>easA</i> cut-site (opposite orientation - 5' side) (no product)	65, 150 s
12	CGAGGTCGACACAGCAAAGTC + GTATCCCTCGTCCGAGAACG	<i>N. fumigata easA</i> – <i>C. africana cloA</i> – pBChygro construct in <i>easA</i> cut-site (opposite orientation - 3' side) (no product)	64, 150 s

^a Underlines indicate unique restriction sites used for cloning fusion PCR product: GTCGAC: *SalI* and GCGGCCGC: *NotI*.

^b Expected product size based on wild-type locus and subject to insertions/deletions following CRISPR.

Table 2. Concentration (μM) of accumulating precursors and pathway end products in engineered strains of *Neosartorya fumigata* (*N.f.*) and *Metarhizium brunneum* (*M.b.*) 10 days post inoculation

Species and pathway end product	Agroclavine	LA ^a	Festuclavine	DHLA ^b	dihydroLAH ^c
<i>N.f.</i> LA	7.76 \pm 1.87	0.19 \pm 0.08	n.d. ^d	n.d.	n.d.
<i>M.b.</i> LA	0.61 \pm 0.06	4.12 \pm 0.54	n.d.	n.d.	n.d.
<i>N.f.</i> DHLA	n.d.	n.d.	4.10 \pm 0.94	0.11 \pm 0.02	n.d.
<i>M.b.</i> DHLA	n.d.	n.d.	0.08 \pm 0.01	0.48 \pm 0.29	n.d.
<i>M.b.</i> dihydroLAH	n.d.	n.d.	n.d.	0.23 \pm 0.09	0.04 \pm 0.01

^alysergic acid

^bdihydrolysergic acid

^cprovisional dihydrolysergic acid α -hydroxyethylamide

^dnot detected

Chapter 3

Two satellite gene clusters enhance ergot alkaloid biosynthesis capacity of *Aspergillus leporis*

Abstract

Ergot alkaloids are fungal specialized metabolites that are important in agriculture and serve as sources of several pharmaceuticals. *Aspergillus leporis* is a soil saprotroph that possesses two ergot alkaloid biosynthetic gene clusters encoding lysergic acid amide production. We identified two additional, partial biosynthetic gene clusters within the *A. leporis* genome containing some of the ergot alkaloid synthesis (*eas*) genes required to make two groups of clavine ergot alkaloids, fumigaclavines and rugulovasines. Clavines possess unique biological properties compared to lysergic acid derivatives. Bioinformatic analyses indicated the fumigaclavine cluster contained functional copies of *easA*, *easG*, *easD*, *easM*, and *easN*. Genes resembling *easQ* and *easH*, which are required for rugulovasin production, were identified in a separate gene cluster. The pathways encoded by these partial, or satellite, clusters would require intermediates from the previously described lysergic acid amide pathway to synthesize a product. Chemical analyses of *A. leporis* cultures revealed the presence of fumigaclavine A. Rugulovasin was only detected in a single sample, however, prompting a heterologous expression approach to confirm functionality of *easQ* and *easH*. An *easA* knockout strain of *Metarhizium brunneum*, which accumulates the rugulovasin precursor chanoclavine-I aldehyde, was chosen as expression host. Strains of *M. brunneum* expressing *easQ* and *easH* from *A. leporis* accumulated rugulovasin as demonstrated through mass spectrometry analysis. These data indicate that *A. leporis* is exceptional among fungi in having the capacity to synthesize products from three branches of the

ergot alkaloid pathway and for utilizing an unusual satellite cluster approach to achieve that outcome.

Introduction

Several different fungi in the Eurotiales and Hypocreales produce specialized metabolites known as ergot alkaloids (Wallwey and Li 2011, Florea et al. 2017, Tasker and Wipf 2021, Robinson and Panaccione 2015) (Fig. 1). These fungi occupy a wide variety of niches including soil saprophytes, entomopathogens, and plant endophytes and parasites (Gerhards et al. 2014, Schardl et al. 2006, Young et al. 2015, Leadmon et al. 2020, Panaccione 2023). Ergot alkaloids have historically been associated with negative impacts on humans and other animals due to their potent toxicity and ability to cause convulsive and gangrenous symptoms when ingested (Haarmann et al. 2009). Exposure to some ergot alkaloids can cause psychotropic and narcotic effects, a property that has been used by both Native American cultures and, in more recent history, recreational drug users (Schultes and Hofmann 1973, Hofmann 1980). The ability of these compounds to exhibit a wide array of pharmacological activities is due to their similarity to neurotransmitters and high binding affinity for several neurological receptors, including dopamine, adreno, and 5-hydroxytryptamine receptors (Pertz and Eich 1999, Eich et al. 1985). The activities of clavine-derived ergot alkaloids (Fig. 1) are less understood compared to those of ergopeptines and lysergic acid amides, though some have been shown to possess anticancer, antimicrobial, anti-inflammatory, and insecticidal activities (Eich et al. 1985, Wu et al. 2005, McCabe and Wipf 2016).

Ergot alkaloids are a complex family of chemicals originating from a shared pathway (Fig. 1) that branches at different points depending on the combination of accessory ergot alkaloid synthesis (*eas*) genes present in a particular organism's biosynthetic gene cluster (Panaccione 2023, Tudzynski et al. 1999, Coyle and Panaccione 2005, Unsöld and Li 2005, Schardl et al. 2013, Tsai et al. 1995). Synthesis of chanoclavine-I aldehyde, the common

intermediate shared among several major branches of the ergot alkaloid pathway, requires a set of five shared *eas* genes (*dmaW*, *easF*, *easE*, *easC*, and *easD*). The products of *dmaW* and *easF* prenylate tryptophan at position 4 (Tsai et al. 1995) and methylate the amino group (Rigbers and Li 2008), respectively, before decarboxylative closure of the third ring is carried out by the products of *easE* and *easC*, together generating the simplest clavine—chanoclavine-I (Lorenz et al. 2010, Goetz et al. 2011, Yao et al. 2021). The product of *easD* then oxidizes the primary alcohol of chanoclavine-I to an aldehyde (Wallwey et al. 2010a), generating chanoclavine-I aldehyde, which serves as a major branchpoint for several other ergot alkaloid pathways. Branches to most major classes of ergot alkaloids depend on whether the reductase or isomerase allele of *easA* is present in an organism (Cheng et al. 2010a, Cheng et al. 2010b, Coyle et al. 2010, Wallwey et al. 2010b). The isomerase and reductase products of *easA* catalyze closure of the ergoline D ring before reduction via the product of *easG* occurs, generating either festuclavine or agroclavine, respectively (Wallwey et al. 2010b, Matuschek et al. 2011). Production of lysergic acid amides, such as lysergic acid α -hydroxyethylamide (LAH), is then dependent upon the presence of other tailoring enzymes in an organism's *eas* cluster (Haarmann et al. 2006, Robinson and Panaccione 2014, Bragg et al. 2017, Arnold and Panaccione 2017, Steen et al. 2021, Davis et al. 2020, Correia et al. 2003, Ortel and Keller 2009). Ergopeptides consist of a tripeptide chain linked to D-lysergic acid and are synthesized by the combination of two nonribosomal peptide synthetases (LPS1 and LPS2) together with the Fe²⁺/2-ketoglutarate-dependent dioxygenase encoded by *easH* found in *Claviceps purpurea* (Havemann et al. 2014). EasH is responsible for hydroxylating the α -carbon of the amino acid adjacent to D-lysergic acid, driving cyclolization of the α -carbon with the terminal lactam carbonyl group generated by LPS1/LPS2 (Havemann et al. 2014).

The clavine branches of the ergot alkaloid pathway include those ending in production of fumigaclavines, cycloclavine, and rugulovasines. Production of fumigaclavines A, B, and C in *Aspergillus fumigatus* (synonym *Neosartorya fumigata*) involves the activities of EasM, EasN, and EasL acting on festuclavine in the absence of a CloA allele (Bilovol and Panaccione 2016, Liu et al. 2009, Unsöld and Li 2006). Fumigaclavine C has anti-inflammatory, antitumor, and anti-atherogenic properties, highlighting the potential for clavine-derived medicines (Wu et al. 2005, Zhao et al. 2010, Li et al. 2013, Du et al. 2011). Cycloclavine, originally isolated from seeds of *Ipomoea hildebrandtii* (Stauffacher et al. 1969) and later the fungus *Aspergillus japonicus* (Furuta et al. 1982), possesses insecticidal and anti-parasite activities (Körber et al. 2014). Cycloclavine production in *A. japonicus* is dependent upon a version of the dioxygenase EasH that, together with the reductase version of EasA and EasG, catalyzes the formation of a cyclopropyl ring moiety attached to the clavine ring system (Jakubczyk et al. 2015, Jakubczyk et al. 2016). The *A. japonicus* version of EasH has also been shown to possess the ability to catalyze the asymmetric hydroxylation of other clavines, such as festuclavine and elymoclavine, a result that displays the promiscuity of this enzyme (An et al. 2022). Rugulovasines A and B, originally isolated from several *Penicillium* species including *P. bifforme* (Abe et al. 1969, Dorner et al. 1980), are a stereoisomeric pair of clavines with toxic and hypotensive properties (Nagaoka et al. 1972). Rugulovasine biosynthesis branches from the ergot alkaloid pathway at chanoclavine-I aldehyde and relies upon *easQ*, encoding an aldehyde dehydrogenase, and a version of EasH hypothesized to hydroxylate the same carbon oxidized by EasH from *A. japonicus* during cycloclavine synthesis (Fabian et al. 2018).

Jones et al. (2021) identified two *eas* clusters associated with accumulation of the lysergic acid amide LAH in *Aspergillus leporis*, a member of *Aspergillus* section Flavi originally

isolated from jackrabbit dung (States and Christensen 1966). *Aspergillus leporis* also is capable of infecting the model lepidopteran insect *Galleria mellonella* and produces relatively high concentrations of LAH during infection (Jones et al. 2023). Phylogenetic studies indicated the eight genes required for synthesis of lysergic acid in *A. leporis* were orthologous to those of the ergot alkaloid producers of the fungal family Clavicipitaceae, but the genes required to put lysergic acid into LAH evolved independently in *A. leporis* and two other species of *Aspergillus* compared to those of the Clavicipitaceae (Jones et al. 2021). Further analysis of the genome of *A. leporis* has led us to two additional clusters of genes: one containing homologs of some of the genes required for synthesis of fumigaclavines in *A. fumigatus*, and the other containing two genes associated with rugulovasine biosynthesis in *P. biforme*. The objectives of this present study were to characterize these gene clusters and more fully investigate the ergot alkaloid biosynthesis capacity of *A. leporis*.

Results

Investigation of two partial, clavine-type *eas* clusters in *Aspergillus leporis*. Through investigation into alleles of *easA*, *easD*, and *easG* that were observed in *A. leporis* but not associated with the two lysergic acid amide gene clusters described by Jones et al. (), we identified a third *eas* cluster containing these three alleles and several other genes associated with fumigaclavine production (Fig. 2A). The *A. leporis* contig ([SWBU01000167.1](#)) containing homologs of *easA*, *easD*, and *easG* was also found to contain apparently intact copies of *easM* and *easN* along with a copy of *easL* that appeared to be a pseudogene due to a 1990-bp insertion (nucleotides 93,081 to 95,071 of this contig), two deletions, and multiple nonsense mutations (Fig. 3). The cluster also contains a copy of a gene called *easK* which is found in the *eas* cluster

of *A. fumigatus* but not in the fumigaclavine-associated *eas* cluster of *P. commune* (Wallwey and Li 2011). No role for the product of *easK* has been found or proposed, and the copy in the *A. leporis* cluster appears to be a pseudogene due to the presence of several nonsense mutations. Accumulation of fumigaclavine A should occur if the copies of *easA*, *easD*, *easG*, *easM*, and *easN* present in this cluster are functional and active at the same time as products of *dmaW*, *easF*, *easE*, and *easC* from one of the lysergic acid amide clusters of *A. leporis*.

The area upstream of the fumigaclavine cluster was analyzed in three increments of 5000 bp at a time by BLASTx before it was concluded that no other *eas* genes were present nearby. The remaining 3251 bp of the contig following the *easA* termination codon were also analyzed by BLASTx and did not possess additional *eas* genes. The area flanking this cluster was found to contain elements related to transposon activity with putative products resembling a transposase ([XP_013329072.1](#)), a pogo transposable element ([RJE23005.1](#)), and a reverse transcriptase ([XP_001395701.2](#)) having been identified nearby. Apart from the copies previously characterized in the lysergic acid amide synthesis clusters of *A. leporis* (Jones et al. 2021), no additional copies of *dmaW*, *easF*, *easE*, or *easC* (which would encode the steps preceding those predicted in the fumigaclavine cluster) meeting minimum criteria of 30% amino acid sequence identity and 70% query coverage could be found within the genome. This observation indicates the fumigaclavine cluster is isolated from, and devoid of, other *eas* genes.

The discovery of a partial fumigaclavine cluster in *A. leporis* prompted additional genome mining for other potential *eas* genes. Through this approach, a copy of *easH* encoding a product with 61% identity to EasH encoded by the *P. camemberti* allele of that gene was identified (Fig. 2B). Another gene, encoding an aldehyde dehydrogenase, was found ~2 kb away and encodes a product with 75% identity with the product of the *P. camemberti* allele of *easQ*.

The genomic context of the *A. leporis easQ* and *easH* homologs was investigated by searching the areas upstream and downstream to test for other potential *eas* genes. Increments of 5000 bp at a time were analyzed by BLASTx, with the process being repeated a total of three times in both directions. Putative genes encoding a metalloprotease ([KAB8075085.1](#)), major facilitator transporter ([KAE8380494.1](#)), NADH-ubiquinone oxidoreductase ([XP_033419163.1](#)), RNA-directed DNA polymerase ([GFF18983.1](#)), kinesin ([KAB8075089.1](#)), and cytochrome P450 oxidoreductase ([RAQ58036.1](#)) were identified nearby. No other *eas* genes were detected, however, indicating that this partial cluster of *easQ* and *easH* is isolated from other genes needed for ergot alkaloid production.

Fumigaclavine A accumulation in *A. leporis* NRRL 3216. Solid (combination of hyphae, conidiophores, and conidia) and liquid (culture fluids) phases of independent cultures of *A. leporis* NRRL 3216 grown in sucrose-yeast extract medium for 14 days accumulated fumigaclavine A (Fig. 4). Extracts from both phases were analyzed by high-performance liquid chromatography (HPLC) with fluorescence detection and compared to a fumigaclavine A standard of known concentration. A peak eluting at 43.8 min matched the peak representing the fumigaclavine A standard in retention time and fluorescence properties. Percent secretion of fumigaclavine A was calculated from eight technical replicates analyzed by HPLC and found to have a mean of 35 (range 9 to 57, median 35), which is approximately three-fold higher than the secretion of fumigaclavine A observed in *A. fumigatus* (Mulinti et al. 2014). Extracts from the solid phase of the cultures were analyzed by liquid chromatography-high resolution mass spectrometry (LC-HRMS) and compared to a fumigaclavine A standard. An analyte of $m/z = 299.1747$ with a single peak occurring at 5.29 min was detected (Fig. 5A), which lines up with

the peak corresponding to the fumigaclavine A standard occurring at 5.33 min (Fig. 5B).

Fragmentation analyses of the m/z 299.1747 analytes revealed matching spectra (Fig. 5C-D).

A strain of *A. leporis* that had been previously modified to disrupt the sole functional copy of *easD* present in the LAH-associated *eas* clusters (Jones et al. 2023) was grown and analyzed alongside the wild type to test whether the availability of increased chanoclavine-I would result in increased accumulation of fumigaclavine A. The *easD* knockout strain of *A. leporis* accumulated significantly more chanoclavine-I ($P = 0.0073$) and fumigaclavine A ($P = 0.0014$) than did wild-type *A. leporis* (Table 1). The rate of conversion of chanoclavine-I to fumigaclavine A did not differ significantly between the two strains ($P = 0.659$), suggesting the observed increase in fumigaclavine A resulted from the availability of additional chanoclavine-I in the *easD* knockout. This observation supports the hypothesis that the fumigaclavine cluster is fed chanoclavine-I intermediate derived from the lysergic acid amide cluster and thus can be considered a satellite cluster relative to the lysergic acid amide cluster. The relative timing of accumulation of LAH and fumigaclavine A is relevant in this context. LAH accumulation peaks sharply at six days, then declines markedly by day 12 under the conditions used (Jones et al. 2021) (Fig. 6). Fumigaclavine A accumulation increased gradually over time, reaching a maximum at 15 days post-inoculation before declining gradually (Fig. 6). Chanoclavine-I, which is a required intermediate in both LAH and fumigaclavine pathways, reached maximum concentration in the six-to-nine-day range and then declined only slightly over the remainder of the three-week culture period. Any chanoclavine-I not converted to LAH during what is typically the optimal period of LAH accumulation in the wild type was then likely available to the enzymes of the fumigaclavine pathway during peak production of that metabolite. The difference in timing of the two pathways also provides a plausible explanation for why the copy of *EasD*

encoded in the fumigaclavine pathway was not observed to complement the *easD* mutation in the LAH pathway (Jones et al. 2023).

Rare rugulovasine accumulation in *A. leporis* NRRL 3216 under conditions that favor ergot

alkaloid accumulation. Rugulovasine A spontaneously stereoisomerizes over time to rugulovasine B; the two stereoisomers then readily interconvert (Rebek et al. 1984). The LC-HRMS approach we used does not allow distinction of the two stereoisomers, so we will refer to the observed analyte demonstrating properties of rugulovasines A/B as simply rugulovasine from here on. Cultures of *P. biforme* NRRL 885 were grown on malt extract agar for 7 days to provide a reference analyte for rugulovasine. Samples were analyzed by LC-HRMS and found to accumulate the m/z 269.1278 ion typical of rugulovasine with a single peak occurring at 5.91 min (Fig. 7A). Cultures of *A. leporis* NRRL 3216 were grown under similar conditions, and among a total of 26 samples ranging in age from 3 to 18 days (including 14 in the 12-day to 18-day range), only one culture at 14 days old was found to accumulate an analyte corresponding to rugulovasine (m/z 269.1278, eluting at 5.88 min) (Fig. 7B). Fragmentation analyses of the parent ions from *P. biforme* and *A. leporis* extracts revealed matching spectra, indicating *A. leporis* is capable of rugulovasine production (Fig. 8). Larvae of *G. mellonella* were inoculated with *A. leporis* to test if insect infection would more consistently elicit rugulovasine production. Extracts from 8-day post-infection larvae were analyzed by LC-HRMS and were found to lack rugulovasine. Extracted ion chromatograms for m/z 269.1278 from *A. leporis* cultures as well as larvae infected with *A. leporis* displayed peaks eluting at approximately 4.99 min and 5.35 min (Fig. 7C-D). The identities of the m/z 269.1278 peaks occurring in panels B-D of Fig. 7 were confirmed to be lysergic acid and its stereoisomer by comparison to the lysergic acid previously documented to accumulate in *G. mellonella* larvae infected with a *lpsB* knockout of *M.*

brunneum (Fig. 7E) (Davis et al. 2020). The lysergic acid stereoisomers appeared in this extracted ion chromatogram because lysergic acid has the same molecular formula as rugulovasine. Fragmentation analyses of the parent ions corresponding to these earlier-eluting m/z 269.1278 ion peaks further confirmed their identity as diastereoisomeric lysergic acid and isolysergic acid (Fig. 9).

Phylogenetics of *A. leporis easQ* and *easH* associate them with ergot alkaloid synthesis

versions of these genes. Since rugulovasines were only detected in single *A. leporis* sample, we examined the versions of EasQ and EasH encoded in the *A. leporis* gene cluster more closely. We conducted phylogenetic analysis of the predicted EasQ along with homologs from *P. biforme* and *P. camemberti eas* clusters as well as non-*eas* cluster homologs found in *A. leporis*, *P. biforme*, *P. camemberti*, *A. fumigatus*, and *M. brunneum*. Homologs were defined as having >30% amino acid sequence identity and 70% query coverage with the version of EasQ encoded in that organism's *eas* cluster. The results showed that the version of EasQ encoded from the allele in the *easQ/easH* satellite cluster of *A. leporis* formed a clade with those encoded within the *P. biforme/P. camemberti* rugulovasine *eas* gene clusters (Fig. 10), though bootstrap support for this clade was marginal. Two non-*eas* cluster homologs of EasQ encoded elsewhere in the *A. leporis* genome met the criteria for inclusion in this data set and were found to form distinct clades with their orthologous, non-*eas* cluster counterparts in the other species.

Phylogenetic analysis of the predicted *A. leporis* EasH protein sequence compared to homologs from rugulovasine, cycloclavine, and ergopeptine producers showed that the version of EasH encoded in the *A. leporis* satellite cluster forms a clade with EasH encoded in *eas* clusters from rugulovasine producers (Fig. 11). Additionally, these phylogenetic data show

strong bootstrap support for the EasH versions required for rugulovasine, cycloclavine, and ergopeptine production having diverged from a recent common ancestor.

Rugulovasine production by heterologous expression of *easQ* and *easH* from *A. leporis* in *M. brunneum*. To more thoroughly test the ability of *easQ* and *easH* from *A. leporis* to catalyze formation of rugulovasine, both genes were placed under the control of the bi-directional *easG/dmaW* promoter of *M. brunneum* and transformed into an *easA* knockout strain of *M. brunneum* (Davis et al. 2020). Fusion PCR was used to generate the expression construct which was then introduced into *M. brunneum* as part of a construct based on pBChygro, a selectable marker conferring hygromycin resistance (Silar 1995). Presence of the fusion construct and hygromycin resistance gene was confirmed through PCR (Fig. 12). The strain of *M. brunneum* expressing *A. leporis easQ* and *easH* genes was analyzed by LC-HRMS and compared to the *easA* knockout background strain and wild-type *P. biforme*, a natural rugulovasine producer, for reference (Dorner et al. 1980). There was no evidence of rugulovasine in the background, *easA* knockout strain of *M. brunneum* (Fig. 13A). The *M. brunneum* strain expressing both *A. leporis* genes was found to produce an analyte of $m/z = 269.1278$ with a single peak that aligns with the peak corresponding to rugulovasine in *P. biforme* (Fig. 13B-C). Fragmentation analyses of the m/z 269.1278 analyte from the *M. brunneum* mutant revealed a spectrum consistent with that of rugulovasine from *P. biforme* (Fig. 13D-E).

Lack of cycloclavine production upon expression of *easH* from *A. leporis* in a mutant strain of *A. fumigatus*. Since versions of EasH involved in cycloclavine synthesis (Jakubczyk et al. 2016, An et al. 2022) oxidize the same carbon likely to be oxidized by the version of EasH involved in rugulovasine synthesis (Fabian et al. 2018), we tested the ability of EasH from *A. leporis*, in conjunction with the products of the required early pathway genes from *A. fumigatus*,

to catalyze formation of cycloclavine. In this study, *easH* from *A. leporis* was placed under the control of the *A. fumigatus easA* promoter and expressed in an *easM* knockout strain of *A. fumigatus* (Bilovol and Panaccione 2016). Fusion PCR was used to generate this construct which was then introduced into *A. fumigatus* as part of a construct prepared in pBCphleo (Silar 1995). Presence of the fusion construct and phleomycin resistance gene were confirmed through PCR (Fig. 12). The strain of *A. fumigatus* expressing *A. leporis easH* was analyzed by LC-MS and compared to the *easM* knockout strain of *A. fumigatus* and wild-type *A. japonicus* Saito NRRL 360, a documented cycloclavine producer (Furuta et al. 1982), for reference. An analyte of *m/z* 239.1, corresponding to cycloclavine (as confirmed by LC-HRMS, Fig. 14), was detected in extracts of *A. japonicus*, but no corresponding metabolite was detected in any of the *A. fumigatus* colonies expressing *easH* from *A. leporis* (Fig. 14). Reverse transcription-polymerase chain reaction (RT-PCR) analyses of triplicate malt extract cultures of this mutant demonstrated the presence of *easH* mRNA (Fig. 15), indicating that failure to generate cycloclavine was not due to lack of *easH* expression.

Discussion

Our data show that *A. leporis* is an unusual species of ergot alkaloid producing fungus as it possesses two partial gene clusters encoding some of the genes necessary for fumigaclavine A and rugulovasine production, in addition to two gene clusters encoding for LAH biosynthesis (one of which is complete, and the other lacks a functional copy of *easD*; Jones et al. 2021). We hypothesize the fumigaclavine and rugulovasine clusters act as satellite clusters of the LAH cluster because they lack steps required for production of early steps, thus requiring intermediates chanoclavine-I or chanoclavine-I aldehyde from one of two previously

characterized LAH gene clusters (Jones et al. 2021). We identified fumigaclavine A in extracts of *A. leporis*, with 65% of the total amount accumulating being retained within the hyphae and/or conidiophores and conidia. An *easD* knockout strain of *A. leporis* (Jones et al. 2023) was found to accumulate fumigaclavine A at more than three times the rate of the wild-type fungus. This result is consistent with the reliance of this pathway on intermediates from the LAH pathway and the observed activation of this satellite pathway at a later point in time relative to LAH accumulation.

We were only able to detect rugulovasine accumulation in a single sample of *A. leporis*, prompting the need to better test functionality of *easQ* and *easH*. Heterologous expression of these genes in an *easA* knockout strain of *M. brunneum* resulted in reliable rugulovasine accumulation in the engineered mutants. This result indicates that the products of *easQ* and *easH* from the satellite cluster are functional and encode the capacity to convert chanoclavine-I aldehyde to rugulovasine. The rarity with which we detected rugulovasine in cultures of *A. leporis* suggests the fungus requires some specific nutritional or environmental conditions to accumulate rugulovasine. Determination of these conditions is beyond the scope of this present study but one factor that may have varied tube-to-tube was gas exchange, since tubes were covered with loosely closed screw caps. The *A. fumigatus* mutant expressing *A. leporis easH* alone failed to produce cycloclavine, indicating specialization among versions of EasH from different pathway branches.

Aspergillus leporis is the only fungus known to possess at least four biosynthetic gene clusters encoding three different branches of the ergot alkaloid pathway. Two of these branches requiring activity of the main branch for early pathway steps. These findings are significant as they support the idea that different offshoots of the ergot alkaloid pathway have evolved to shunt

products into various pathway branches depending on specific environmental conditions. While *A. leporis* is unique among ergot alkaloid producers for possessing multiple satellite gene clusters for core pathway modifications, other fungi have also been found to utilize some discontinuous genetic loci to complete or modify specialized metabolites. Biosynthesis of different trichothecenes in *Fusarium* species is encoded by a set of up to 12 *Tri* genes clustered on chromosome 2 (Brown et al. 2004). A two-gene satellite cluster has been identified on chromosome 1 (Peplow et al. 2003, Gale et al. 2005) while at least two other single-gene satellites have been found elsewhere in the genome (Kimura et al. 1998, Alexander et al. 2004, Merhej et al. 2011). Aspercryptin biosynthesis in *Aspergillus nidulans* relies on the combinatorial action of two different biosynthetic gene clusters (Chiang et al. 2016). The utilization of satellite gene clusters for specialized metabolite biosynthesis has also been characterized in plants, as is seen with α -tomatine in tomato (Itkin et al. 2013), cucurbitacins in cucumber (Shang et al. 2014), and morphine in opium poppy (Guo et al. 2018). Our results provide further evidence that fungi may increase the diversity of their specialized metabolites through multiple, related biosynthetic gene clusters. Potential products of physically separated gene clusters should be considered when taking approaches to mine fungal genomes for novel specialized metabolites or when modifying characterized clusters in mutant strains.

Fumigaclavine A was the fumigaclavine we detected in *A. leporis*, but the genome of the fungus indicates it, or a recent ancestor, once had the capacity to synthesize fumigaclavine C. The final step of fumigaclavine C production in *Aspergillus* species is controlled by the reverse prenyltransferase gene *easL*, or *fgaPT1* (Unsöld and Li 2006). This step is absent from *Penicillium* species that produce fumigaclavines, resulting in cessation of the pathway at fumigaclavine A (Martín et al. 2017). Previous studies of *Penicillium commune* have shown that

this species produces fumigaclavine A as a pathway end product due to lack of *easL* (Unsöld 2006, Vinokurova et al. 2003). Here, we show that *A. leporis* also accumulates fumigaclavine A (as opposed to fumigaclavine C) due to inactivation of *easL* by an insertion that alters the reading frame and prevents its product from being translated correctly. Interestingly, the same set of genes is also found in *Penicillium roqueforti*, which produces isofumigaclavines A and B (stereoisomers of fumigaclavines A and B), but the genes are split into two clusters encoded by separate areas of the genome (Fernández-Bodega et al. 2017).

Cycloclavine is an uncommon ergot alkaloid found only in a few species of fungi that possess a specific version of EasH (Jakubczyk et al. 2015, Jakubczyk et al. 2016). Our phylogenetic data indicate that the EasH responsible for cycloclavine production shares a common ancestor with the versions required for rugulovasine production and those involved in ergopeptine biosynthesis. While we demonstrated the ability of *A. leporis* EasH (together with EasQ) to catalyze rugulovasine production, it was unable to catalyze formation of cycloclavine when engineered alone in an appropriate mutant background in *A. fumigatus*. This result indicates that a degree of specialization exists among the different versions of EasH. Investigations into any differences in their crystal structures as well as their substrate-binding specificity may provide clues regarding differences in their mechanisms.

Evolutionary data across fungal species suggest that the ancestor to all ergot alkaloid producers may have been related to extant *Aspergillus* species and that neofunctionalization of *easH* coupled with entire cluster duplications played an important role in ergot alkaloid diversification (Florea et al. 2017). Our results show that *A. leporis* retains the capacity for production of two clavine branches of the pathway that rely on obtaining an intermediate from one or both of the duplicated gene clusters encoding lysergic acid amide production. Jones et al.

(2021) previously proposed that genes encoding the final three steps of the LAH pathway in *A. leporis* evolved independently from those catalyzing similar steps in the Clavicipitaceae and that lysergic acid amides provide an advantage to *A. leporis* during infection of a model insect (Jones et al. 2023). The persistence of multiple ergot alkaloid synthesis clusters suggests that a variety of ergot alkaloids confers a benefit to the fungus, perhaps depending on the environment the fungus finds itself in. Further studies into the ecology of the fungus may provide clues as to the nature of these specific benefits.

Materials and Methods

Identification of novel *A. leporis* eas clusters. The variants of EasD ([KAB8071224.1](#)), EasA ([KAB8071228.1](#)) and EasG ([KAB8071227.1](#)) noted by Jones et al. (2021) as encoded by homologs not associated with either of the two characterized LAH-associated gene clusters were analyzed by tBLASTn against the whole-genome shotgun database for *A. leporis*. The single contig that each of these genes was found to originate from (GenBank accession number [SWBU01000167.1](#)) was downloaded and annotated for *easD*, *easG*, and *easA*. The areas adjacent to these genes were analyzed in 5-kb fragments by BLASTx to determine presence of other potential ergot alkaloid genes. Copies of genes with products resembling EasM and EasN were noted along with copies of *easL* and *easK* that appear to be pseudogenes. The areas flanking this cluster of *eas* genes were searched in successive 5 kb fragments three times in either direction before it was concluded no other *eas* genes were present nearby.

Penicillium biforme EasH was analyzed by tBLASTn against the whole-genome shotgun database for *Aspergillus* species. From the returned matches, *A. leporis* was chosen for further analysis. The matching contig (GenBank accession number [SWBU01000070.1](#)) was downloaded

and annotated as described above, revealing the presence of a homolog of *easQ* adjacent to *easH*. The areas adjacent to these genes were analyzed in successive 5-kb fragments by BLASTx to investigate the presence of other potential ergot alkaloid genes. The process was repeated three times in either direction before we concluded no other ergot alkaloid synthesis genes were detected.

Growth and maintenance of fungi. Cultures of *A. leporis* NRRL 3216 and an *easD* knockout of *A. leporis* (Jones et al. 2023) were maintained on sucrose-yeast extract agar medium (per liter, 20 g sucrose, 10 g yeast extract, 1 g magnesium sulfate-heptahydrate, and 15 g agar). Cultures were grown at 30°C for at least 7 days before testing for ergot alkaloids. Cultures of *M. brunneum* ARSEF 9354 and its mutant derivatives were maintained on sucrose-yeast extract agar medium and were grown for at least 10 days prior to collecting conidia for injection into *G. mellonella* larvae. Cultures of the previously engineered *easM* knockout strain of *A. fumigatus* (Bilovol and Panaccione 2016) were maintained at 37°C on malt extract agar medium (per liter, 6.0 g malt extract, 1.8 g maltose, 6.0 g dextrose, 1.2 g yeast extract, and 15 g agar) and were grown for at least 7 days before testing for ergot alkaloids.

Sample preparation for alkaloid analyses. To measure the number of moles of fumigaclavine A retained in the hyphae compared to the quantity secreted into the medium liquid, eight cultures of *A. leporis* NRRL 3216 were grown, prepared and harvested as described by Jones et al. (2021). For the comparison of fumigaclavine A accumulation in wild type versus the *easD* knockout, seven replicate cultures were compared. Replicate cultures were inoculated with a common spore suspension (30,000 conidia/tube) and grown in 0.5 mL of sucrose-yeast extract medium in 2-mL screw cap tubes (part number 02-681-343; Fisher Scientific, Pittsburgh, PA) with the lids slightly ajar to allow gas exchange. For malt extract agar cultures of *P. biforme* NRRL 885 and *A.*

japonicus NRRL 360, alkaloids were extracted from ~400 μ L samples of colonized medium with 400 μ L of methanol. Samples were rotated end-over-end (40 rpm) at room temperature for 1 hr and clarified by centrifugation. The *P. biforme* extract served as reference for rugulovasines as it has been characterized previously as containing these compounds, whereas the *A. japonicus* extract provided a reference for cycloclavine (Furuta et al. 1982, Dorner et al. 1980, Fabian et al. 2018). Extracts from these reference materials were prepared at least two times for each isolate. Mutant cultures of *A. fumigatus* generated during this study were grown on malt extract agar medium for 7 days before the conidiating surface of the entire Petri dish was extracted by repeatedly washing with 2 mL methanol. The entire volume of each *A. fumigatus* extract was concentrated to ~200 μ L in a vacuum concentrator prior to analysis. Wild-type *A. leporis* and mutants of *M. brunneum* generated during this study were grown on sucrose-yeast extract agar medium for 10 days prior to injection of their conidia into *G. mellonella* larvae. After 8 days, the larval cadavers were bead beaten with 10 3-mm-diameter glass beads in 1 mL methanol at 6 m/s for 30 s. The resulting extracts were then rotated end-over-end at 40 rpm for 1 hour before being clarified by centrifugation. For HPLC analyses, 20 μ L of each sample was injected, and for LC-HRMS analyses, 10 μ L of each sample was injected.

HPLC analyses. Samples were analyzed for ergot alkaloids by HPLC with fluorescence detection by methods described in detail previously (Panaccione et al. 2012). The column was a 150- by 4.6-mm inner-diameter, 5- μ m particle size Prodigy C₁₈ column (Phenomenex, Torrance, CA), and the mobile phase was a 55-min, binary, multilinear gradient of 5% acetonitrile to 75% acetonitrile in 50 mM aqueous ammonium acetate. Chanoclavine and fumigaclavine A were detected using excitation and emission wavelengths of 272 nm and 372 nm, respectively, and LAH was detected by excitation at 310 nm and recording emission at 410 nm. For secretion

analyses, alkaloids were quantified according to Davis et al. (2020). Chanoclavine-I was quantified by comparing peak areas to an external standard curve prepared from chanoclavine-I standard (Alfarma, Prague, Czech Republic). Fumigaclavine A was relative to an external standard curve prepared from fumigaclavine A (Alexis Biochemicals, San Diego, CA). LAH was quantified by comparing peak areas to an external standard curve prepared from ergonovine (Sigma-Aldrich, St. Louis, MO), which contains the identical fluorophore; thus, LAH values must be considered as relative to ergonovine as opposed to absolute.

LC-HRMS analyses. Initial LC-MS analyses were conducted on a Thermo LCQ Deca XP plus mass spectrometer connected to a Thermo Surveyor HPLC system (Thermo Scientific, Waltham, MA) as described previously (Fabian et al. 2018). High-resolution mass spectra were collected on a Thermo Scientific Q Exactive mass spectrometer coupled to a Thermo Accela 1250 ultra-high-performance liquid chromatography (UHPLC) system. Separations were performed on a 150-mm by 4.6-mm inner-diameter, 2.6- μ m particle size Kinetex Evo C₁₈ column (Phenomenex, Torrance, CA) subjected to a gradient prepared by combining mobile phase A (5% acetonitrile, 0.1% formic acid) and mobile phase B (75% acetonitrile, 0.1% formic acid). The sample was loaded at 95% A plus 5% B and held for 1 min before ramping linearly to 40% A plus 60% B at 10 min at a flow rate of 300 μ L/min. The mass spectrometer was operated in positive ion mode and programmed with data-dependent acquisition settings. Analytes were electrospray ionized with a spray voltage of 3.5 kV and a capillary temperature of 300°C. Precursor scans were acquired at 70,000 resolution (at m/z 200) over an m/z range of 150 to 400. Ions of m/z = 239.1535, 269.1278, and 299.1747 were selected for higher-energy collisional-dissociation (HCD) fragmentation (normalized collisional energy [NCE] = 30) and were analyzed at 35,000 resolution.

Phylogenetic analyses. The respective protein sequence translated for EasQ from *eas* clusters of *A. leporis*, *P. biforme*, and *P. camemberti* were used as the query in a BLASTp search for homologous proteins in the NCBI database for each organism. A cutoff of at least 30% identity over 70% query coverage was used to select matches from the returned list to be included in the data set for phylogenetic analysis. The objective of these searches was to find the two closest homologs of a particular *eas* gene in an organism's genome. We set thresholds based in part on values discussed by Pearson (Pearson 2013) and on empirical experience from a similar study (Jones et al. 2021). Comparisons including sequences that did not meet these criteria resulted in alignments that trimmed off numerous informative amino acids from other well-aligning homologs. If more than two proteins from a given species met those criteria, only the top two matches were used. Since *M. brunneum* and *A. fumigatus* lack an *eas* cluster-associated version of EasQ, the EasQ sequences from *A. leporis* and *P. camemberti* were both used to search *M. brunneum* and *A. fumigatus* databases and the top three matches from both species were chosen (provided they met the criteria delineated above). When the BLASTp search resulted in fewer matches than outlined above, a tBLASTn search was performed against the whole-genome shotgun database for that organism. If hypothetical proteins queried in this manner met the cutoff criteria described above, the protein sequences were deduced by BLASTx comparison of the appropriate regions of the identified contigs. Accession numbers for homologs not already identified as a functional *eas* cluster-associated EasQ can be found in Figure 10. This process was repeated for EasH alleles with the only change being the inclusion of organisms having versions of EasH shown to catalyze key steps in the synthesis of cycloclavine (*A. japonicus* and *Byssoschlamys spectabilis*) or ergopeptines (*C. purpurea* and *Periglandula ipomoeae*). Accession numbers for homologs not already identified as a functional EasH and associated with *eas*

clusters can be found in Figure 11. Alignments and phylogenetic analyses were performed in MEGA X (Kumar et al. 2016). Once both sets of proteins for EasQ and EasH were assembled, sequences were aligned by MUSCLE as contained in MEGA X, accepting the defaults, and aligned proteins were trimmed by eye. Model tests of both data sets indicated that the Le and Gascuel (LG) model using a discrete Gamma distribution (+G) was most appropriate, so this was used for maximum likelihood analyses of both the EasQ and EasH data sets (Le and Gascuel 2008). One-thousand bootstrap analyses were performed for both data sets, and bootstrap values of 50% or higher were included at the relevant nodes. Neighbor-joining trees constructed with 1,000 bootstrap analyses were consistent with the data derived from maximum likelihood analyses (not included).

Preparation of transformation constructs. Genomic DNA (gDNA) was extracted from wild-type *A. leporis*, wild-type *M. brunneum*, and *easM* ko *A. fumigatus* samples according to the GeneClean spin protocol (MP Biomedicals, Solon, OH). The *A. leporis* gDNA was used as template in PCRs with primer combinations 1 and 3 (Table 2) to generate the *A. leporis easQ* and *A. leporis easH* fragments with their native 3' untranslated regions (UTRs) (nucleotides 47,107 to 48,732 and nucleotides 51,683 to 51,702, respectively, in the record under GenBank accession number [SWBU01000070.1](https://www.ncbi.nlm.nih.gov/nuccore/SWBU01000070.1)) with 5' overlaps for the *M. brunneum* bidirectional *easG/dmaW* promoter (Davis et al. 2020) (Fig. 16). These and all subsequent PCRs were performed with Phusion green hot start II high-fidelity PCR master mix (Thermo Scientific, Waltham, MA) and followed similar protocols as described previously by Davis et al. (2020) and with primers and reaction conditions detailed in Table 2. All products were gel purified using a ZymoClean gel DNA recovery kit (Zymo) prior to performing fusion PCR. The *M. brunneum* gDNA was used as template with primer combination 2 to amplify the bidirectional *easG/dmaW* promoter with

overlaps for *A. leporis easQ* and *A. leporis easH* (Fig. 16). An equimolar ratio of the *A. leporis easQ*, *M. brunneum* bidirectional promoter, and *A. leporis easH* fragments were fused using primer combination 6 (Fig. 17). The final product included unique restriction sites for *MluI* and *XhoI* near their termini allowing for double digestion, gel purification, and ligation into pBCygro (Fungal Genetics Stock Center, Manhattan, KS) (Silar 1995) generating *A. leporis easQ-A. leporis easH*- pBCygro. Competent *Escherichia coli* cells were transformed with this plasmid and plated on LB medium (per liter, 10 g tryptone, 5 g yeast extract, 5 g NaCl, and 15 g agar) supplemented with chloramphenicol (25 g/mL). Plasmid products were harvested from selected colonies and purified using a Zyppy plasmid miniprep kit (Zymo). Correct assembly was verified through double digestion with *MluI/XhoI*. The plasmid was linearized using *SnaBI* and purified with a PCR purification kit (Zymo) prior to fungal transformation.

DNA from the *easM* knockout of *A. fumigatus* was used as template with primer combination 4 to amplify the *easA* promoter (Robinson and Panaccione 2014) with an overlap for *A. leporis easH* (Fig. 16). Primer combination 5 was used with the *A. leporis* gDNA template to generate *A. leporis easH* with a 5' overlap for the *A. fumigatus* promoter. Equimolar ratios of *A. fumigatus* promoter and *A. leporis easH* fragments were fused together using primer combination 7 (Fig. 17). The *A. fumigatus* promoter-*A. leporis easH* final product included restriction sites for *MluI/XbaI* and was processed as described above with the substitution of pBCphleo (Fungal Genetics Stock Center, Manhattan, KS) (Silar 1995) as the parent plasmid, generating *A. leporis easH*-pBCphleo. Correct assembly of the plasmid was confirmed through double digestion with *MluI/XbaI*. The plasmid was linearized using *AleI* and purified using a PCR purification kit prior to fungal transformation.

Transformation of *M. brunneum* and *A. fumigatus*. To test the capacity of EasQ and EasH from *A. leporis* to generate rugulovasines from chanoclavine-I aldehyde, protoplasts from an *M. brunneum easA* knockout strain were prepared and transformed with a construct containing *A. leporis easQ* and *A. leporis easH* cloned into pBChygro according to a previously described protocol (Davis et al. 2020). This strain was selected as the recipient as it accumulates chanoclavine-I aldehyde, the precursor to rugulovasines A/B. Transformants were plated in TM102 medium (per liter, 310 g sucrose, 10 g malt extract, 10 g peptone, 2 g yeast extract, 1 g magnesium sulfate-heptahydrate, 0.5 g monobasic potassium phosphate, 0.5 g dibasic potassium phosphate, 0.5 g potassium chloride, 0.05 g chloramphenicol, and 15 g agar) supplemented with hygromycin (InvivoGen, San Diego, CA) at 600 $\mu\text{g/mL}$ and incubated at 30°C. Upon surfacing, colonies were transferred to sucrose-yeast extract agar medium supplemented with hygromycin at 300 $\mu\text{g/mL}$ and incubated at 30°C to allow further growth under selection. Genomic DNA was extracted from selected colonies and checked by PCR for presence of the introduced constructs. Primer combinations 8 and 10 were used to verify the presence of *A. leporis easQ* and *A. leporis easH* portion of the construct and the hygromycin resistance gene, respectively, in the *M. brunneum* background (Fig. 12).

To test the ability of *A. leporis* EasH to generate cycloclavine in a conducive genomic context, protoplasts of an *easM* knockout strain of *A. fumigatus* (Bilovol and Panaccione 2016) were transformed with a construct comprised of *A. leporis easH* cloned into pBCphleo. This strain was selected as the recipient because it accumulates festuclavine and its precursor chanoclavine-I aldehyde while leaving *easA*_{red} intact for cycloclavine production. Transformants were plated in TM102 supplemented with phleomycin at 200 $\mu\text{g/mL}$ (InvivoGen, San Diego, CA) and incubated at 37°C. Upon surfacing, colonies were transferred to malt extract agar

medium supplemented with phleomycin at 100 µg/mL and incubated at 37°C to allow further growth under selection. Genomic DNA was extracted from selected colonies and checked by PCR for presence of the introduced constructs. Primer combinations 9 and 11 were used to verify the presence of *A. leporis easH* and the phleomycin resistance gene, respectively, in the *A. fumigatus* background (Fig. 12).

RNA extraction and RT-PCR. Triplicate cultures of the *A. fumigatus* mutant expressing *A. leporis easH* were grown in 25 mL malt extract medium (lacking agar) inside of deep-dish culture plates and incubated overnight at 37°C. The plates were kept still to ensure formation of a single mat of hyphae on the surface of the broth with sparse conidia beginning to develop. RNA was extracted from approximately 100 mg of a conidiating portion of the mat with the Plant RNeasy kit (Qiagen), treated with DNase I (Qiagen), and reverse transcribed with Superscript IV (Invitrogen, Carlsbad, CA). RNA extraction and cDNA synthesis of replicates were performed concurrently to ensure consistency. Template cDNA from each replicate was diluted 1:100 prior to PCR amplification. Primer combinations 12 and 13 were used to amplify portions of *easH* and an endogenous β-tubulin encoding gene (GenBank accession number [XP_752456.1](#)) from each cDNA sample as well as from gDNA isolated from a malt extract agar culture of the mutant (Fig. S7). Because *easH* lacks introns, amplification of a β-tubulin encoding gene was carried out with primers flanking an intron to serve as a control for cDNA quality.

Statistical analyses. Concentrations of chanoclavine-I and fumigaclavine A in cultures (n= 7) of wild-type and *easD* knockout strains of *A. leporis* were measured as described above (under HPLC analyses) and used to calculate the percent conversion of precursor to product (Table 1). Data were checked by Brown-Forsythe tests for normality of variances. Data for chanoclavine-I accumulation did not pass ($P < 0.05$) and were therefore analyzed using a Wilcoxon's rank sum

test. The variances of both fumigaclavine A accumulation and overall percent conversion were found to be normally distributed by Brown-Forsythe tests and were subsequently analyzed using paired t-tests. All statistical analyses were performed with the JMP software package (SAS, Cary, NC).

Acknowledgements

This chapter has been published in Applied and Environmental Microbiology under the doi: [10.1128/aem.00793-23](https://doi.org/10.1128/aem.00793-23). I would like to acknowledge co-author Abigail Jones for her contribution in developing the *easD* knockout strain of *A. leporis* and assistance in setting up and analyzing time-course experiments.

This research was funded by NIH grant 2R15-GM114774-3, with additional salary support for D.G.P. from USDA Hatch project NC1183. A.M.J. is a Beckman Scholar supported by the Arnold and Mabel Beckman Foundation. This paper is published with the approval of the West Virginia Agriculture and Forestry Experiment Station as article number 3460. We thank Bo Xue (BioNano Research Facility, WVU) for assistance running LC-HRMS samples.

Figures and Tables

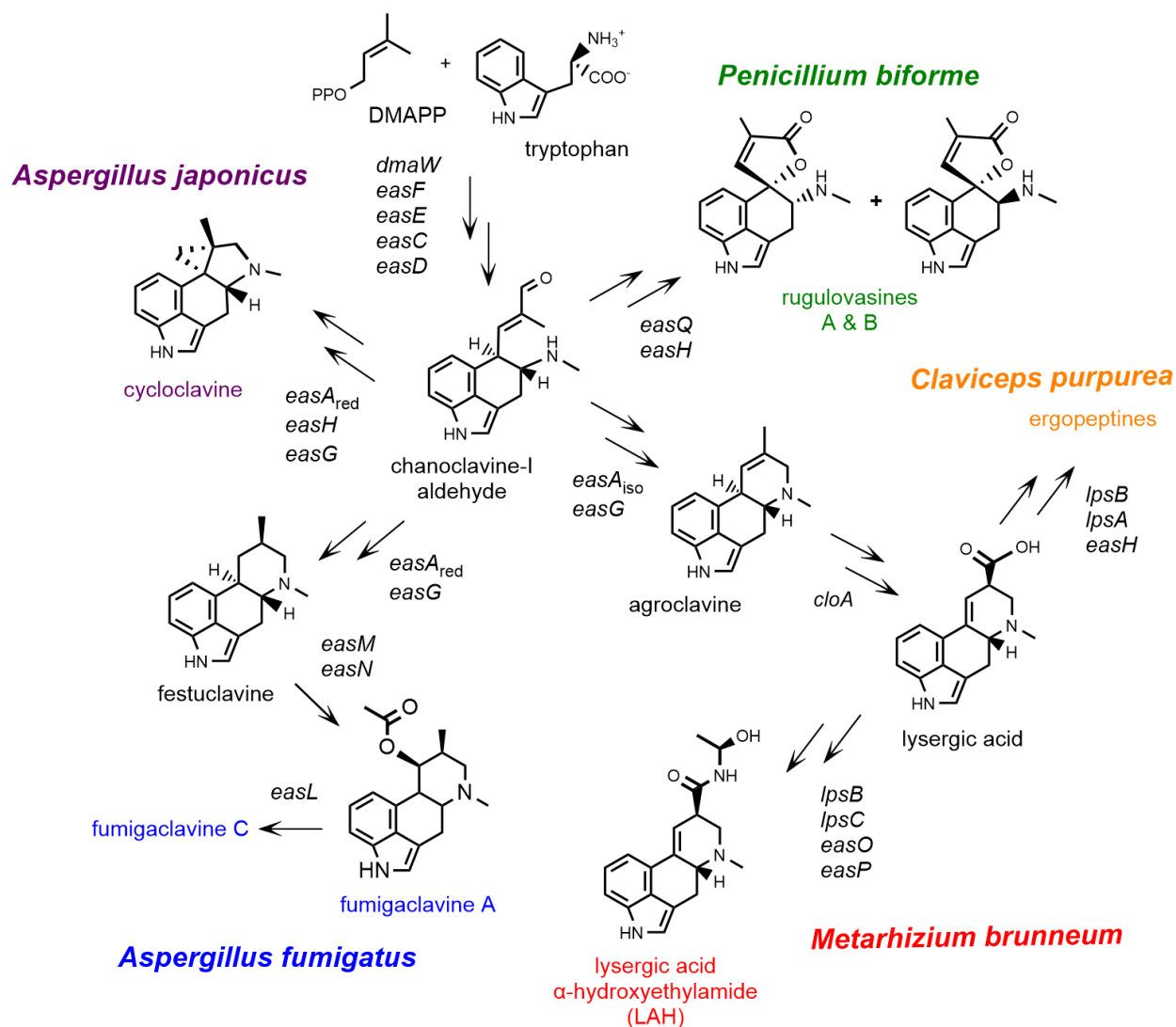


Fig 1. Simplified pathways to different ergot alkaloids. All pathways begin with the same core set of genes (*dmaW*, *easF*, *easE*, *easC*, *easD*) and branch depending on the combination of other *eas* genes present. The pathway branches involving the isomerase *easA* allele can lead to production of lysergic acid amides, as are found in *M. brunneum* (Leadmon et al. 2020) (labeled

in red) and ergopeptines as found in *C. purpurea* and several *Epichloë* species (Florea et al. 2017, Robinson and Panaccione 2015, Haarmann et al. 2009) (labeled in orange). The pathway branches involving the reductase *easA* allele can lead to production of fumigaclavines, as are found in *A. fumigatus* (Gerhards et al. 2014) (labeled in blue) and cycloclavine, which is found in *A. japonicus* (Furuta et al. 1982, Jakubczyk et al. 2015) (labeled in purple). The pathway leading to production of rugulovasines A/B in *P. biforme* involves keto-enol tautomerization of chanoclavine-I aldehyde and the activity of the protein products of *easQ* and *easH* (Fabian et al. 2018) (labeled in green). Versions of *easH* are highlighted to distinguish the function of their protein products. DMAPP, dimethylallylpyrophosphate; red, reductase; iso, isomerase. Lysergyl peptide synthetases 1 (LPS1), 2 (LPS2), and 3 (LPS3) are encoded by *lpsA*, *lpsB*, and *lpsC*, respectively.

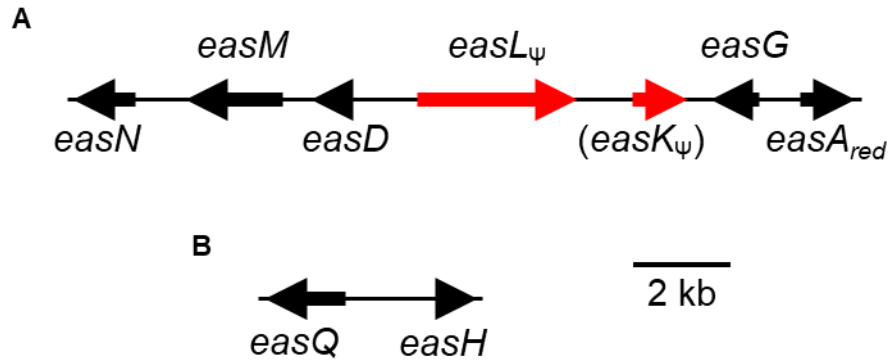


Fig 2. Clusters containing genes potentially associated with fumigaclavine or rugulovasine synthesis in *A. leporis*. Black arrows indicate functional gene copies and red arrows with Ψ in the gene name indicate hypothesized pseudogenes. The role for *easK* has not been characterized, but it has been identified in fumigaclavine clusters of other fungi (Robinson and Panaccione 2015, Gerhards et al. 2014). Scale bar included for approximate sizes of genes and intergenic regions.

```

      10      20      30      40      50      60      70      80      90     100
Aleporis  ....|....|....|....|....|....|....|....|....|....|....|....|....|....|
Afumigatus ATGACGAAGGGTGATGTCCAAGTATTCCATTTCGGAAGAGAAACTACGCGATCCATTTGAAGTATTGAGTCTAACCCCTTTCATTTCAACATGAAGATCACC
-          ***** ** * ***** ***** * *****

      110     120     130     140     150     160     170     180     190     200
Aleporis  ....|....|....|....|....|....|....|....|....|....|....|....|....|....|
Afumigatus GGCTGTGGTGGGAACAGGGAGGCTTCAGTACGGCGGACTATCTACGGCGGACTATCCGGACAAAATCGAAAAAACTAATTTTACCCGTCAACGCTAGTAT
-          -----

      210     220     230     240     250     260     270     280     290     300
Aleporis  ....|....|....|....|....|....|....|....|....|....|....|....|....|....|
Afumigatus TCTGCCAGCAGAACAATTATATTAGAGGACTTGCTTAGTTTCACTTAAAGGCTAATCTCCTGAGCACTATGTAAAGATGCAAGTCTGCTCAGATGT
-          -----

      310     320     330     340     350     360     370     380     390     400
Aleporis  ....|....|....|....|....|....|....|....|....|....|....|....|....|....|
Afumigatus TGTACACAGGGCCTGTACACTAGGCGTGTTGAAACAATGCAAAAGAAAATTTCGTATGTATTTTATAAGATAATAGGGTTGTCCTCTTCTCCTGTCTCCC
-          -----

      410     420     430     440     450     460     470     480     490     500
Aleporis  ....|....|....|....|....|....|....|....|....|....|....|....|....|....|
Afumigatus CCTCGTCTCTCCTTGCTGGATGAATCCAAATTGATTGGATTCTTGGCCTCCCCCTCCTCCGGGTCTAAGTTAATCAGAAGTTGGGTTTGTCCACCTCC
-          -----

      510     520     530     540     550     560     570     580     590     600
Aleporis  ....|....|....|....|....|....|....|....|....|....|....|....|....|....|
Afumigatus TTGTCTGCTATGTAGTTGGCTTCCAGCAGGAACCTCATGTACCTCTAATTGATTATCCCGTACAGAGCATAGTCTCCCATCGTCTGGCCATTTACAGTTG
-          -----

      610     620     630     640     650     660     670     680     690     700
Aleporis  ....|....|....|....|....|....|....|....|....|....|....|....|....|....|
Afumigatus GCACATGCTCCGCCTCAAAGCCAGGCAGATGCCGGCAATCGGAAAAGGGTCGAAATCCTGGACGAGTACGGCACCTTGTACAGGTGGGCCAACTGAGCC
-          -----
                                     ACGGCAACCCATGCAG-----
                                     ***** * * ***

```

```

      710      720      730      740      750      760      770      780      790      800
Aleporis  .....|.....|.....|.....|.....|.....|.....|.....|.....|.....|
Afumigatus CCACGAGATTAAATCAACAGGGCATTAAATATACGACGGCCGGTGGCTCTCTATTTGCTCAGCACGAACGCAGCCGCGTACGAA TGA AACTCGTTATCCTG
-          -----CAACA-----
          *****

      810      820      830      840      850      860      870      880      890      900
Aleporis  .....|.....|.....|.....|.....|.....|.....|.....|.....|.....|
Afumigatus GAAGGGCTAGAACCGGGTGCTGTTGTATAGTGTGTATAAAAGGTCTTAG CTGTTGACCCTTAATTGGCAAGCTAGGGTATTGTCCGGCGGGAGTAACCTG
-          -----

      910      920      930      940      950      960      970      980      990      1000
Aleporis  .....|.....|.....|.....|.....|.....|.....|.....|.....|.....|
Afumigatus CAATAG CCGGGAGAACAGGCCTCCCAGAGTGAAAACAGGAGCGTTGTTATTATTATTGGTTGA ATTAAGGTTGTAGAAGAAACTAGTAGCAGTATGAACT
-          -----

      1010     1020     1030     1040     1050     1060     1070     1080     1090     1100
Aleporis  .....|.....|.....|.....|.....|.....|.....|.....|.....|.....|
Afumigatus GTATAGCAGCCAGGTGCAGAGCACTCACAGATGCAGAATGCTCGCATAGAAGCCGTATAGCTCGTATAAAAGAGTTAGTAATATGCTTCAGATATCAAAA
-          -----ACAGACGAAG-----
          ***** * **

      1110     1120     1130     1140     1150     1160     1170     1180     1190     1200
Aleporis  .....|.....|.....|.....|.....|.....|.....|.....|.....|.....|
Afumigatus GAACAAAACTTAACAAGTAATAGCTTGTACGCCATGGTAGTAGTAATAGTTATGGTGTTAATGAAGAAGAGAAGAAGACAAAGAGAGCAAGAA TAGACA
-          -----

      1210     1220     1230     1240     1250     1260     1270     1280     1290     1300
Aleporis  .....|.....|.....|.....|.....|.....|.....|.....|.....|.....|
Afumigatus TCAATAGCTGCATATATCTTGATATTGTACGGAGCTAGCTTGAGATACCTATTAATTAACCAGATAAAGTTAGGTCCTAGGACAATG TAA GCTTCTTGAT
-          -----AGGTTCAAGATCAATG-----
          ***** * ** *****

      1310     1320     1330     1340     1350     1360     1370     1380     1390     1400
Aleporis  .....|.....|.....|.....|.....|.....|.....|.....|.....|.....|
Afumigatus GCCGTTGTAGATTATTTAATCATCTTCGTACAGCAGCTGGGGCAAGCTCTCGATATAGAGAA TAA AGCCGGTCCCTGATAATTATTAGTATTATGTATTT
-          -----GAGAGCTCCATTTGAGGTATTGAGTCGGACCCT-----TGTTTT-
          ** *** ** * * ** ** ** **

```

	1410	1420	1430	1440	1450	1460	1470	1480	1490	1500
<i>Aleporis</i>									
<i>Afumigatus</i>	AATA TAA CTATATGATAAACCTAGCGATAAGAAAGCCCTGGCTCCAAAAATGCTGATGAAG TAA GGTCCGTCCATAATCTTCAATTTGCCTCTTGAAAG									
-	-----									
	1510	1520	1530	1540	1550	1560	1570	1580	1590	1600
<i>Aleporis</i>									
<i>Afumigatus</i>	CTCCGTACGAAGCTGAAC TAA TACTCTTTCTACCTCTGCTTGAGTAGCAATGGTATTTGTTGTACAGCGGTACAGGCCTTAGCGGTGCCGAATATATTT T									
-	-----									
				TCAGCATGAGGACC				ACAGGCTTTGGTGG		
			** * *	** * *				** * *	** * *	
	1610	1620	1630	1640	1650	1660	1670	1680	1690	1700
<i>Aleporis</i>									
<i>Afumigatus</i>	AGAGTTTCGAGCCTCAATATTAAAGCCTTCTTGT TG TAGAACATGAAGCATTTCCTTTTCTTCAAGGCCAACCTGGTAAAAGAGAACCTTTATCCGGGTAT									
-	-----									
				GAACGGGCAG			CTTCAAAGCTTGCC			
			** * *	* * *			** * *	** * *		
	1710	1720	1730	1740	1750	1760	1770	1780	1790	1800
<i>Aleporis</i>									
<i>Afumigatus</i>	GAAGAATCTCATT TAA TGTTGCTGTATGGTTCTGCTTTTTAATGCCCCAGGTTCGAAGACGGGTATCAATCGTATAAGAAGTTACTTCAACCCCATACCG									
-	-----									
	1810	1820	1830	1840	1850	1860	1870	1880	1890	1900
<i>Aleporis</i>									
<i>Afumigatus</i>	ATGAGC TAG GAGACAAAGGGAAGAGGTAGAAGTATGGCTTTTATA TAG ATCTATAATCTCGGCCTTGATGGCTCAAGATCAAGAGAGGGGCGAGGCATG									
-	-----									
	1910	1920	1930	1940	1950	1960	1970	1980	1990	2000
<i>Aleporis</i>									
<i>Afumigatus</i>	ATAAAATTC TGA TACCTTAGAGCTGATGAAGA TAA TTTGTCAACCAAGAAAAATACAGTATCACGCCTGAATTGGTGTTCATGGCGTCTTTTTAGTGCAGT									
-	-----									
	2010	2020	2030	2040	2050	2060	2070	2080	2090	2100
<i>Aleporis</i>									
<i>Afumigatus</i>	GGTATTGTCCGATATAATTGAGAAAGCTACACCGCTAGTTAGGGATAGAT TAA AGGCGGCCAGTAAAGCGGTATACCGAGATAAAACAGGTAAAATTAGTT									
-	-----									


```

                2110      2120      2130      2140      2150      2160      2170      2180      2190      2200
Aleporis      .....|.....|.....|.....|.....|.....|.....|.....|.....|.....|.....|.....|.....|.....|.....|.....|
Afumigatus    TTTTCGATTTTGTTCGGA TAG TCCGCCGTATATATC TGA GGCTCGCAAATAACAGCGTGGCATCTCAGTACCAACATCTGC TGA CGTTCTACTCCGTCTA
-              ACATACCTTAGGCTTGCAAAGTACAGTGTGGGATCTCAGTACCAGCATCTGTTGATGTTCTACTCCGTCTA
                * * * * *
                2210      2220      2230      2240      2250      2260      2270      2280      2290      2300
Aleporis      .....|.....|.....|.....|.....|.....|.....|.....|.....|.....|.....|.....|.....|.....|.....|.....|
Afumigatus    CGCGTCGAACCTCGGCCATGGCCTAACGAGAAGAGTGATAACGTTAACTGGGTCTGCGGTATCTCCCCGGGAGGCAAGAATCTGGAGCTTAGCATGAAC
-              CGCGCCCAATTTGGGACCTTGGCCCAACGACAAGCGAGATAATGTTCACTGGGTCTGCGGTATCTGCCCTGGAGGCGAGAACCTGGAGATTAGCATGAAC
                * * * * *
                2310      2320      2330      2340      2350      2360      2370      2380      2390      2400
Aleporis      .....|.....|.....|.....|.....|.....|.....|.....|.....|.....|.....|.....|.....|.....|.....|.....|
Afumigatus    TACCAGCAGCAGTCCAAGTGCAGTGTGCGCATAG CTGCCGAGACAATTGGGCCCT TGA CAGGCACCGAGAAGGATCCATCTAACATGA TCGCCGAGAAAA
-              TACCAACAAGGAGCGAAATGCACAGTTCGCATCGCTGCTGAAACCATTACACCCGCGGCCGGTACCGATAAGGACCCTTTCAACCTAACCGCTGAGAAGA
                * * * * *
                2410      2420      2430      2440      2450      2460      2470      2480      2490      2500
Aleporis      .....|.....|.....|.....|.....|.....|.....|.....|.....|.....|.....|.....|.....|.....|.....|.....|
Afumigatus    AGC TGA TTGAGGATCTCAGAGCTCTCCAGCCGGACCTCAATTTCAATTGGTTTGATCATTCTAACCGAGGTTGTGCTGCCCGAGGAGGTGGCTTT TGA G
-              AGATGATCGAGGATCTTAAGGCCCTCCAGCCAAACCTGAACTTCACCTGGTTTAATCATTTCAGCGGGAGGTTCTGGTGCCGGAAGAGGTGGCTCTAAA
                * * * * *
                2510      2520      2530      2540      2550      2560      2570      2580      2590      2600
Aleporis      .....|.....|.....|.....|.....|.....|.....|.....|.....|.....|.....|.....|.....|.....|.....|.....|
Afumigatus    CCATAAGAAGGCTATCGATACAGTCCCCTTCAAAAACCAAAGACTCCATGGACTCGATTTGGCTGAAGGGGCCCTTCATGCTCAAGTCATACTTCATGCCT
-              CAATGACGAAATTATCTCCAAAGTCCCATTCAAGAATCAGAGACTCCATGGGCTCGATCTGAGTGAAGGAGCATTATGTTGAAGTCCTACTTCATGCCT
                * * * * *
                2610      2620      2630      2640      2650      2660      2670      2680      2690      2700
Aleporis      .....|.....|.....|.....|.....|.....|.....|.....|.....|.....|.....|.....|.....|.....|.....|.....|
Afumigatus    TCAATCCGCTCCGCTGTCACTGGAGTTGAGACCACACAAATCATGTTGACTCTATCCGAAAGCTGGGGTTGGAGAACAACAACCTTCAACTCCGCTTTGG
-              GCGATTGCTCCGCCATCACTGGGGTTGAGAACACACAGATCATGTTGAAATCTATCCGAAAGCTGAAATCTCAAGAATGCCAACTTTATCTCCGCTCTGA
                * * * * *
                2710      2720      2730      2740      2750      2760      2770      2780      2790      2800
Aleporis      .....|.....|.....|.....|.....|.....|.....|.....|.....|.....|.....|.....|.....|.....|.....|.....|
Afumigatus    ACATGTTGCAGGACTGGA TGA TTCTACCAATGGTCGATCTATGGAGCATTGGGATGGAGTTTCTACGATGCGATCGACGCCGAGAAAGCCAGGATCAA
-              GTACGCTAGAAGACTGGATGGTTCCAACGAATGGCCGTTTATGGAGTATTGGGATGGTATTTCTATGACGCGGTCGATGCATGTAAGCCAGGATCAA
                * * * * *

```

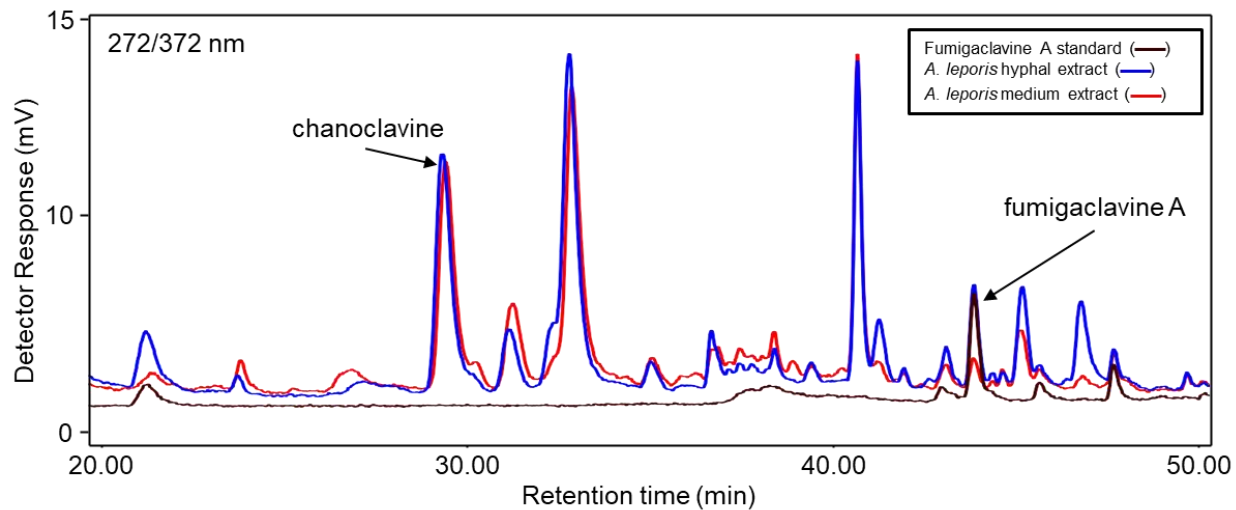



Fig 4. HPLC chromatogram of wild type *A. leporis* solid and liquid extracts compared to fumigaclavine A standard. Hyphal and medium extracts were from the same culture, which is representative of the multiple cultures analyzed for Table 1 and for the secretion study summarized in the text. Fluorescence was detected at 372 nm after excitation at 272 nm. Peaks corresponding to characterized ergot alkaloids are indicated.

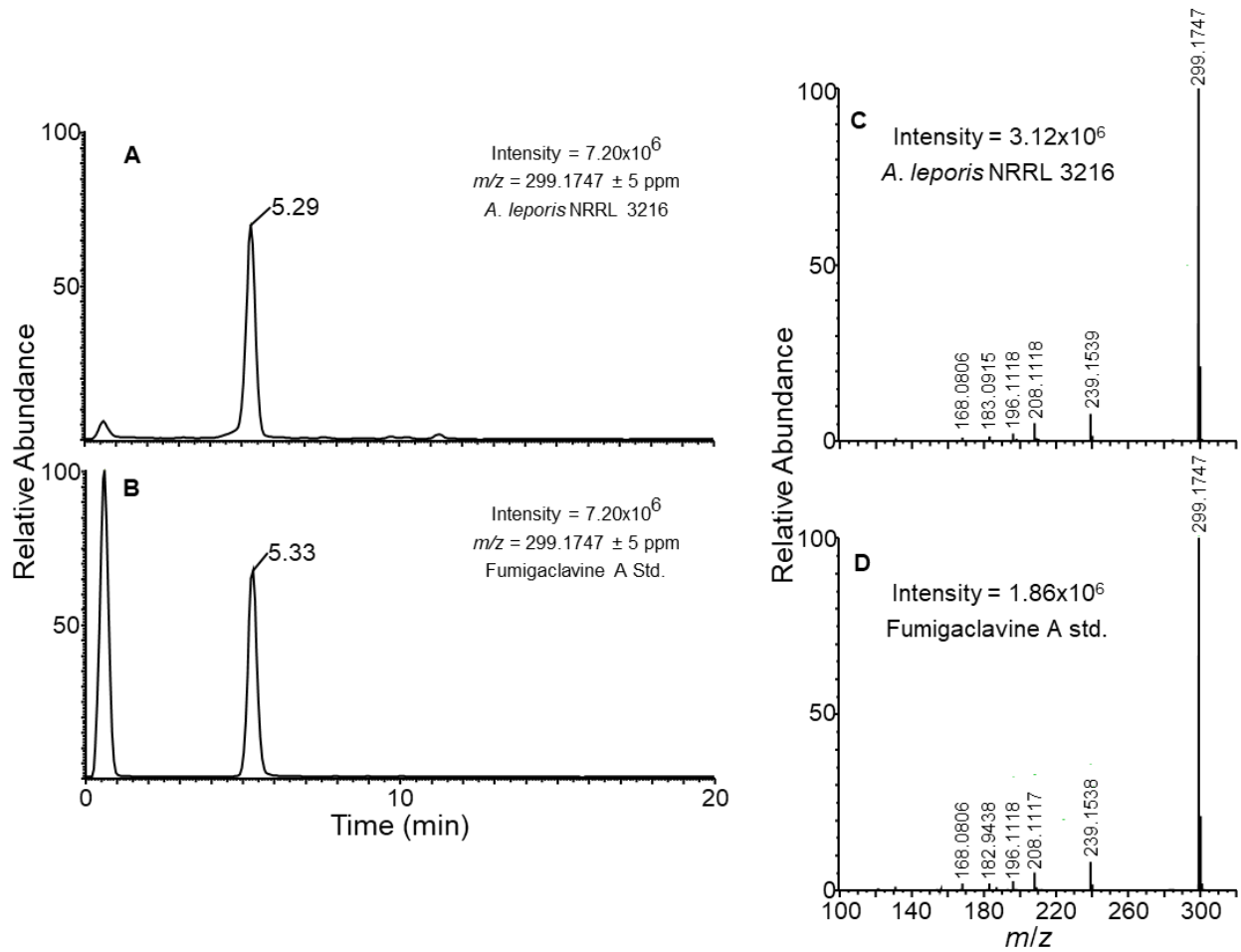


Fig 5. LC-HRMS of *A. leporis* hyphal extract compared to fumigaclavine A standard.

Extracted ion chromatograms of (A) wild-type *A. leporis* NRRL 3216 hyphal extracts and (B) 400 ng/ μ L fumigaclavine A standard analyzed at m/z 299.1747 ± 5 ppm. (C-D) High resolution MS spectra resulting from fragmentation of parent ions shown in panels A and B. Instrument resolution accurate to < 5 ppm.

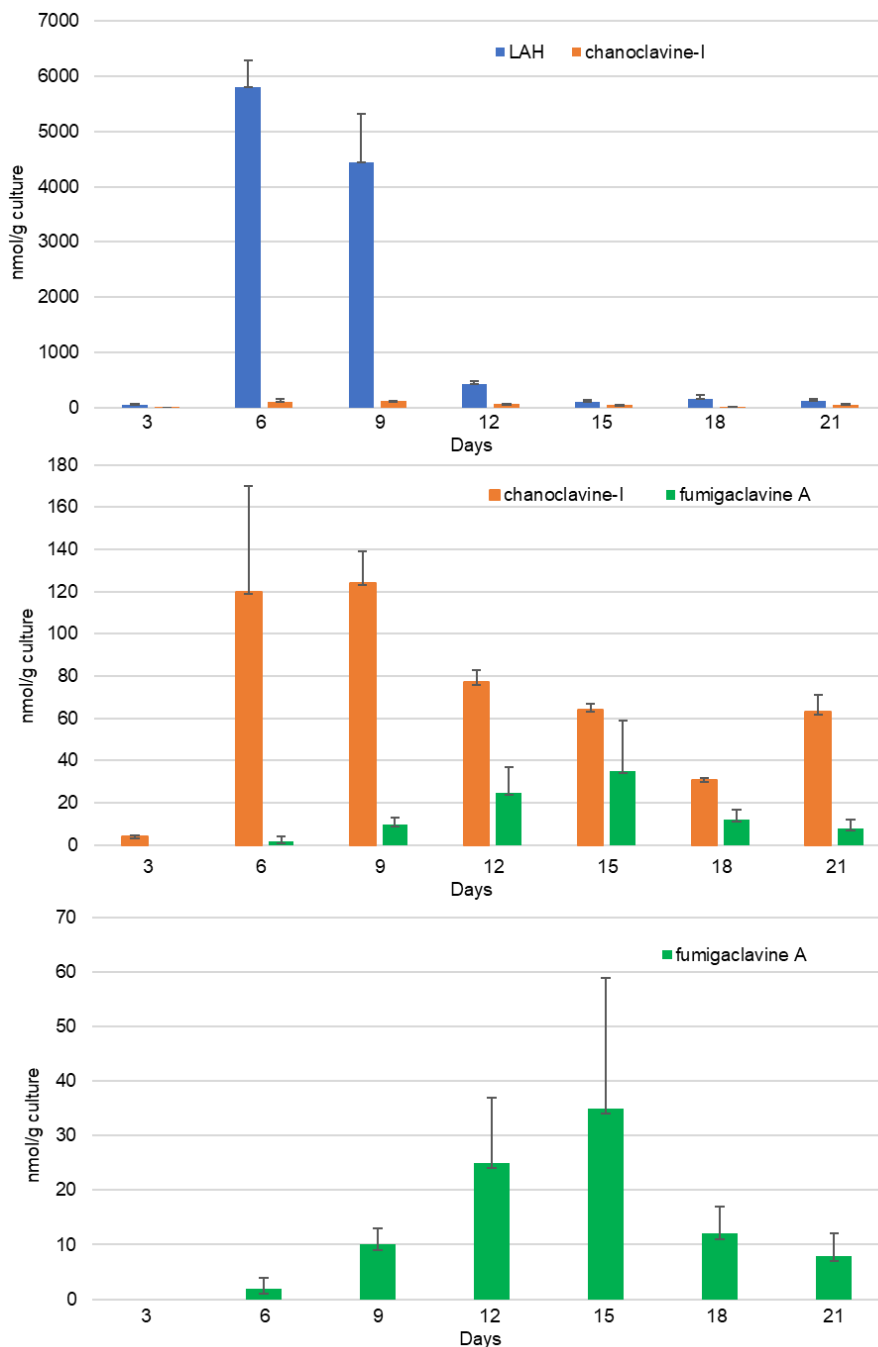


Fig. 6. Accumulation of lysergic acid α -hydroxyethylamide (LAH), chanoclavine-I, and fumigaclavine A in cultures of *A. leporis* NRRL 3216 over time. Bars represent means (n = 3), and error bars correspond to standard error. Values for chanoclavine-I and fumigaclavine A are rescaled in lower panels to provide detail. Experiment was conducted at room temperature.

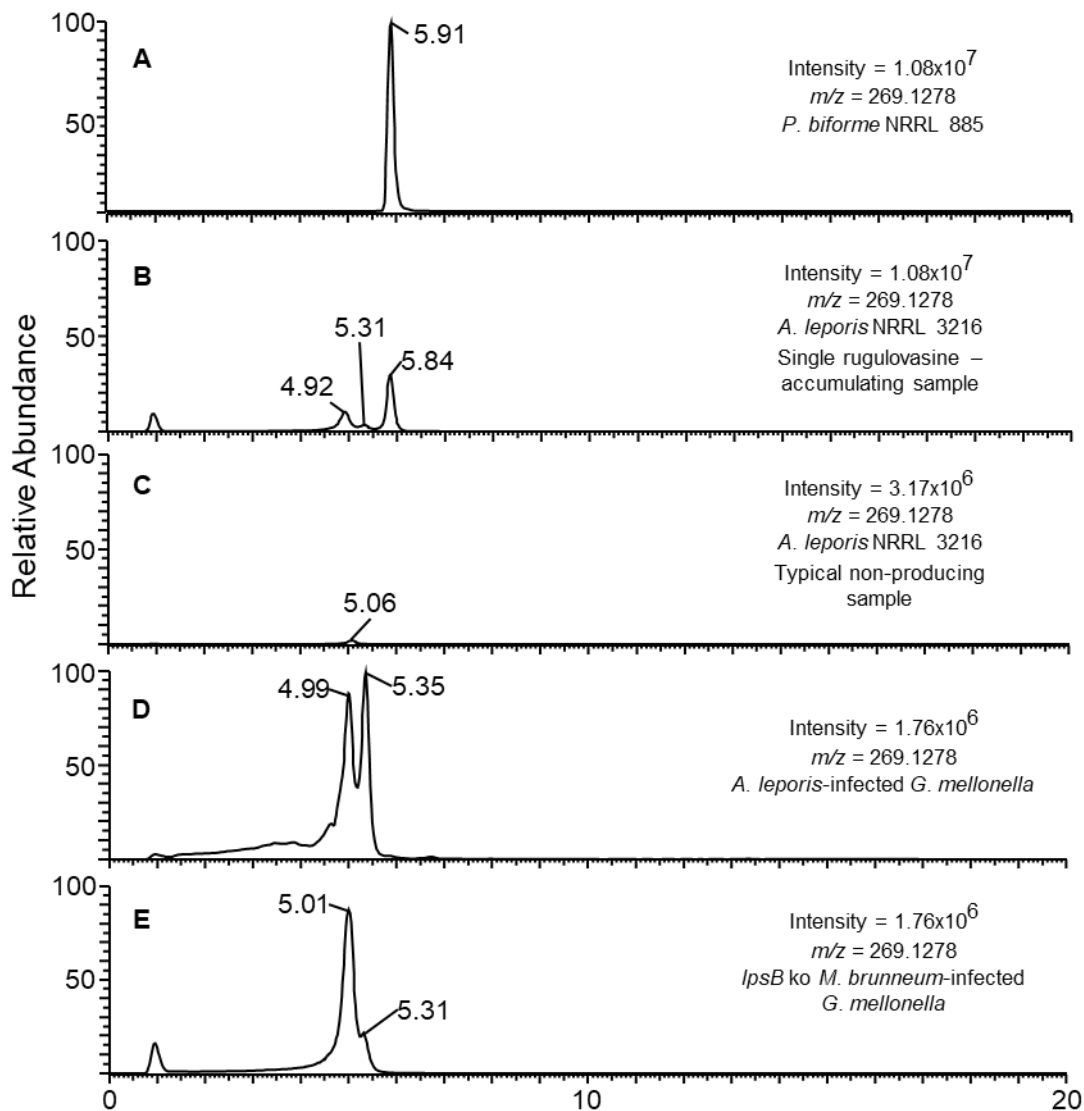


Fig 7. LC-HRMS analyses of *P. biforme* and single rugulovasine-producing *A. leporis* culture compared to typical *A. leporis* culture, *A. leporis*-infected *G. mellonella*, and *G. mellonella* infected with *lpsB* knockout of *M. brunneum*. Extracted ion chromatograms of (A) *P. biforme* NRRL 885 malt extract culture, (B) single rugulovasine-producing *A. leporis* NRRL 3216 malt extract culture, (C) typical rugulovasine-nonproducing *A. leporis* NRRL 3216 malt extract culture, (D) *A. leporis*-infected *G. mellonella*, and (E) *lpsB* knockout *M. brunneum*-infected *G. mellonella* analyzed at m/z 269.1748 ± 5 ppm. Instrument resolution accurate to < 5 ppm.

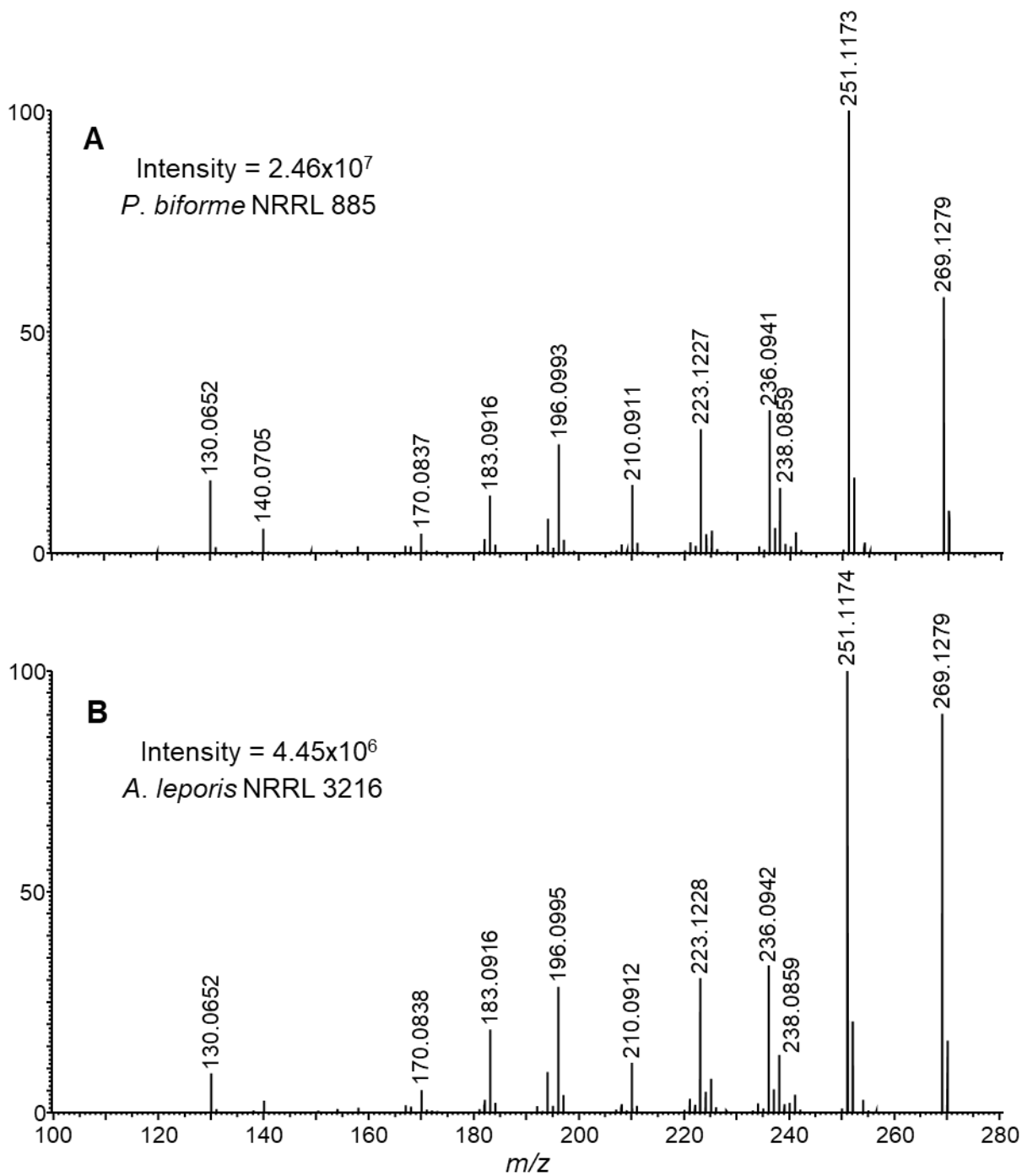


Fig 8. High resolution MS spectra of ions resulting from fragmentation of m/z 269.1278 parent ion in *P. biforme* compared to suspected rugulovasine-accumulating *A. leporis* sample.

Instrument resolution accurate to < 5 ppm.

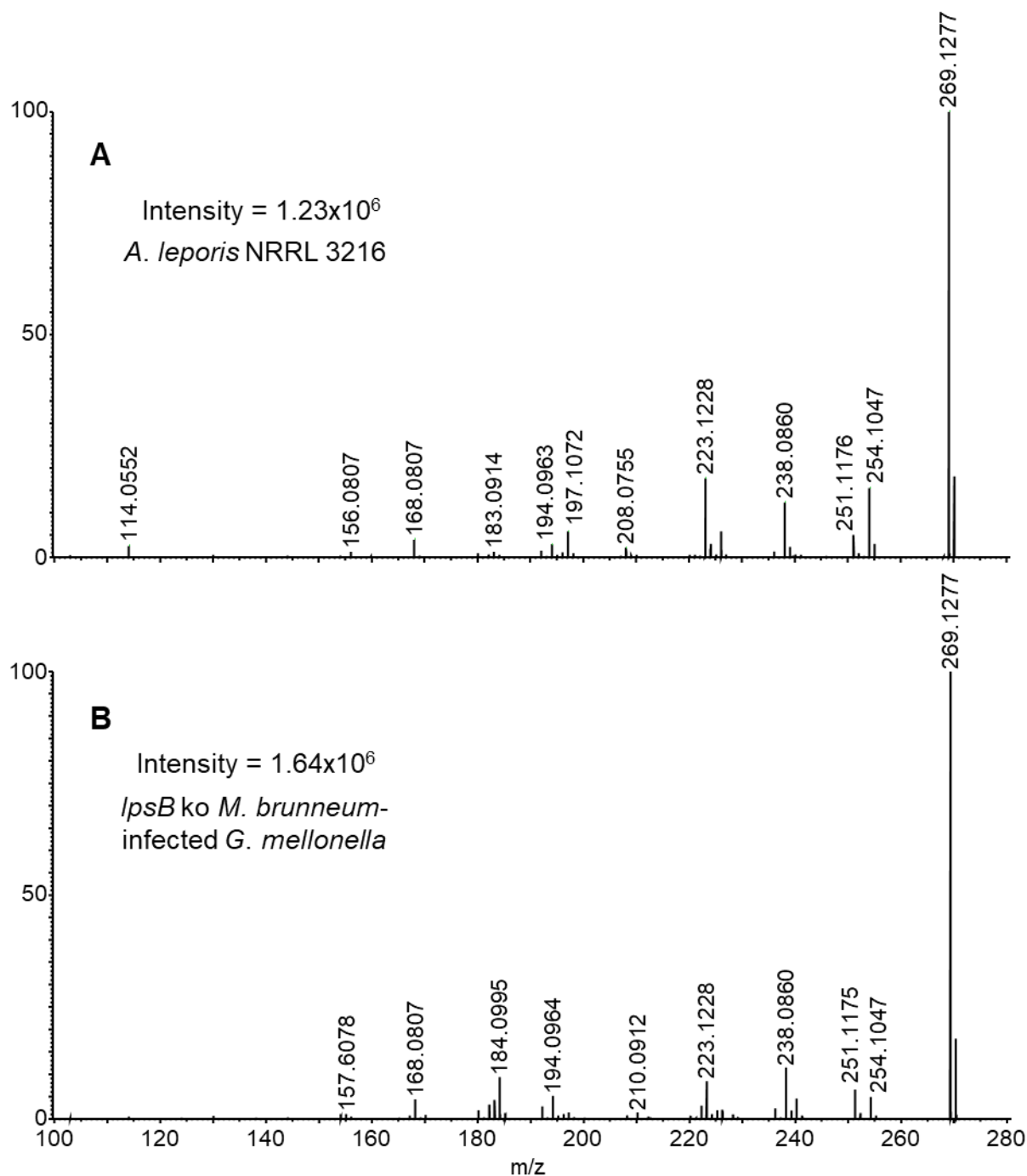


Fig 9. High resolution MS spectra of ions resulting from fragmentation of m/z 269.1278 parent ion in typical *A. leporis* sample compared to lysergic acid from *lpsB* knockout *M. brunneum*-infected *G. mellonella*. Instrument resolution accurate to < 5 ppm.

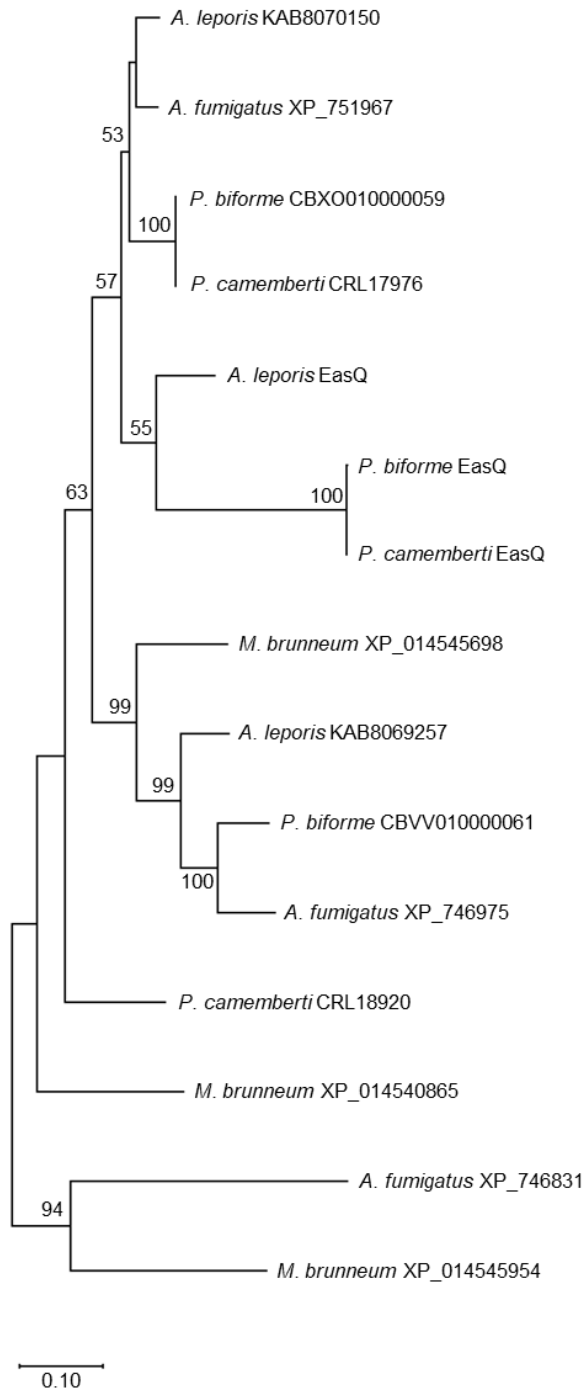


Fig 10. Maximum likelihood tree for amino acid sequences of EasH encoded in eas clusters and homologs from species producing differing branches of ergot alkaloids. Homologs had

at least 30% amino acid sequence identity over 70% query coverage and are identified by species and NCBI accession number. The tree presented has the greatest log likelihood of 1,000 bootstrapped trees calculated with the Le and Gascuel (LG) model (Le and Gascuel 2008) using a discrete Gamma distribution (+G) in MEGA X (Kumar et al. 2016); bootstrap values of 50% or higher are indicated at the corresponding nodes. Clades possessing ergot alkaloid pathways for rugulovasine, cycloclavine, and ergopeptine production are highlighted in green, purple, or orange, respectively. Tree is unrooted. The bar represents changes per site.

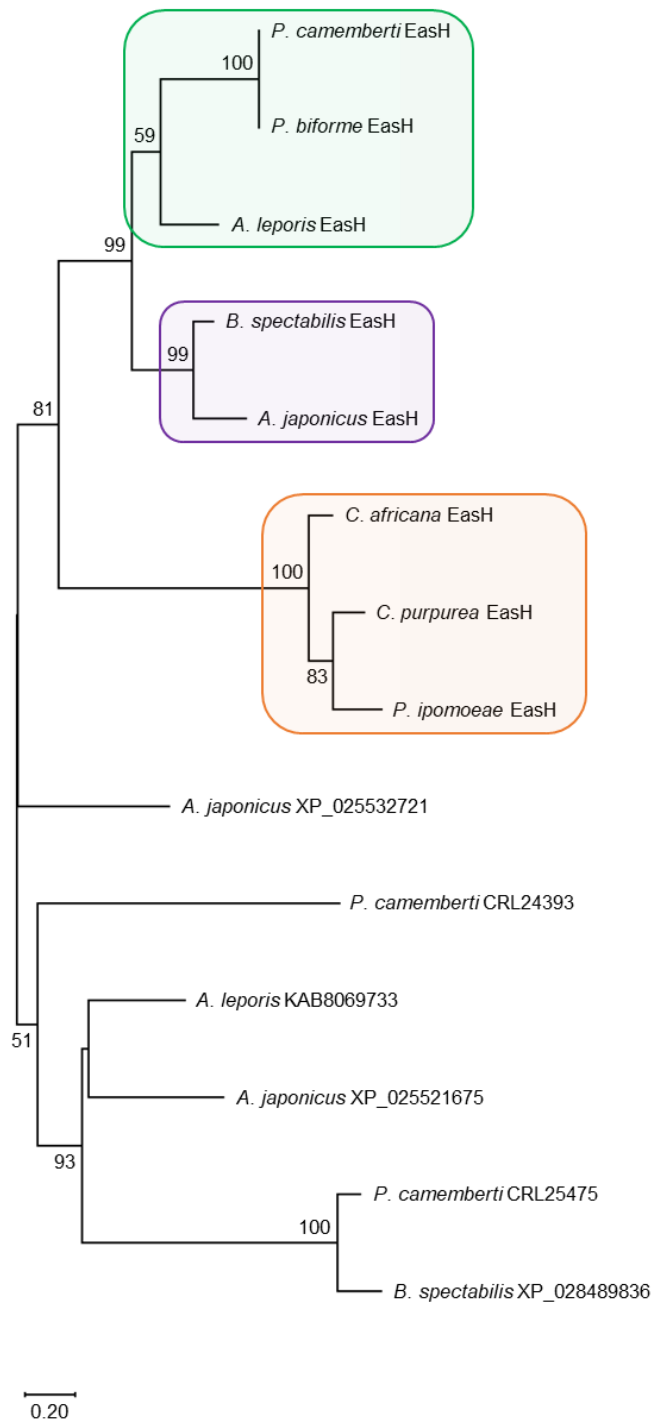


Fig 11. Maximum likelihood tree for amino acid sequences of EasH encoded in *eas* clusters and homologs from species producing differing branches of ergot alkaloids. Homologs had

at least 30% amino acid sequence identity over 70% query coverage and are identified by species and NCBI accession number. The tree presented has the greatest log likelihood of 1,000 bootstrapped trees calculated with the Le and Gascuel (LG) model (Le and Gascuel 2008) using a discrete Gamma distribution (+G) in MEGA X (Kumar et al. 2016); bootstrap values of 50% or higher are indicated at the corresponding nodes. Clades possessing ergot alkaloid pathways for rugulovasine, cycloclavine, and ergopeptine production are highlighted in green, purple, or orange, respectively. Tree is unrooted. The bar represents changes per site.

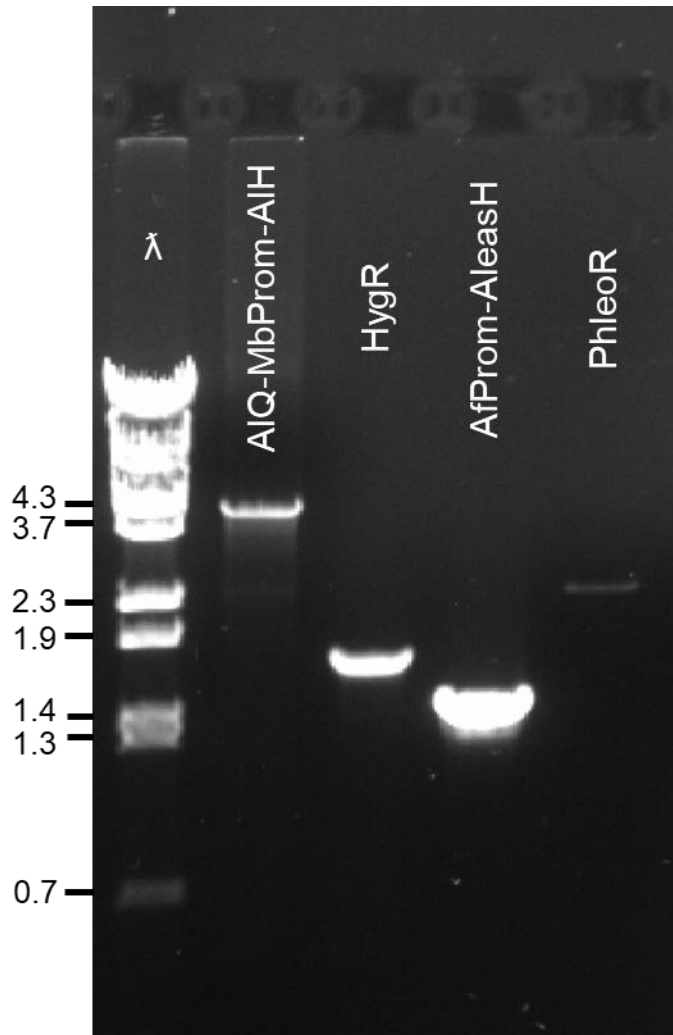


Fig 12. Verification of fusion constructs and resistance genes in *M. brunneum* and *A. fumigatus* mutants. PCR products from primer combinations 8-11 (listed in Table 2) generated using genomic DNA from *M. brunneum* and *A. fumigatus* mutants generated during this study. Sizes of relevant fragments from *Bst*EII-digested bacteriophage lambda DNA are indicated to the left. Gel was stained with ethidium bromide. AIQ-MbProm-AIH, *A. leporis easQ* – *M. brunneum easG/dmaW* promoter – *A. leporis easH* fusion product; AfProm-AIH, *A. fumigatus easA* promoter – *A. leporis easH* fusion product. HygR, hygromycin resistance gene. PhleoR, phleomycin resistance gene.

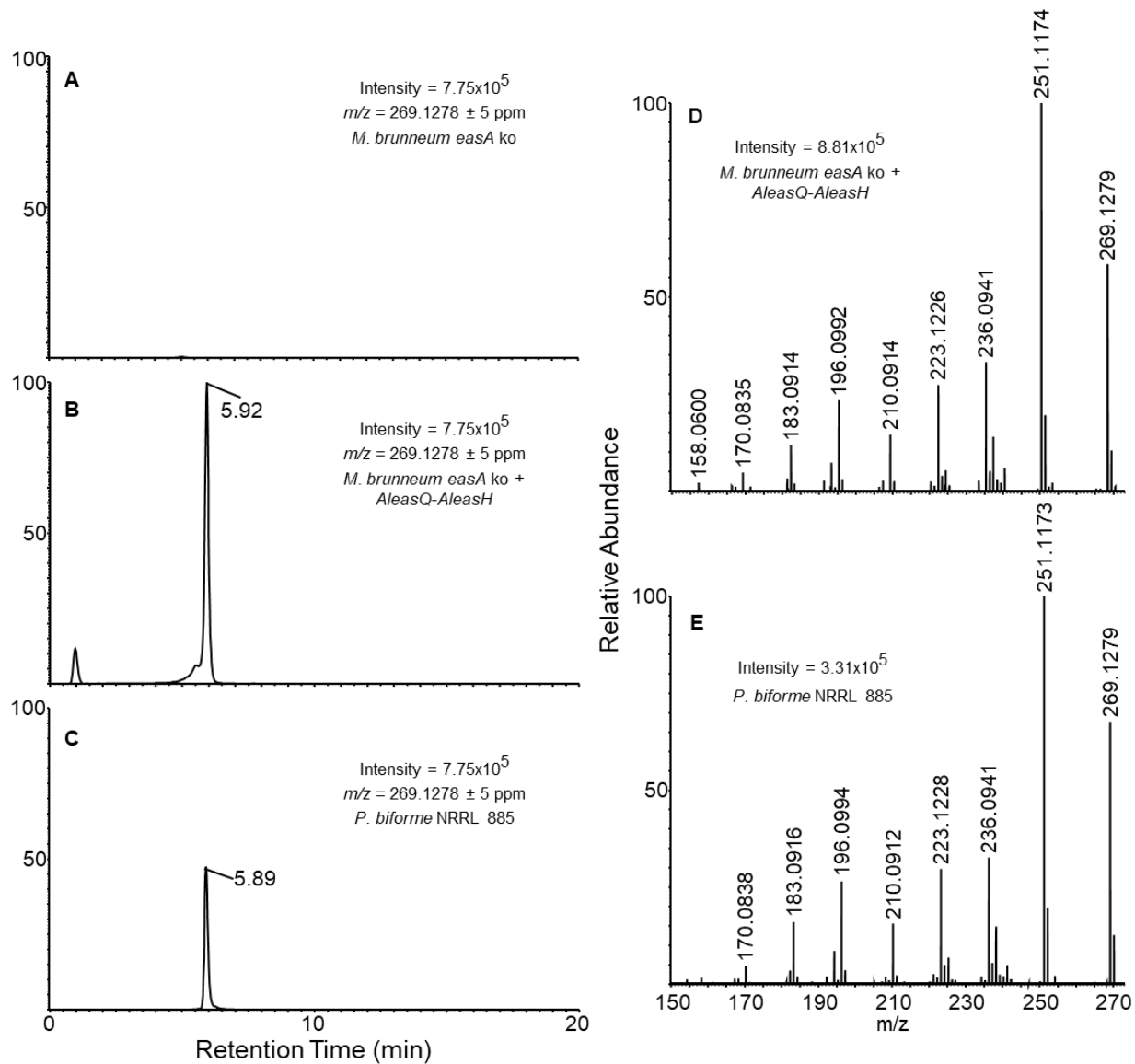


Fig 13. LC-HRMS analyses of *M. brunneum* mutant expressing *easQ* and *easH* from *A. leporis* compared to the background strain of *M. brunneum* (*easA* knockout) and *P. biforme* NRRL 885. Extracted ion chromatograms of (A) *easA* knockout strain of *M. brunneum*, (B) *M. brunneum* mutant expressing *easQ* and *easH* from *A. leporis*, and (C) *P. biforme* analyzed at m/z 269.1278 ± 5 ppm. (D-E) High resolution MS spectra resulting from fragmentation of parent ions shown in panels B and C. Instrument resolution accurate to < 5 ppm.

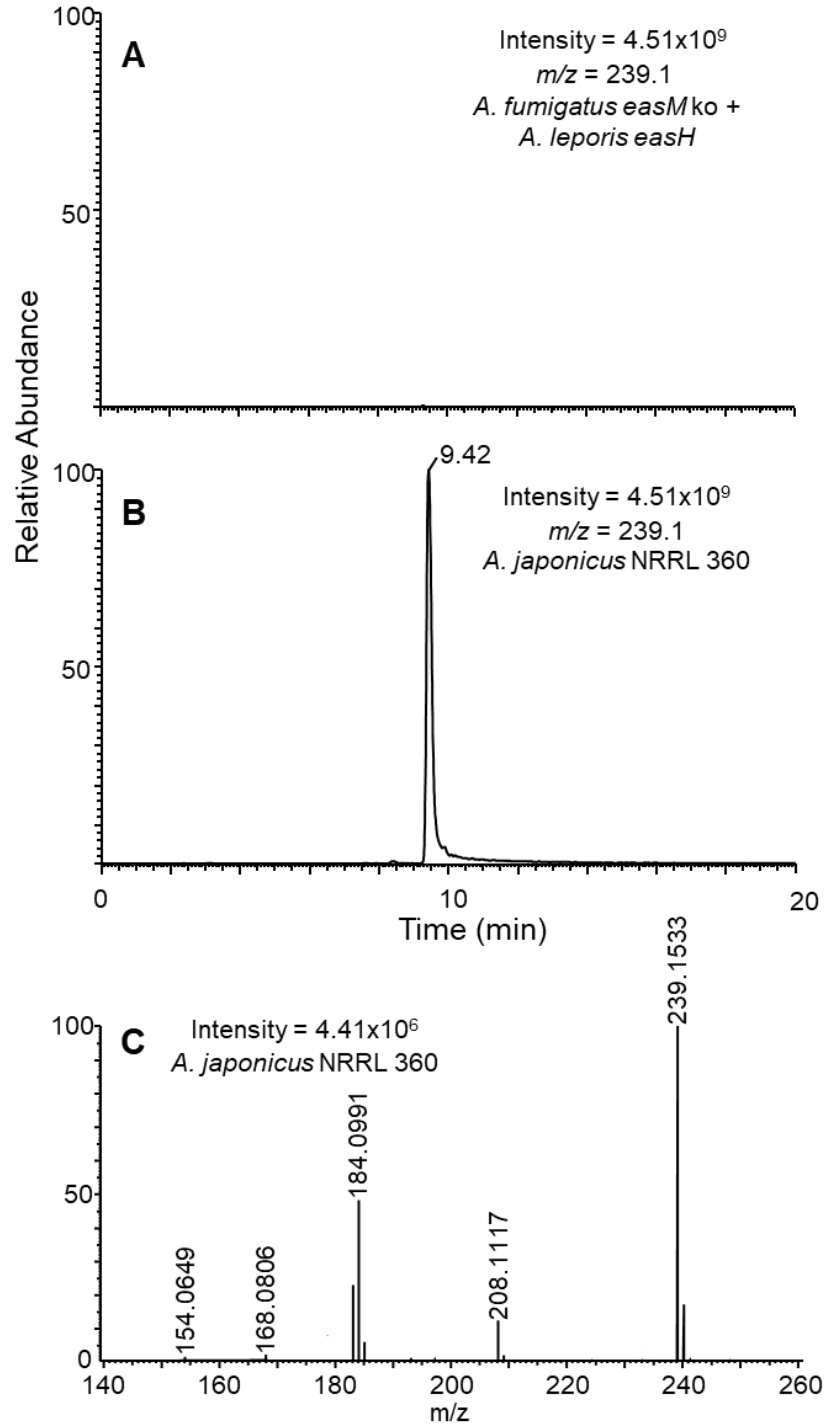


Fig 14. LC-MS analysis of *easM* knockout *A. fumigatus* augmented with *A. leporis easH* compared to *A. japonicus* NRRL 360. Extracted ion chromatograms of (A) *easM* knockout *A. fumigatus* expressing *easH* from *A. leporis*, and (B) *A. japonicus* analyzed at m/z 239.1. (C) LC-

HRMS fragmentation spectrum of the m/z 239.1533 parent ion from *A. japonicus* showing fragments which match those reported for cycloclavine by Jakubczyk et al. (2015) (154.0646, 168.0801, 184.0987, 208.1117 for parent ion of m/z 239.1540).

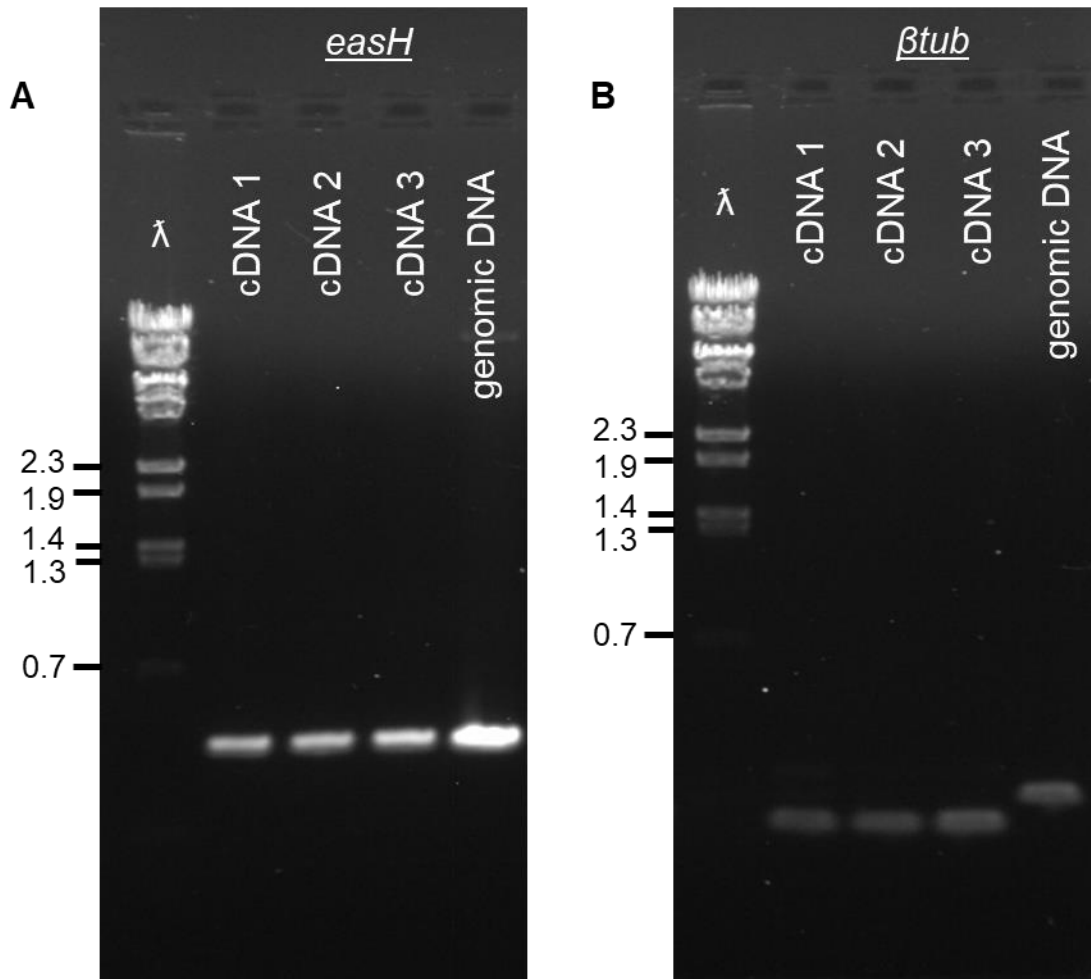


Fig 15. RT-PCR analysis of *A. fumigatus* mutant expressing *A. leporis easH* alone. PCR products from primer combinations (A) 12 and (B) 13 (listed in Table 2) generated using cDNA from three independent MEA cultures of the *A. fumigatus* mutant compared to genomic DNA isolated from the mutant. *betub* was used as an endogenous control for cDNA quality as *easH* lacks introns. Sizes of relevant fragments from *Bst*EII-digested bacteriophage lambda DNA are indicated to the left. Gel was stained with ethidium bromide.

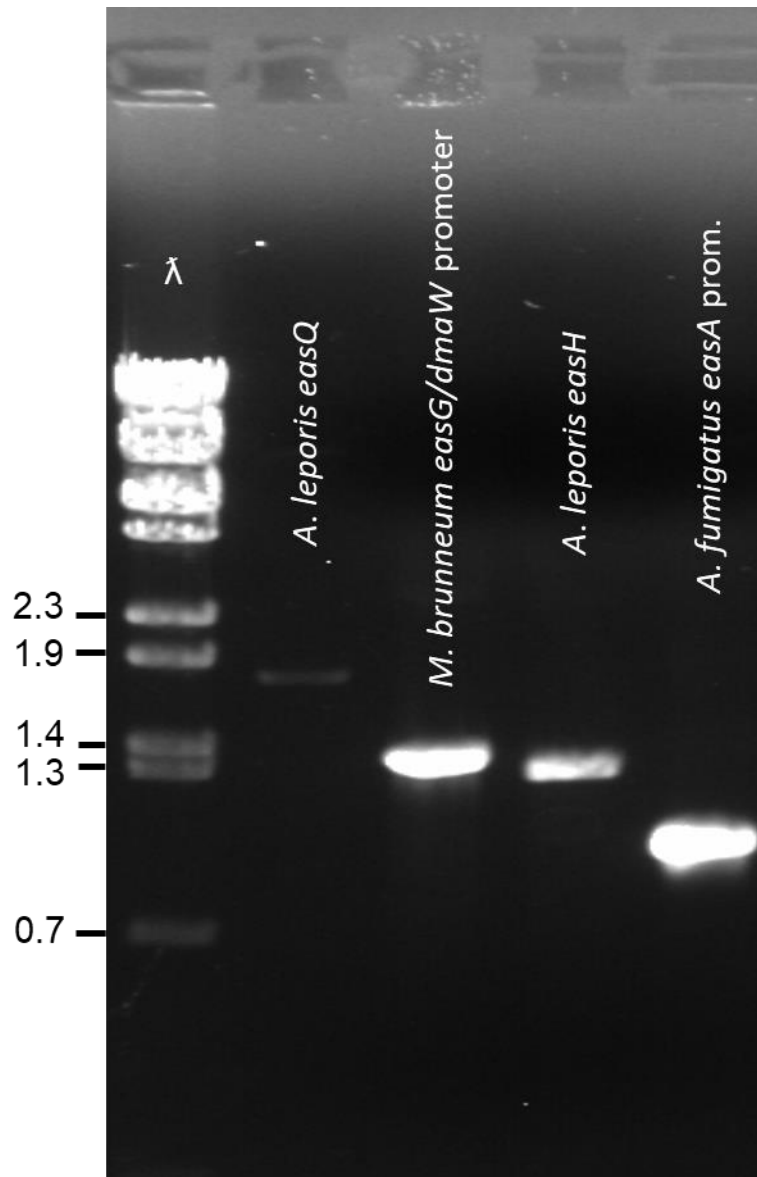


Fig 16. Analysis of PCR products used for generating different fusion constructs. PCR products from primer combinations 1-4 (listed in Table 2) prior to fusion PCR. Sizes of relevant fragments from *Bst*EII-digested bacteriophage lambda DNA are indicated to the left. Gel was stained with ethidium bromide.

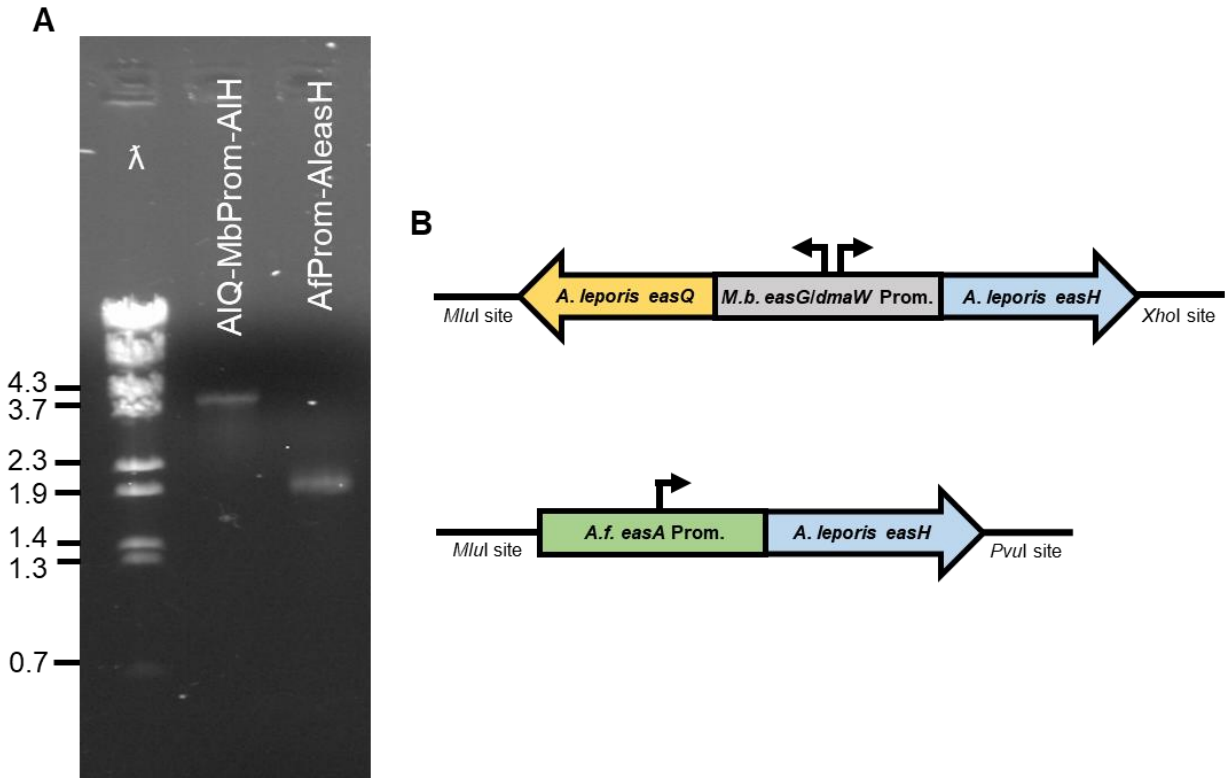


Fig 17. Construction of the *A. leporis easQ*-*M. brunneum* promoter-*A. leporis easH* and *A. fumigatus* promoter-*A. leporis easH* expression constructs. (A) PCR products from primer combinations 6 and 7 (Table 2) prior to ligation into vector backbone. Sizes of relevant fragments from *Bst*EII-digested bacteriophage lambda DNA are indicated to the left. Gel was stained with ethidium bromide. AIQ-MbProm-AIH, *A. leporis easQ* – *M. brunneum easG/dmaW* promoter – *A. leporis easH* fusion product; AfProm-AIH, *A. fumigatus easA* promoter – *A. leporis easH* fusion product. (B) Graphics displaying the orientation and components of the AIQ-MbProm-AIH and AfProm-AIH expression constructs. Prom., promoter.

Table 1. Accumulation (mean \pm standard error; n = 7) of chanoclavine-I and fumigaclavine A in cultures of *A. leporis* grown in sucrose-yeast extract medium for 14 days at 30 °C

Strain	Chanoclavine-I (nmol/g fungus)	Fumigaclavine A (nmol/g fungus)	Percent conversion ^a
<i>A. leporis</i> NRRL 3216	92 \pm 7 A ^b	84 \pm 21 A	43 \pm 7 A
<i>A. leporis easD ko</i>	454 \pm 91 B	274 \pm 41 B	40 \pm 3 A

^aPercent of chanoclavine-I converted to fumigaclavine A

^bMeans within a column that differ significantly ($P < 0.05$) are indicated with different letters

Table 2. Primers and PCR Protocol Information

Primer pair	Primer sequences (5' to 3') ^a	Product (length in base pairs)	Annealing temperature (°C), Extension time (s)
1	CTCA <u>ACGCGT</u> GAACGAATAGACGTCGACCC + CCATCTCGGAAAAGAAAAATGTCGGGATTCGTGGTCCA	<i>A. leporis easQ</i> + overlap with <i>M. brunneum easG/dmaW</i> promoter (1877 bp)	63, 60
2	TGGACCACGAATCCCGACATTTTTCTTTTCCGAGATGG + CGGTGGTGGGAACCGTCATCGTAAACCAGAGTATTATG	<i>M. brunneum easG/dmaW</i> promoter + overlaps for <i>A. leporis easQ</i> & <i>A. leporis easH</i> (1325 bp)	53, 60
3	CATAATACTCTGGTTTACGATGACGGTCCCACCACCG + CGT <u>ACTCGAGCAGCAAGGGGTAGGGAATGA</u>	<i>A. leporis easH</i> + overlap with <i>M. brunneum easG/dmaW</i> promoter (1140 bp)	64, 60
4	CGTA <u>ACGCGT</u> GCTTCTAATCCACCAAGTACTTG + CGGTGGTGGGAACCGTCATGGTGCGGAGTGCCTACTCTA	<i>A. fumigatus easA</i> promoter + overlap with <i>A. leporis easH</i> (827 bp)	65, 30

5	TAGAGTAGGCACTCCGCACCATGACGGTCCCACCACCG + CGTATCTAGACAGCAAGGGGTAGGGAATGA	<i>A. leporis easH</i> + overlap with <i>A. fumigatus easA</i> promoter (1140 bp)	64, 60
6	CTCAACGCGTGAACGAATAGACGTCGACCC + CGTACTCGAGCAGCAAGGGGTAGGGAATGA	<i>A. leporis easQ</i> – <i>M. brunneum easG/dmaW</i> promoter – <i>A. leporis easH</i> fusion (4281 bp)	72, 150
7	CGTAAACGCGTGCTTCTAATCCACCAAGTACTTG + CGTACTCGAGCAGCAAGGGGTAGGGAATGA	<i>A. fumigatus easA</i> promoter – <i>A. leporis easH</i> fusion (1916 bp)	72, 60
8	TCCGCCAATTAGGGTTCGAC + CAGCGTACCGACCTCCATC	<i>A. leporis easQ</i> – <i>M. brunneum easG/dmaW</i> promoter – <i>A. leporis easH</i> -pBChygro mutant verification (3914 bp)	65, 120
9	TCCGTCTCCATTGGCTCTTG + CTATTCCTTTGCCCTCGGAC	Verification of hygromycin resistance gene in <i>M. brunneum</i> mutants (1835 bp)	64, 60
10	GAAGAGACTGAGGGTGGTGG + AACAAGCAAGCCCAAGCAAC	<i>A. fumigatus easA</i> promoter – <i>A. leporis easH</i> fusion – pBCphleo mutant verification (1309 bp)	64, 60

11	GTACCCGGGGATCTTTTCGAC + ACCAAAGGCCATCTTGGTAC	Verification of phleomycin resistance gene in <i>A. fumigatus</i> mutants (2644 bp)	63, 90
12	CAATCCTCAGTGCGCTACAAG + GACGCATGTTGCGCCATTC	<i>A. leporis easH</i> fragment (446 bp cDNA and genomic DNA)	64, 30
13	GCTGGAGCGTATGAACGTC + GTTGTTACCAGCACCGGAC	<i>A. fumigatus βtub</i> fragment (172 bp cDNA and 237 bp genomic DNA)	65, 30

^a Underlines indicate unique restriction sites used for cloning fusion PCR product: ACGCGT: *Mlu*I, CTCGAG: *Xho*I, and TCTAGA: *Xba*I

Chapter 4

Localization of EasT, a novel ergot alkaloid transporter protein

Abstract

Ergot alkaloids are a group of specialized metabolites that exhibit diverse pharmaceutical properties and are produced by various species of fungi. Purification and chemical modification of ergot alkaloids has facilitated the development of medicines aimed at a variety of neurological diseases and disorders including migraines, dementia, Parkinson's disease, and others. This study focuses on the localization and function of EasT, a putative membrane-bound transporter hypothesized to be involved in ergot alkaloid biosynthesis in the soil saprotroph *Aspergillus leporis*. Initial protein sequence analysis of EasT indicated a resemblance to membrane-bound major facilitator superfamily transporters from other fungi, including vesicular amine transporters and multidrug resistance pumps. Fusion of CFP to EasT at either the C- or N-terminus and subsequent transformation into *Aspergillus fumigatus*, a clinically significant ergot alkaloid producer, was employed to study localization of EasT and its effect on the levels of fumigaclavines and other, precursor ergot alkaloids within the fungus. Another set of strains was prepared by first transforming *A. fumigatus* with mCherry tagged for peroxisomal localization before addition of either EasT-CFP or CFP-EasT. The results indicate that EasT alters the ergot alkaloid profile of *A. fumigatus* and localized to discrete enclosures within the cytoplasm of the fungus, as opposed to plasma membrane. These particles were distinct from peroxisomes and potentially correspond to vesicular structures. The findings suggest that EasT plays a role in the transport of ergot alkaloids or their intermediates between subcellular compartments,

contributing to the regulation of their biosynthesis. This study enhances our understanding of the biosynthesis and trafficking of ergot alkaloids, providing insight into their cellular dynamics.

Introduction

Ergot alkaloids are a group of specialized metabolites produced by several different species of fungi and possess a variety of different pharmaceutically relevant properties (Schardl et al 2006; Wallwey and Li 2011; Florea et al 2017; Tasker and Wipf 2021; Robinson and Panaccione 2015). Species of ergot alkaloid-producing fungi capable of infecting grain crops have historically caused mass poisoning events, with symptoms of ergotism including convulsions, hallucinations, and gangrene (Haarmann et al 2009). More recently, medicines aimed at treating migraines (Rothlin 1955), dementia (Flynn and Ranno 1999), Parkinson's disease (Montastruc et al. 1993), and other health conditions have been developed by utilizing the property of ergot alkaloids to bind to different neurological receptors (Pertz et al. 1999).

The main classes of ergot alkaloids include clavines, lysergic acid amides, and ergopeptines. Some fungi in the Aspergillaceae, such as *Aspergillus fumigatus*, produce festuclavine and fumigaclavines (Coyle et al. 2005) while fungi in several genera of the family Clavicipitaceae including *Metarhizium brunneum* and *Epichloë festucae* produce lysergic acid and its downstream derivatives (Leadmon et al. 2020, Schardl et al. 2013). The enzymatic steps in most branches of the ergot alkaloid have been characterized, with biosynthesis of the major branchpoint intermediate, chanoclavine-I aldehyde, requiring a set of five genes (*dmaW*, *easF*, *easE*, *easC*, and *easD*) shared by most ergot alkaloid producers (Tsai et al. 1995, Rigbers et al. 2008, Lorenz et al. 2010, Goetz et al. 2011, Yao et al. 2021, Wallwey et al. 2010a). The combination of other tailoring genes present in an organism's ergot alkaloid biosynthetic gene cluster (BGC) then determines which major class(es) of ergot alkaloids are produced (Cheng et al. 2010a, Cheng et al. 2010b, Coyle et al. 2010, Wallwey et al. 2010b, Matuschek et al. 2011, Haarmann et al. 2006, Robinson and Panaccione 2014, Bragg et al. 2017, Arnold and Panaccione

2017, Steen et al. 2021, Davis et al. 2020, Correia et al. 2003, Ortel and Keller 2009, Havemann et al. 2014, Bilovol and Panaccione 2016, Liu et al. 2009).

The genes responsible for specialized metabolite biosynthesis in fungi are typically clustered close together on a chromosome in a BGC, allowing for their co-regulation. Different bioinformatic tools such as fungiSMASH and SMURF have been developed to mine fungal genomes for BGCs and to predict their potential products based upon the protein domains present (Blin et al. 2019). These techniques can be combined with traditional gene knockout, heterologous expression, and *in vivo* enzyme studies to allow for the characterization of enzyme activities. The subcellular localization of, and interactions between, individual enzymes is understudied in comparison and is further complicated by the highly dynamic nature of fungal cells and their organelles (Read 2018).

Synthesis of specialized metabolites requires multiple steps. Some steps may occur in the cytosol, whereas as others may occur in subcellular compartments. Localization of enzymes and movement of pathway intermediates is important in completing a pathway. To date, few published studies have investigated the location of ergot alkaloid synthesis at a subcellular level, but considerable research has been done on the synthesis of two other groups of fungal specialized metabolites—aflatoxins and trichothecenes. Aflatoxins are a group of highly carcinogenic polyketide hepatotoxins produced primarily by *Aspergillus parasiticus* and *Aspergillus flavus* (Frisvad et al. 2019). Aflatoxin biosynthesis has been studied extensively and all 25 genes and their enzymatic activities have been characterized previously (reviewed by Caceres et al. 2020). The subcellular localization of many of these enzymes has also been studied using a combination of different techniques including fluorescence protein fusions and immunofluorescence microscopy. Production of aflatoxins has been shown to rely on the co-

localization of vesicles, enzymes, and other cellular machinery into concentrated areas dubbed aflatoxisomes (Chanda et al. 2009). Trichothecenes are a group of >200 sesquiterpene mycotoxins produced by different genera of fungi including several *Fusarium* species (Grove 2007). Previous studies have identified regions of *F. graminearum* hyphae that resemble aflatoxisomes (referred to as simply “toxisomes”) which have been shown to involve the reorganization of the endoplasmic reticulum (ER) and the transport of vesicles by way of actin filaments (Menke et al. 2013, Boenisch et al. 2017).

The localization of each enzymatic step in the ergot alkaloid pathway is still in the early stages of investigation. Work by Nielsen et al. (2014) determined that EasE relies on the presence of ER-targeting signal for activity in yeast, but a putative peroxisomal-targeting signal present in EasC was found to be nonessential. Recently, our lab (Jones et al. 2021) identified a putative membrane-bound transporter gene present in one of the lysergic acid α -hydroxyethylamide (LAH) gene clusters within *Aspergillus leporis*, a member of the *Aspergillus* section Flavi originally isolated from rabbit dung (States and Christensen 1966). Initial studies have determined that the transporter encoded by this gene, dubbed *easT*, is not responsible for the high amount of ergot alkaloid secretion observed in this fungus, but knockout of the gene reduces the overall yield of ergot alkaloids (Jones, unpublished). Heterologous expression of *easT* in a strain of *A. fumigatus* previously engineered to produce lysergic acid again did not improve secretion but did affect accumulation of pathway intermediates and end product (Jones, unpublished). These observations indicate that the product of *easT* significantly affects accumulation but not secretion of ergot alkaloids. The objective of this present study was to tag EasT using a fluorescent label to visualize localization of the transporter when introduced into *A. fumigatus*.

Results

EasT protein sequence comparisons and analysis.

The product of the predicted *easT* gene without introns was used as the subject of a BLASTp search. The results of this search indicated that EasT is similar to a number of other major facilitator superfamily transporters, general substrate transporters, and multidrug resistance efflux pumps from other fungi. One match included a vesicular amine transporter from *Aspergillus uvarum* with 97% query coverage and 51% amino acid sequence identity ([XP_025489032.1](#)). Other matches included the tetracycline resistance protein TetA from *Penicillium expansum* ([KGO39363.1](#)) with 94% query coverage and 49% amino acid sequence identity and the pyrrolopyrazine cluster-associated transporter *ppzB* from *Metarhizium rileyi* ([A0A166Z003.1](#)) with 92% query coverage and 51% amino acid sequence identity.

Hydrophobicity analysis of EasT using the TMHMM program (Krogh et al. 2001) predicted 12 transmembrane segments which is also supported by a Kyte-Doolittle Hydropathy plot (Fig. 1) (Kyte and Doolittle 1982). The presence of 12 transmembrane domains is consistent with other members of the major facilitator superfamily of membrane transporters (Reddy et al. 2012).

EasT expression alters *A. fumigatus* ergot alkaloid profile.

To test the localization of EasT, the gene encoding it from *A. leporis* was cloned into cyan fluorescent protein (CFP) expression vectors for tagging at either the N- or C-terminus. The combined protein-encoding sequences were placed under control of the *A. fumigatus* *gpdA* promoter. A strain of *A. fumigatus* was also engineered using a plasmid for constitutive mCherry with the C-terminal PTS1 tripeptide (-SKL) for peroxisomal targeting (Elleuche and Pöggeler 2008). Both the peroxisomal-labeled strain and the wild-type fungus were transformed with the CFP-EasT (i.e., amino terminal labeled) and EasT-CFP (carboxy terminal labeled) vectors. The

presence of mCherry-SKL, either EasT-CFP fusion construct, and marker conferring resistance to hygromycin/phleomycin in each of the four mutants was confirmed by PCR (Fig. 2 and 3). To test whether active enzyme was being expressed, solid (combination of hyphae, conidiophores, and conidia) and liquid (culture fluids) phases of independent cultures of wild-type and all four mutant *A. fumigatus* strains grown in malt extract medium for 8 days were analyzed by high-performance liquid chromatography (HPLC) with fluorescence detection and compared to a fumigaclavine A standard curve. A peak eluting at 43.8 min matched the peak representing the fumigaclavine A standard in retention time and fluorescence properties. Peaks corresponding to fumigaclavine B (22.0 min), chanoclavine-I (30.0 min), festuclavine (41.4 min), and fumigaclavine C (59.0 min) were deduced based on their fluorescence properties, and their elution times, and their presence or absence in previously engineered mutants of *A. fumigatus* (Coyle and Panaccione 2005, Coyle et al. 2010, Goetz et al. 2011, Bilovol and Panaccione 2016). The average concentration of each ergot alkaloid in solid and liquid phases was calculated from six samples, and heterologous expression of EasT significantly decreased accumulation of total ergot alkaloids in the solid phases of *A. fumigatus* strains expressing the EasT-CFP fusion, while CFP-EasT seemed to have less of an impact (Figure 4; Table 1). In liquid phases, mutants expressing EasT tagged on either terminus accumulated similar quantities of ergot alkaloids compared to the wild type, though modest increases in secreted festuclavine and fumigaclavine B were observed in some mutants (Figure 4). Secretion of two intermediates in the fumigaclavine pathway was affected in some but not all *easT*-expressing strains (Table 2). One of four *easT*-expressing strains secreted significantly more festuclavine than the wild type and three of four secreted more fumigaclavine B. None of the *easT*-expressing mutants varied significantly from

the wild type in secretion of the pathway end product (fumigaclavine C) or in secretion of total ergot alkaloids.

Localization of CFP-EasT and EasT-CFP in *A. fumigatus*.

Hyphae and conidiophores of all four mutants (wildtype + EasT-CFP, wildtype + CFP-EasT, mCherry-SKL + EasT-CFP, and mCherry-SKL + CFP-EasT) were analyzed using fluorescence microscopy to determine the localization of EasT within the cells of mutants. Small spherical structures corresponding to peroxisomes could be seen in hyphae of either mCherry-SKL mutant strain (Figs. 5A and 6A). Smaller, discrete CFP-labeled spheres were found throughout hyphae and localized independently of the tagged peroxisomes. These smaller structures seemed to correspond to some type of budding vesicle that can be seen throughout conidiophores under DIC lighting (Figs. 5B and 6B). The localization of EasT to these spheres occurred regardless of the N- or C-terminal tag, a feature which is common in integral membrane proteins as the transmembrane domains are known to influence localization (Cosson et al. 2013, Guna and Hegde 2018). Expression of *easT*-CFP and CFP-*easT* transcripts and synthesis of corresponding proteins were confirmed via RT-PCR and western blotting (Fig. 7). Both mutants successfully transcribed mRNA with the expected size of the fusion product with introns spliced out (Fig. 7A). The expected fusion proteins of 82 kD were also confirmed in membrane fractions of proteins isolated from both mutants (Fig. 7B).

Discussion

The ability of EasT to alter ergot alkaloid accumulation and its localization to discrete spots throughout fungal cells correlates well with its predicted function as a membrane-bound

transporter of ergot alkaloids and/or pathway intermediates. BLASTp and hydropathy analyses show that EasT possesses a 12 transmembrane domain (TMD) structure like that of other major facilitator superfamily (MFS) proteins. Other matches included vesicular amine transporters which are responsible for transport of neurotransmitters in mammals (Blakely and Edwards 2012). The resemblance of ergot alkaloids to neurotransmitters supports a role for this type of transporter.

The microscopy data presented here indicate a role for EasT in transport of ergot alkaloids and/or their intermediates into or out of small subcellular compartments. Trafficking of pathway intermediates into subcellular compartments within cells is a common feature for mycotoxin biosynthesis as is seen with toxisomes associated with aflatoxin and trichothecene synthesis which result from various vesicle-vacuole fusions along a biosynthetic pathway (Keller 2015). EasT localizes to discrete spots which resemble small vesicles along some internal structure within fungal cells and its resemblance to other vesicular amine transporters hints to this role in *A. leporis*. Mutants expressing mCherry targeted to peroxisomes showed localization independent of EasT, indicating that EasT is targeted to some other membrane-bound structure or organelle. These results are consistent with the role of EasT as a transporter involved in ergot alkaloid production.

The gene encoding EasT was introduced into *A. fumigatus*, a species which produces fumigaclavines in a system that has not been documented to require any related transporters but may rely on transporters encoded outside of the *eas* cluster. Expression of *easT* in the otherwise functioning fumigaclavine pathway of *A. fumigatus* had negative consequences for fumigaclavine accumulation. *Aspergillus fumigatus* presumably has evolved its own mechanisms for completing its ergot alkaloid pathway and expressing an additional transporter (which was

done here primarily for localization purposes) interfered with fumigaclavine accumulation in some of the *easT*-expressing strains. Wild-type *A. fumigatus* transformed with EasT fused to CFP at either the C- or N-terminus showed a decrease in production of most of its ergot alkaloid profile. The impact of EasT was more significant when CFP was fused to the C-terminus, indicating that there may be some form of interference in the N-terminal fusion protein. Other studies have shown that MFS proteins can be tagged with little to no difference in their performance relative to non-tagged (native) versions (Chen et al. 2021). Despite the interference of EasT with fumigaclavine accumulation, the data support a role for this protein in moving ergot alkaloid pathway intermediates within the cell.

The decrease in total concentrations of ergot alkaloids seen in mutants expressing EasT could be due to intermediates being sequestered away from the native enzymes with some (e.g., fumigaclavine B) possibly “leaking” out of cells. This “leaking” could be due to exocytosis of fused vesicles (or toxisomes) or by some unknown mechanism not involving EasT following sufficient vesicle fusion and toxisome accumulation. This exocytosis scenario is supported by an increase in the amounts of festuclavine and fumigaclavine B secreted in some of the *easT*-expressing mutants along with a lack of observed EasT localization to the plasma membrane. A similar process involving fused vesicles being released from cells occurs during aflatoxin biosynthesis and secretion in *A. parasiticus* (Roze et al. 2011, Kenne et al. 2014).

Overall, EasT appeared to localize to discrete regions of *A. fumigatus* cells resembling vesicles and, in the heterologous system in which it was expressed, impacted the production of fumigaclavines negatively. Results from *A. leporis* (Jones, unpublished) have indicated that EasT plays a positive role in promoting lysergic acid amide accumulation and has no significant role in their secretion. Taken together, these observations suggest that EasT is not a plasma

membrane exporter of ergot alkaloids but rather plays a role in the intracellular transport of ergot alkaloids or their precursors.

Methods

Growth and maintenance of fungi. Cultures of wild-type *A. fumigatus* FGSC A1141 (=WVU1943) (Coyle and Panaccione 2005) and its transformants were grown on malt extract agar (MEA) medium (per liter, per liter, 6.0 g malt extract, 1.8 g maltose, 6.0 g dextrose, 1.2 g yeast extract, and 15 g agar) at 37 °C. Cultures of wild-type *A. leporis* NRRL 3216 were maintained on sucrose-yeast extract (SYE) agar medium (per liter, 20 g sucrose, 10 g yeast extract, 1 g magnesium sulfate-heptahydrate, and 15 g agar).

Preparation of transformation constructs. Genomic DNA (gDNA) was extracted from wild-type *A. fumigatus* and wild-type *A. leporis* samples according to the GeneClean spin protocol (MP Biomedicals, Solon, OH). The *A. fumigatus* gDNA was used as template in a PCR with primer combination 1 (Table 3) to generate the *A. fumigatus* GPDH promoter (nucleotides 3,418,743 to 3,419,708 of GenBank accession number [VBRB01000006.1](#)) fragment with restriction sites for *SacI* and *SpeI* near the termini (Fig 6). These and all subsequent PCRs were performed with Phusion green hot start II high-fidelity PCR master mix (Thermo Scientific, Waltham, MA) and followed similar protocols as described previously by Davis et al. (2020) and with primers and reaction conditions detailed in Table 3. All PCR products were gel purified using a ZymoClean gel DNA recovery kit (Zymo) prior to performing ligation. pBChygro (Fungal Genetics Stock Center, Manhattan, KS; Silar 1995) plasmid was used as template with primer combination 2 to amplify the hygromycin resistance gene along with the accompanying

promoter and 3' untranslated region (3'UTR) (Fig. 6). The phleomycin resistance gene and flanking regions were similarly amplified from pBCphleo plasmid (Fungal Genetics Stock Center, Manhattan, KS; Silar 1995) using primer combination 3 (Fig. 6). Primer sets 2 and 3 included restriction sites for *SbfI* near both termini—allowing for digestion, purification, and subsequent ligation into downstream vectors.

pDS221 plasmid (Addgene plasmid #34981; Strickland et al. 2012) was used with primer combination 4 to amplify the mCherry gene and introduced an additional set of bases (TCGAAGTTGTAG) coding for the peroxisomal targeting signal and a stop codon (Fig 6). Additionally, the primers included restriction sites for *SpeI* and *Sall*. The plasmid pAG426GPD-EYFP-*ccdB* (Addgene plasmid #14348) was used as a backbone for mCherry expression experiments. The native promoter in this plasmid was excised via double-digestion using *SacI/SpeI*. This and all subsequent digestions were gel purified using a ZymoClean gel DNA recovery kit (Zymo) prior to performing ligation. The *A. fumigatus* GPDH promoter was similarly double-digested and purified before both fragments were ligated together, generating AfGPDH-EYFP-*ccdB*. One Shot™ *ccdB* Survival™ 2 T1^R cells (Thermo Scientific, Waltham, MA) were used for propagation of this and all other plasmids containing the *ccdB* gene. Bacterial transformants were plated on LB medium (per liter, 10 g tryptone, 5 g yeast extract, 5 g NaCl, and 15 g agar) supplemented with chloramphenicol (25 µg/mL). These and all other plasmid products were harvested from selected colonies and purified using a Zyppy plasmid miniprep kit (Zymo). AfGPDH-EYFP-*ccdB* and the hygromycin cassette fragment were then digested using *SbfI*, purified, and ligated together, generating AfGPDH-EYFP-*ccdB*-HygR. The EYFP-*ccdB* portion of this plasmid was then excised using *SpeI/SalI* while the same enzyme pair was used to treat the mCherrySKL fragment. The gel purified fragments were then ligated together

generating AfGPDH-mCherrySKL-HygR. This plasmid did not require *ccdB*-competent *E. coli* cells and transformants were plated on LB medium supplemented with ampicillin (100 µg/g/mL). Primer combination 5 was used to verify correct assembly of the AfGPDH-CherrySKL portion and its presence in fungal transformants (Fig. 2).

The *A. leporis* gDNA was used as template with primer combination 6 to amplify *A. leporis easT* without the native stop codon (nucleotides 24,443 to 26,176 from Genbank accession number [SWBU01000104.1](https://www.ncbi.nlm.nih.gov/nuccore/SWBU01000104.1)) (Jones *et al.* 2023). Primer combination 7 was used to amplify the same region, albeit with the native stop codon and 3'UTR (nucleotides 24,187 to 26,176 from same accession). The plasmids pAG426GPD-*ccdB*-Cerulean and pAG426GPD-Cerulean-*ccdB* (Addgene plasmids #14396 and #14420, respectively) were digested using *SacI/SpeI* and gel purified. Both fragments were ligated using the AfGPDH promoter fragment, generating AfGPDH-*ccdB*-Cerulean and AfGPDH-Cerulean-*ccdB*. The phleomycin resistance cassette fragment was then digested using *SbfI* before being ligated into both plasmids, generating AfGPDH-*ccdB*-Cerulean-PhleoR and AfGPDH-Cerulean-*ccdB*-PhleoR. These plasmids served as recipients in exponential megapriming PCR reactions (Ulrich *et al.* 2012, Lund *et al.* 2014) using primer sets 8 and 9 together with the products generated from combinations 6 and 7, respectively, which served as the megaprimers. The linear products (Fig. 7) were then purified, phosphorylated, and self-ligated, generating AfGPDH-*easT*-Cerulean-PhleoR and AfGPDH-Cerulean-*easT*-PhleoR plasmids for *E. coli* transformation. Primer combinations 10 and 11 were used to verify correct assembly of the AfGPDH-*easT*-Cerulean and AfGPDH-Cerulean-*easT* and portions, respectively, and their presence in fungal transformants (Fig. 2).

Transformation of *A. fumigatus*. To test whether EasT potentially co-localizes with peroxisomes, protoplasts of wild-type *A. fumigatus* FGSC A1141 were prepared and transformed with AfGPDH-mCherrySKL-HygR according to a previously described protocol (Bilovol and Panaccione 2016). Transformants were plated in TM102 supplemented with hygromycin (InvivoGen, San Diego, CA) at 200 $\mu\text{g}/\text{mL}$ and incubated at 37 °C. Upon surfacing, colonies were transferred to MEA supplemented with hygromycin at 100 $\mu\text{g}/\text{mL}$ and incubated at 37 °C to allow further growth under selection. Genomic DNA was extracted from selected colonies and checked by PCR for presence of the hygromycin resistance cassette (primer combination 2) and AfGPDH-mCherrySKL (primer combination 5) (Figs. 2 and 3). Once a desired mutant was obtained, this strain and wild-type *A. fumigatus* were used as the recipients for both AfGPDH-*easT*-Cerulean-PhleoR and AfGPDH-Cerulean-*easT*-PhleoR plasmids. Transformations and plating were carried out as described above, with the substitution of phleomycin at the same concentrations as hygromycin. Genomic DNA was extracted from selected colonies and checked by PCR for presence of the phleomycin resistance cassette (primer combination 3) and either AfGPDH-*easT*-Cerulean (primer combination 10) or AfGPDH-Cerulean-*easT* (primer combination 11) (Figs. 2 and 3).

Sample preparation and alkaloid analyses. Small petri dishes with 5 mL malt extract medium inoculated with 100,000 conidia per plate and grown for 8 days at 37 °C in darkness. Solid mats containing hyphae, conidiophores, and conidia were separated from the remaining liquid medium by vacuum filtration through nylon filters. The filters were dried in petri dishes at 35 °C in total darkness until completely dry before measuring total fungal mass. The portion recovered from each filter was then recorded before being extracted using a 20X volume of methanol (50 mg per mL). Liquids were collected through a funnel into falcon tubes and the volume of each sample

was measured by pipetting. A 0.5 mL portion of the liquid was mixed with an equal volume of methanol, and both solid and liquid portions were centrifuged to pellet solid material before HPLC with fluorescence detection. Peak areas of festuclavine, fumigaclavine A, fumigaclavine B, and fumigaclavine C were used to approximate their quantities relative to an external standard curve generated using known concentrations of pure fumigaclavine A standard (Alexis 411 Biochemicals, San Diego, CA). Thus, the quantities of festuclavine, fumigaclavine B, and fumigaclavine C are relative to fumigaclavine A and not absolute. Chanoclavine-I peak areas were used to approximate their quantities relative to an external standard curve generated using known concentrations of pure chanoclavine-I standard (obtained from Dr. Miroslav Flieger, The Czech Academy of Sciences, Czech Republic). Samples were analyzed for ergot alkaloids by HPLC with fluorescence detection by methods described in detail previously (Panaccione et al. 2012). The column was a 150- by 4.6-mm inner-diameter, 5- μ m particle size Prodigy C₁₈ column (Phenomenex, Torrance, CA), and the mobile phase was a 55-min, binary, multilinear gradient of 5% acetonitrile to 75% acetonitrile in 50 mM aqueous ammonium acetate. Ergot alkaloids were detected using excitation and emission wavelengths of 272 nm and 372 nm, respectively. For secretion analyses, alkaloids were quantified according to Davis et al. (2020).

Statistical analyses. Concentrations of chanoclavine-I, festuclavine, and fumigaclavines A, B, and C in cultures (n = 6) of wild-type, EasT-CFP, CFP-EasT, mCherry-SKL + EasT-CFP, and mCherry-SKL + CFP-EasT strains of *A. fumigatus* were measured as described above (under HPLC analyses) and used to calculate the total nmol produced per gram fungus (Table 1) and secretion (Table 2) of each product. Data were checked by Brown-Forsythe tests for normality of variances. The variances for chanoclavine-I, festuclavine, fumigaclavine B, and fumigaclavine C, and total ergot alkaloid accumulation as well as fumigaclavine B and fumigaclavine C secretion

were found to be normally distributed by Brown-Forsythe tests ($P > 0.05$) and were subsequently analyzed using ANOVA and, when ANOVA indicated a significant effect of strain, Tukey's HSD test to test for differences among means by strain. Data for fumigaclavine A accumulation and the secretion of chanoclavine-I and festuclavine did not pass Brown-Forsythe tests ($P < 0.05$) and were therefore analyzed with nonparametric tests. These data were initially tested using Wilcoxon's signed-rank test and, when Wilcoxon's test indicated a significant effect of strain, a Steel-Dwass multiple comparison test to assess differences among means by strain. All statistical analyses were performed with the JMP software package (SAS, Cary, NC).

Fluorescence Microscopy. To observe the expression of fluorescent proteins, 5×10^3 conidia of each mutant strain were suspended in 200 μ L of malt extract medium (lacking agar) in wells of Nunc™ Lab-Tek™ II chamber slides (Thermo Scientific, Waltham, MA) and incubated in humidified chambers in total darkness at 37 °C for 24 hours. Each chamber was rinsed twice with 200 μ L PBS, mounted using SlowFade Glass Soft-set Antifade medium (Thermo Scientific, Waltham, MA) and a # 1.5 coverslip, and were then sealed using clear nail polish. A Zeiss LSM 710 Confocal microscope with AiryScan equipped with an AxioObserver.Z1 (Carl Zeiss AG, Oberkochen, Germany) was used to image slides of mounted cells. ZEN lite 2011 software was used for image generation and analysis (Carl Zeiss AG).

RT-PCR. Cultures of the wild-type *A. fumigatus* and EasT-CFP-expressing and CFP-EasT-expressing *A. fumigatus* mutants were grown in 25 mL malt extract medium (lacking agar) inside of deep-dish culture plates and incubated at 37°C for 24 hours in total darkness. The plates were kept still to ensure formation of a single mat of hyphae on the surface of the broth with sparse conidia beginning to develop. RNA was extracted from approximately 100 mg of a conidiating portion of the mat with the Plant RNeasy kit (Qiagen), treated with DNase I (Qiagen), and

reverse transcribed with Superscript IV (Invitrogen, Carlsbad, CA). RNA extraction and cDNA synthesis were performed concurrently. Template cDNA was diluted 1:20 prior to PCR amplification. Primer combinations 12 and 13 were used to amplify portions of the *easT*-CFP and CFP-*easT* fusions, respectively, from either cDNA sample as well as from gDNA isolated from a malt extract agar culture of either mutant. Primers were designed such that they included part of the CFP portion and flanked all *easT* introns.

Western Blotting. The Mem-PER™ eukaryotic membrane protein extraction kit (Thermo) was used to extract membrane proteins from ~100 mg of the same mutants used for RNA extraction above. Protein fractions were quantified using a Pierce™ BCA assay kit (Thermo). SDS-PAGE was carried out by loading 20 µg of protein from duplicates of each mutant's membrane fraction into wells of a Novex™ Tris-Glycine, 4-20% polyacrylamide Mini Gel (Thermo). The gel was run at 60-120 mV for 1.5 hours in Tris-glycine running buffer (25 mM Tris, 192 mM glycine, 0.1% SDS, pH 8.3). Proteins were transferred to a nitrocellulose membrane using an Owl™ HEP Series Semidry Electroblothing system (Thermo) and Bjerrum Schafer-Nielsen transfer buffer (48 mM Tris, 39 mM glycine, 20% methanol, 0.04% SDS, pH 9.2) at 15 V constant for 1 hour. The membrane was rinsed in Tris-buffered saline (TBS; 0.05 M Tris, 0.15 M sodium chloride, pH 7.6) and blocked using 3% gelatin in TBS for 1 hour at room temperature. A monoclonal rabbit anti-GFP antibody (Cell Signaling Technology) was diluted 1:1000 in TBS + Tween 20 (TBST; Tris-buffered saline + 0.1% Tween 20) with 1% gelatin for incubation with the membrane overnight at 4 °C. The membrane was then rinsed three times for 5 min each with TBST. Immun-Blot goat anti-rabbit IgG-Alkaline Phosphatase (GAR-AP) conjugate antibody (Bio-Rad) was diluted 1:3000 in TBST with 1% gelatin and incubated with the membrane at room temperature for 1 hour. The membrane was then rinsed three times for 5 min each with TBST

followed by one 5-min wash in TBS before the colorimetric developing solution (Bio-Rad) was added. The reaction was quenched after 4 hours by rinsing with pure water and the membrane was photographed using a lightbox and iPhone camera. The image was changed to monotone and the contrast settings were adjusted to boost band visibility.

Acknowledgements

This research was funded by NIH grant 2R15-GM114774-3, with additional salary support for D.G.P. from USDA Hatch project NC1183.

pDS221 was a gift from Dr. Michael Glotzer. pAG426GPD-EYFP-*ccdB*, pAG426GPD-*ccdB*-Cerulean, and pAG426GPD-Cerulean-*ccdB* were gifts from Dr. Susan Lindquist. Special thanks to Dr. Amanda Ammer (ZEISS Microscopy) and Dr. Neil Billington (WVU) for their assistance and training on the Zeiss 710 machine. Dr. Joe Lynch (WVU) provided valuable advice and guidance for performing Western Blots.

Imaging experiments were performed in the WVU Imaging Facilities which have been supported by the WVU Cancer Institute, the WVU HSC Office of Research and Graduate Education, and NIH grants P20RR016440, P30GM103488, P20GM121322, and U54GM104942. Addition support for the Zeiss LSM 710 with Airyscan was provided by NIH grants P30GM103503 and P20GM103434.

Figures and Tables

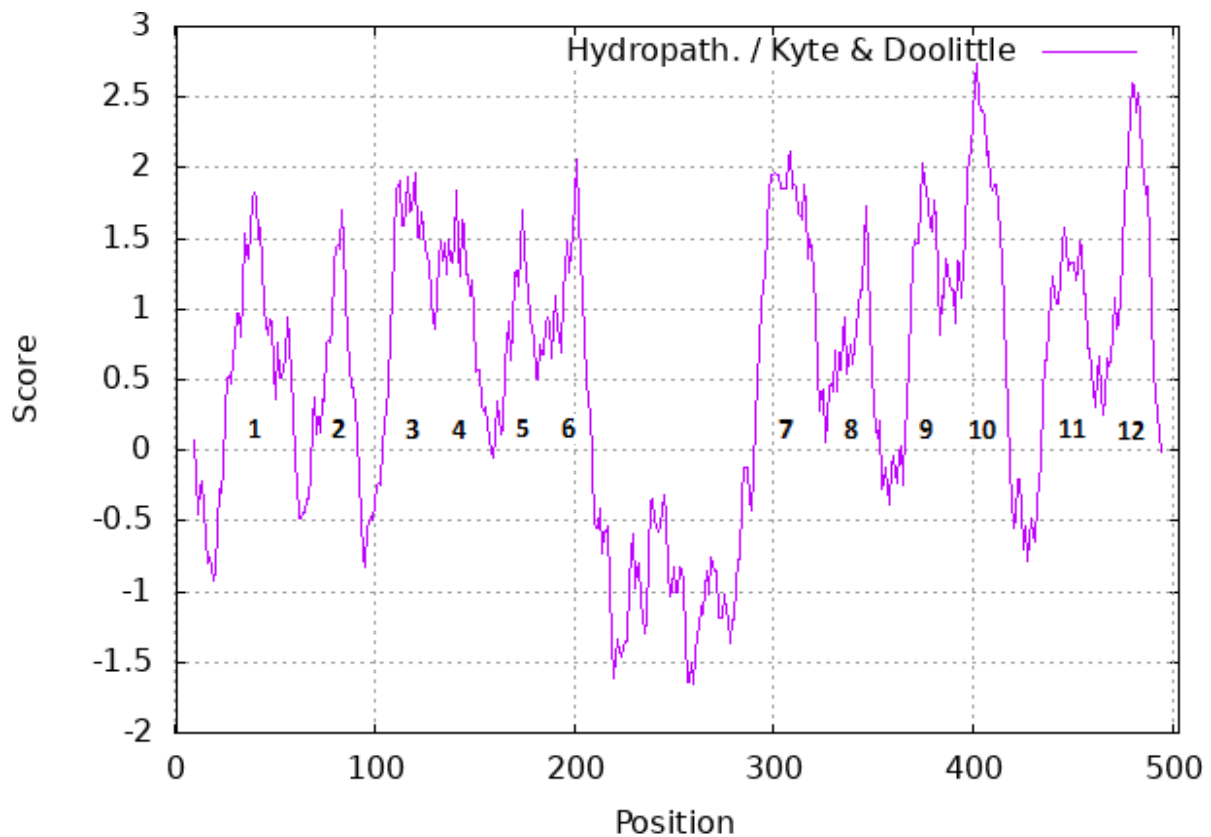


Fig 1. Kyte-Doolittle Hydropathy plot derived from EasT amino acid sequence. A window size of 19 amino acids was used to search for transmembrane regions in this protein. The hydrophobic residues are shown above zero, whereas the hydrophilic residues are below zero. Derived hydrophobic regions are numbered. Generated using ProtScale (web.expasy.org)

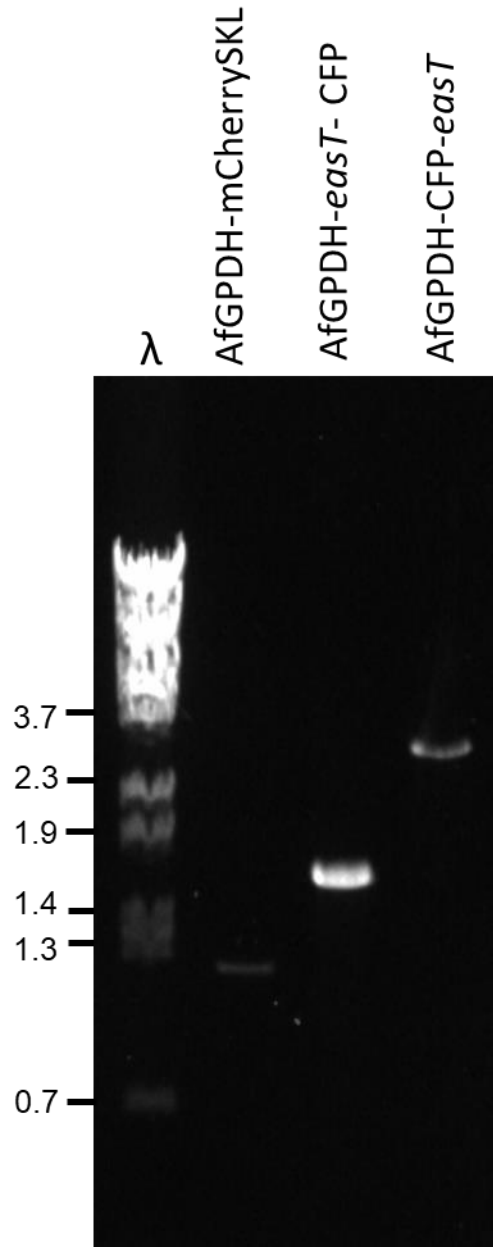


Fig 2. Verification of construct presence in mutants. DNA gel showing amplified mCherry fusion with promoter and both versions of tagged EasT with promoter amplified from mutant genomic DNA using primer combinations 5 and 10-11 (listed in Table 3). Sizes of relevant fragments from *Bst*EII-digested bacteriophage lambda DNA are indicated to the left. Gel was stained with ethidium bromide.

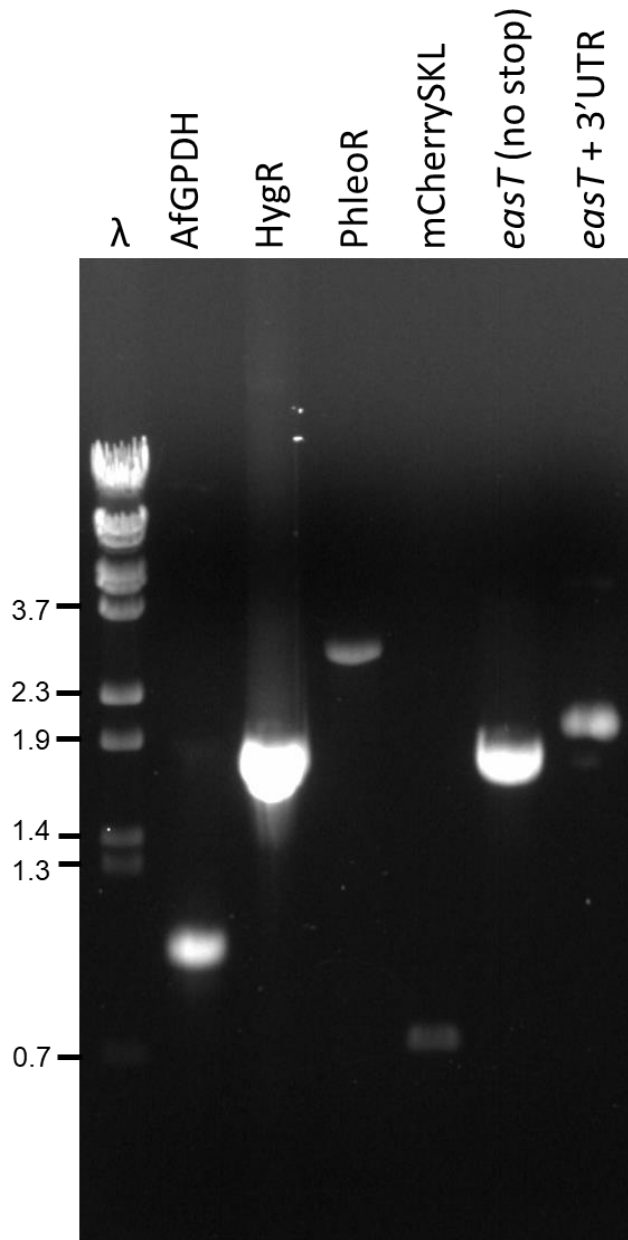


Fig 3. Amplification of fragments used for plasmid construction. PCR products from primer combinations 1-4 and 6-7 (listed in Table 3) digestion or exponential megapriming PCR. Sizes of relevant fragments from *Bst*EII-digested bacteriophage lambda DNA are indicated to the left. Gel was stained with ethidium bromide.

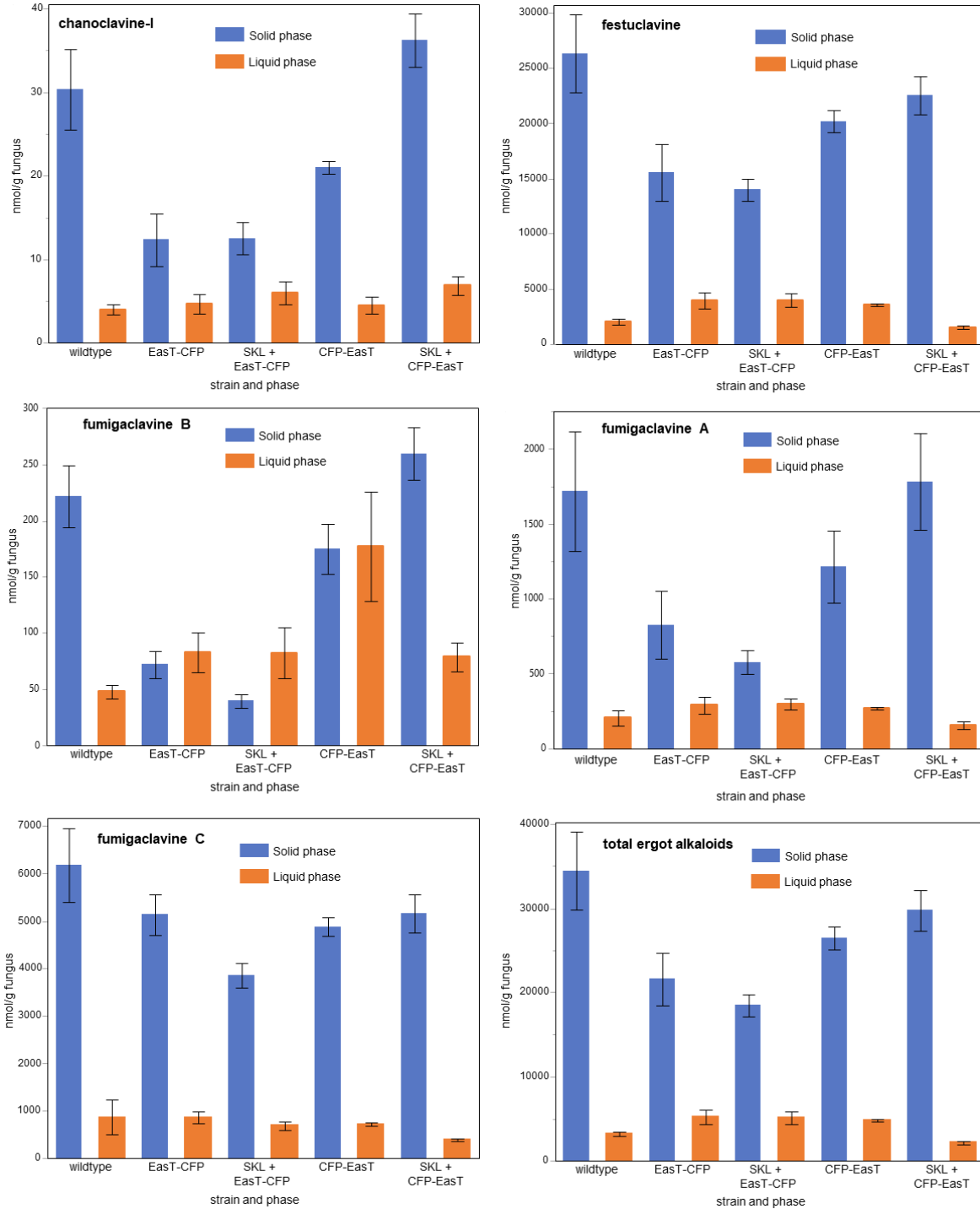


Fig 4. Total nmol of each ergot alkaloid measured in wildtype and mutant strains of *A. fumigatus*. Accumulation of ergot alkaloids in solid (blue) and liquid (orange) phases of wild-type and mutant *A. fumigatus* strains grown in malt extract medium for 8 days at 37 °C. Data

represent means and standard errors for six cultures of each strain. Means within a column that differ significantly ($P < 0.05$) are indicated with different letters. Solid samples are marked with capital letters and liquids are marked with lowercase letters. Means of chanoclavine-I and festuclavine were calculated relative to a standard curve of chanoclavine-I and means of fumigaclavines A, B, and C were calculated relative to a standard curve of fumigaclavine A. Consequently, values for ergot alkaloids should be considered relative rather than absolute.

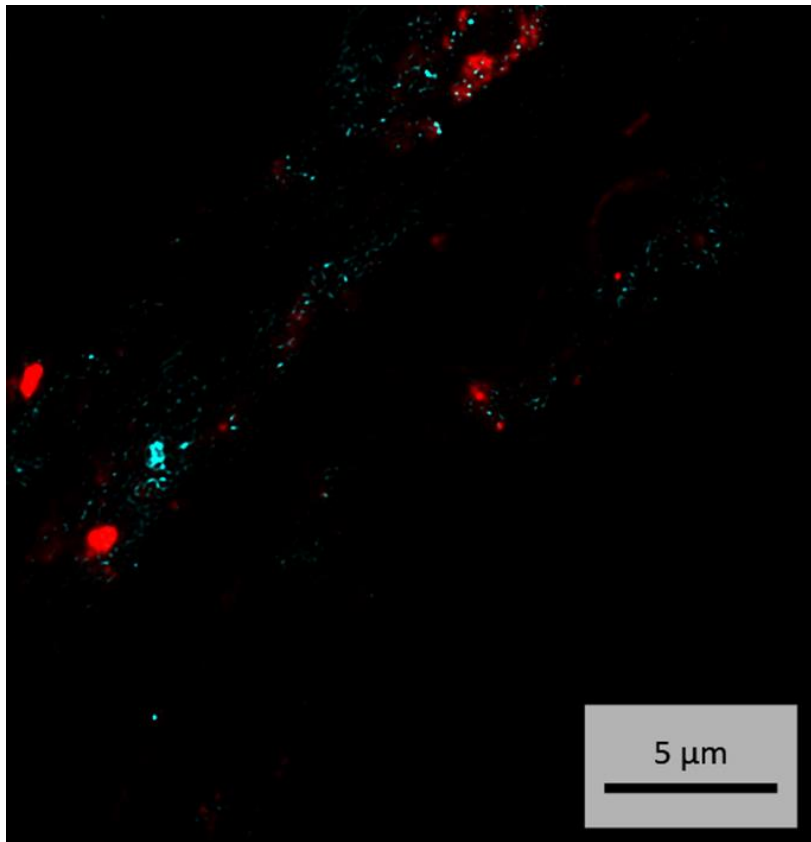
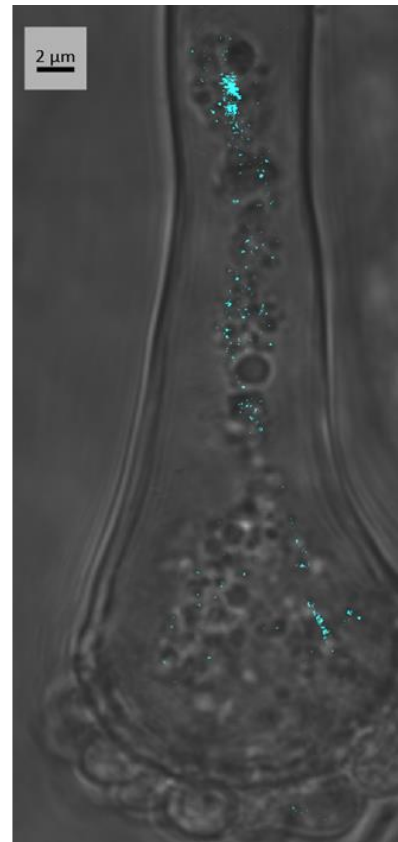
A**B**

Fig 5. Localization of EasT- CFP and mCherry-SKL fusion proteins in mutants. (A)

Localization of EasT-CFP and mCherry-SKL fusions in mutant hyphae and (B) localization of EasT-CFP in another hyphae and conidiophore with DIC. Scale bars included.

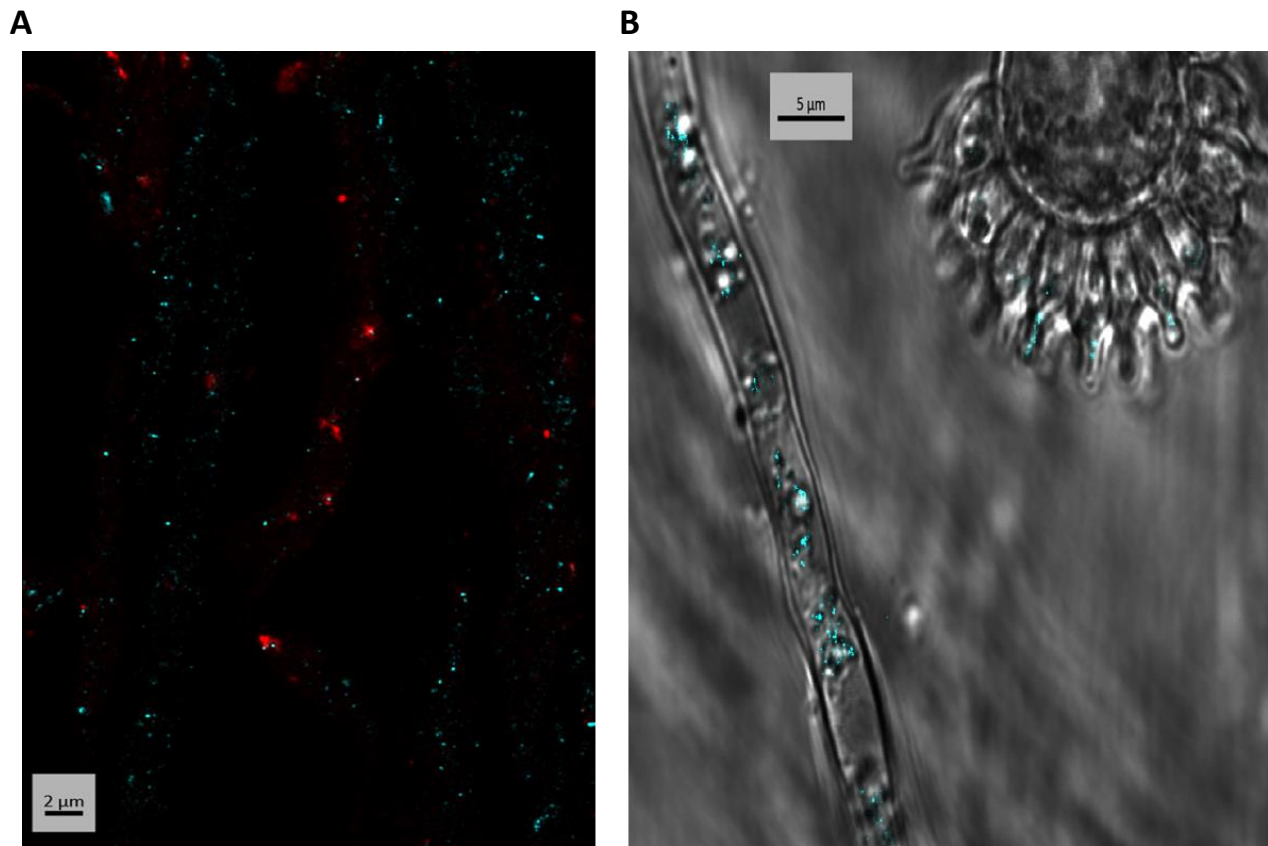


Fig 6. Microscopy of CFP-EasT and mCherry-SKL fusion proteins in mutants. (A)

Localization of CFP-EasT and mCherry-SKL fusions in mutant hyphae and (B) localization of CFP-EasT in another hyphae and conidiophore with DIC. Scale bars included.

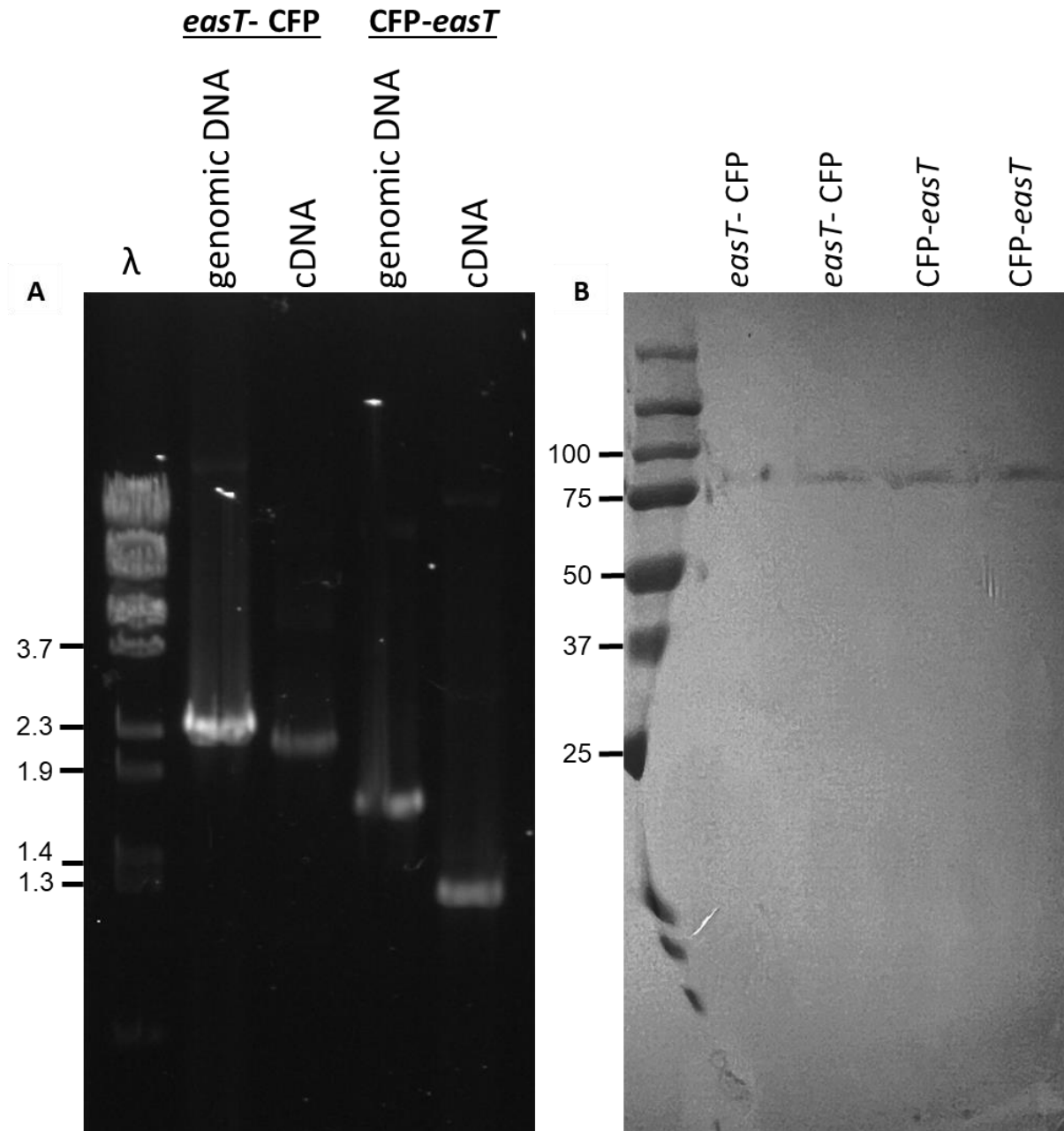


Fig 7. Verification of mRNA and protein expression. (A) DNA gel showing products amplified from genomic DNA and cDNA of *A. fumigatus* mutants expressing *easT*-CFP and CFP-*easT* fusions using primer combinations 12-13 (listed in Table 3), respectively. Sizes of relevant fragments from *Bst*EII-digested bacteriophage lambda DNA are indicated to the left. Gel was stained with ethidium bromide. (B) Western blot analysis of membrane fractions from the same

mutants as panel A. Sizes of Precision Plus pre-stained protein marker (Bio-Rad) fragments in first lanes are indicated to the left of the blot. Membrane marker lane is distorted due to high amounts of detergent in samples.

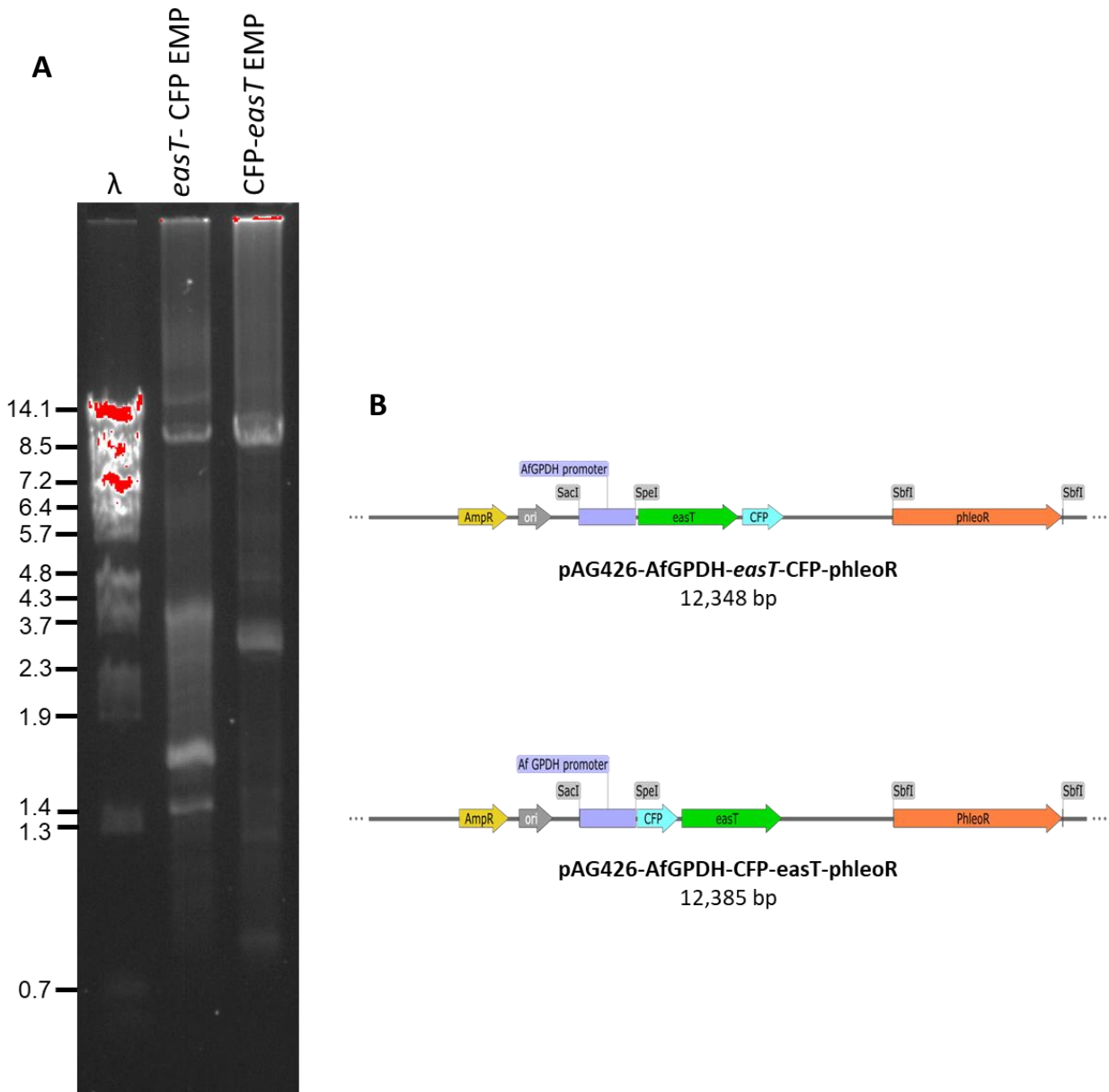


Fig 8. Exponential megapriming PCR products and schematics for CFP-EasT and EasT-CFP fusion expression. (A) Products from exponential megapriming PCRs using primer combinations 8 and 9 (listed in Table 3) prior to gel purification, phosphorylation, and ligation (B) Schematics showing the components and their orientation on the linear plasmid. Sizes of

relevant fragments from *Bst*EII-digested bacteriophage lambda DNA are indicated to the left of the gel. Gel was stained with ethidium bromide.

Table 1. Accumulation (mean \pm standard error; n = 6) of ergot alkaloids in cultures of *A. fumigatus* grown in malt extract medium for 8 days at 37 °C

Strain	Chanoclavine-I ($\mu\text{mol/g}$ fungus)	Festuclavine ($\mu\text{mol/g}$ fungus) ^a	Fumigaclavine B ($\mu\text{mol/g}$ fungus) ^b	Fumigaclavine A ($\mu\text{mol/g}$ fungus)	Fumigaclavine C ($\mu\text{mol/g}$ fungus) ^b	Total ($\mu\text{mol/g}$ fungus)
Wildtype <i>A. fumigatus</i> (<i>A.f.</i>)	0.04 \pm 0.004 AB ^c	28 \pm 4 A	0.3 \pm 0.03 AB	2 \pm 0.4 A	7 \pm 0.7 A	38 \pm 4 A
<i>A.f.</i> + EasT-CFP	0.02 \pm 0.004 C	20 \pm 2 B	0.2 \pm 0.03 BC	1 \pm 0.2 A	6 \pm 0.3 AB	27 \pm 2 AB
<i>A.f.</i> + CFP-EasT	0.03 \pm 0.001 BC	24 \pm 1 AB	0.4 \pm 0.05 A	1 \pm 0.2 A	6 \pm 0.2 AB	31 \pm 1 AB
<i>A.f.</i> + mCherry-SKL + EasT-CFP	0.02 \pm 0.003 C	18 \pm 1 B	0.1 \pm 0.02 C	1 \pm 0.1 A	5 \pm 0.2 B	24 \pm 1 B
<i>A.f.</i> + mCherry-SKL + CFP-EasT	0.04 \pm 0.004 A	24 \pm 4 AB	0.3 \pm 0.02 A	2 \pm 0.3 A	6 \pm 0.4 AB	32 \pm 2 AB

^aValues were estimated relative to fluorescence of chanoclavine-I

^bValues were estimated relative to fluorescence of fumigaclavine A

^cMeans within a column that differ significantly ($P < 0.05$) are indicated with different letters

Table 2. Percent secretion (mean \pm standard error; n = 6) of ergot alkaloids in cultures of *A. fumigatus* grown in malt extract medium for 8 days at 37 °C

Strain	Chanoclavine-I	Festuclavine	Fumigaclavine B	Fumigaclavine A	Fumigaclavine C	Total
Wildtype <i>A. fumigatus</i> (A.f.)	13 \pm 3 A ^a	8 \pm 1 B	19 \pm 3 A	15 \pm 7 AB	13 \pm 5 A	9 \pm 1 AB
<i>A.f.</i> + EasT-CFP	30 \pm 6 A	23 \pm 6 AB	53 \pm 4 B	31 \pm 8 AB	15 \pm 3 A	21 \pm 5 B
<i>A.f.</i> + CFP-EasT	17 \pm 3 A	15 \pm 1 AB	47 \pm 7 B	21 \pm 3 AB	13 \pm 1 A	15 \pm 1 AB
<i>A.f.</i> + mCherry-SKL + EasT-CFP	30 \pm 4 A	22 \pm 4 A	61 \pm 7 B	36 \pm 5 B	15 \pm 2 A	22 \pm 3 B
<i>A.f.</i> + mCherry-SKL + CFP-EasT	16 \pm 2 A	7 \pm 1 B	24 \pm 4 A	9 \pm 2 A	7 \pm 1 A	7 \pm 1 A

^aMeans within a column that differ significantly ($P < 0.05$) are indicated with different, non-overlapping letters

Table 3. Primers and PCR Protocol Information

Primer pair	Primer sequences (5' to 3') ^a	Product (length in base pairs)	Annealing temperature (°C), Extension time (s)
1	AGTCGGAGCTCCGCAGATTCTAGAAGTCCTG + GCTAGACTAGTTGTGTAGATTCGTCTGGTAC	<i>A. fumigatus</i> GPDH promoter (990 bp)	61, 30
2	GTCACCTGCAGGTCCGTCTCCATTGGCTCTTG + AGCTCCTGCAGGCTATTCCTTTGCCCTCGGAC	Hygromycin resistance gene including promoter and 3'UTR (1851 bp)	64, 60
3	GTCACCTGCAGGGTACCCGGGGATCTTTCGAC + AGCTCCTGCAGGTACATGCGTACACGCGTCTG	Phleomycin resistance gene including promoter and 3'UTR (2945 bp)	65, 90
4	GCTAGACTAGTATGGTGAGCAAGGGCGAG + GGTCAGTCGACCTACAACCTTCGACTTGTACAGCTCGTCCATGC	mCherry gene with terminal nucleotides for -SKL amino acid sequence (742 bp)	53, 60

5	<p>CTGCTATAGAGCTTCTGGGC + CTACAACCTTCGACTTGTACAGC</p>	<p>Verification of <i>A. fumigatus</i> GPDH promoter with mCherry (1203 bp)</p>	61, 60
6	<p>ACAAGTTTGTACAAAAAAGCTGAACGAGAAATGGTACGTTATTTTCGGCTG + ACCACTTTGTACAAGAAAGCTGAACGAGAACCGTCAGCATGTCTTCGCTT</p>	<p><i>A. leporis easT</i> with stop codon and 3'UTR and <i>attR1/2</i> overlaps (1793 bp)</p>	61, 60
7	<p>ACAAGTTTGTACAAAAAAGCTGAACGAGAAATGGTACGTTATTTTCGGCTG + ACCACTTTGTACAAGAAAGCTGAACGAGAAATACAGATCCGGAGATGATG</p>	<p><i>A. leporis easT</i> with stop codon and 3'UTR and <i>attR1/2</i> overlaps (2070 bp)</p>	60, 60
8	<p>GATGGGCTGCAGGAATTCGATATCAAGCTTAATGGTGAGC + ACCACTTTGTACAAGAAAGCTGAACGAGAACCGTCAGCATGTCTTCGCTT</p>	<p>Linear <i>AfeasTCFP-</i> PhleoR plasmid from exponential megapriming PCR (12,348 bp)</p>	72, 390
9	<p>GCCGGTACCCAATTCGCCCTATAGTGAGTC + ACCACTTTGTACAAGAAAGCTGAACGAGAAATACAGATCCGGAGATGATG</p>	<p>Linear <i>AfCFPeasT-</i> PhleoR plasmid from exponential megapriming PCR (12385 bp)</p>	72, 240

10	<p>GTACGTTATTTTCGGCTGTCC + CTGAACGAGAACCGTCAG</p>	<p><i>A. fumigatus</i> GPDH promoter- <i>A. leporis easT</i>- CFP verification (1741 bp)</p>	65, 60
11	<p>CTGCTATAGAGCTTCTGGGC + CGTAATACGACTCACTATAGGG</p>	<p><i>A. fumigatus</i> GPDH promoter- CFP- <i>A. leporis easT</i> verification (3349 bp)</p>	61, 120
12	<p>GTACGTTATTTTCGGCTGTCC + GTTACTTGTACAGCTCGTCC</p>	<p><i>A. leporis easT</i> -CFP fusion for RT-PCR (2266 bp cDNA and 2512 bp genomic DNA)</p>	61, 90
13	<p>CACATGAAGCAGCACGACTT + CCCTTCTCTCTGGCTCGAG</p>	<p>CFP- <i>A. leporis easT</i> fusion for RT-PCR (1224 bp cDNA and 1470 bp genomic DNA)</p>	64, 60

^a Underlines indicate unique restriction sites used for cloning fusion PCR product: GAGCTC: *SacI*, ACTAGT: *SpeI*, CCTGCAGG: *SbfI*, and GTCGAC: *SalI*

^b Italics mark *attR1* and *attR2* sites for exponential megapriming PCR.

Chapter 5

Summary

The results presented in this dissertation showcase the diversification of ergot alkaloid biosynthesis in natural and engineered fungi. The work presented in Chapter 2 shows that the species *Metarhizium brunneum* can be engineered to switch production from LA amides to DHLA, an uncommon but pharmaceutically relevant ergot alkaloid, by silencing specific native genes while introducing alternative alleles from other species. This work also demonstrated the ability of this fungus to produce a completely novel ergot alkaloid, dubbed dihydroLAH, through a similar engineering strategy. The work presented in Chapter 3 shows that the fungus *A. leporis*, which is already a unique species in terms of genomic arrangement of its clusters, possesses two partial, satellite clusters for different clavines that require intermediates from its main LAH clusters to complete synthesis of their products. The results presented in Chapter 4 demonstrate the activity and localization of a potential ergot alkaloid transporter, dubbed EasT, that is present in *A. leporis* by introducing the gene encoding the transporter into *A. fumigatus*.

Metarhizium brunneum is a generalist entomopathogen used as a powerful biocontrol agent for many different insect species (Russell et al. 2010, Dogan et al. 2017, Castrillo 2011, Nishi and Sato 2017, Reddy et al. 2014, Han et al. 2021) and is also capable of beneficially colonizing plant roots to help relieve nutritional deficiencies (Liao et al. 2014, Krell et al. 2018). This fungus produces the pharmaceutically relevant LA amides LAH and ergonovine, with large amounts accumulating during insect pathogenesis (Leadmon et al. 2020). The fungus also secretes most of its ergot alkaloids into the growth medium, a trait that is very useful for chemical purification (Leadmon et al. 2020). Depending on enzyme-substrate specificity, *M.*

brunneum could be engineered to produce and secrete dihydro ergot alkaloid equivalents of its natural profile, including DHLA and the hypothetical dihydroLAH. The results presented here showed that the fungus is indeed capable of producing and secreting both of these products. To engineer DHLA production, CRISPR-Cas9 gene editing was used to silence both the isomerase *easA* locus and *lpsB* locus while copies of the reductase *easA* from *A. fumigatus* and a synthetic *cloA* based on that of *C. africana* were introduced. DihydroLAH production was achieved the same way, but while leaving the *lpsB* locus intact to produce an enzyme that acts on DHLA. The fungus is shown to be capable of secreting both products, though at lower levels compared to LA and LAH in the wild-type. This study shows that *M. brunneum* has the potential to serve as a platform in which to produce pharmaceutically relevant ergot alkaloids and novel derivatives of these compounds.

Aspergillus leporis, originally isolated from jackrabbit dung (States and Christensen 1966), is a soil saprotroph that was previously identified by our lab to possess two gene clusters encoding LAH production (minus one pseudogenized *easD* copy; Jones et al. 2021). Later work showed that the fungus produces relatively high concentrations of LAH during infection of insects with smaller amounts accumulating in culture (Jones et al. 2023). Two partial gene clusters containing sets of genes related to production of fumigaclavines and rugulovasines were identified in separate areas of the *A. leporis* genome. The results here show that one cluster contains functional copies of the reductase allele of *easA*, *easG*, *easD*, *easM*, and *easN* that encode production of fumigaclavine A. Production of fumigaclavine A was found to peak around 14 days which is subsequent to a significant decrease in LAH levels. Rugulovasines could only be detected in a single sample of 14-day old *A. leporis* cultures, prompting the need to further test the functionality of the two genes present in the second partial gene cluster. Introduction of

these genes into a strain of *M. brunneum* engineered to accumulate chanoclavine-I allowed for production of rugulovasines, confirming their function. These data indicate that *A. leporis* is exceptional among fungi in having the capacity to synthesize products from three branches of the ergot alkaloid pathway and for utilizing an unusual satellite cluster approach to achieve that outcome.

Previously, a novel gene encoding a putative major facilitator family transporter was identified in one of the *A. leporis* LAH gene clusters (Jones et al. 2021). *Aspergillus fumigatus*, a distant relative of *A. leporis*, is a common airborne saprotroph known to produce the fumigaclavine branch of the ergot alkaloid pathway and can cause infections in individuals with compromised immune systems (Denning 1998, Panaccione and Coyle 2005). To study the localization of the product of *easT* and its activity on fumigaclavine production, the gene was cloned into *A. fumigatus* for overexpression with a fluorescent tag on either the C- or N-terminus. Colocalization with peroxisomes was also tested by transforming either tagged EasT into a strain expressing mCherry with a known peroxisomal localization signal. The results here showed that EasT reduced production of ergot alkaloids while localizing to small, vesicular structures within fungal cells. The effect was stronger in strains engineered with the C-terminal tagged EasT, indicating some form of interference in the N-terminal version. These results conflict with other studies in our lab (Jones, unpublished) which showed a positive effect of EasT on ergot alkaloid accumulation both in *A. leporis* and in previously engineered strain of *A. fumigatus*. Further work is needed before final conclusions can be drawn around the exact role that EasT plays in ergot alkaloid production. One possible difference for the interference of EasT with ergot alkaloid accumulation in *A. fumigatus* observed here is that the transporter is being added to a heterologous system that presumably has evolved to function without and

presumably with its own transporters. Intermediates may have been moved into or out of compartments resulting in spatial separation from enzymes that would otherwise catalyze the next steps in the pathway.

Overall, this research demonstrates that genetic engineering can be used as a powerful platform to study the diversification of ergot alkaloid production across fungal species. This research applied powerful gene editing tools including CRISPR-Cas9 and heterologous expression to non-model fungi to address questions that could not be addressed directly in model organisms. This work also shows how the relatively easy cultivation of fungi that secrete most of their alkaloids can provide us with a means for studying the production of rare or novel ergot alkaloids in systems that require far less chemical purification than is traditionally needed.

References

- Abe M, Ohmomo S, Ohashi T, Tabuchi T. 1969. Isolation of chanoclavine (I) and two new interconvertible alkaloids, rugulovasine A and B, from cultures of *Penicillium concavo-rugulosum*. *Agric Biol Chem* 33:469–471. <https://doi.org/10.1080/00021369.1969.10859341>.
- Alexander NJ, McCormick SP, Larson TM, Jurgenson JE. 2004. Expression of Tri15 in *Fusarium sporotrichioides*. *Curr Genet* 45:157–162. <https://doi.org/10.1007/s00294-003-0467-3>.
- An C, Zhu F, Yao Y, Zhang K, Wang W, Zhang J, Wei G, Xia Y, Gao Q, Gao SS. 2022. Beyond the cyclopropyl ring formation: fungal Aj_EasH catalyzes asymmetric hydroxylation of ergot alkaloids. *Appl Microbiol Biotechnol* 106:2981–2991. <https://doi.org/10.1007/s00253-022-11892-4>.
- Arnold SL, Panaccione DG. 2017. Biosynthesis of the pharmaceutically important fungal ergot alkaloid dihydrolysergic acid requires a specialized allele of *cloA*. *Appl Environ Microbiol* 83:e00805-17. <https://doi.org/10.1128/AEM.00805-17>.
- Barrow KD, Mantle PG, Quigley FR. 1974. Biosynthesis of dihydroergot alkaloids. *Tet Lett* 15:1557–1560. [https://doi.org/10.1016/S0040-4039\(01\)93135-1](https://doi.org/10.1016/S0040-4039(01)93135-1).
- Beaulieu WT, Panaccione DG, Ryan KL, Kaonongbua W, Clay K. 2015. Phylogenetic and chemotypic diversity of *Periglandula* species in eight new morning glory hosts (Convolvulaceae) *Mycologia* 107:667–678. <https://doi.org/10.3852/14-239>.
- Bernier L, Cooper RM, Charnley AK, Clarkson JM. 1989. Transformation of the entomopathogenic fungus *Metarhizium anisopliae* to benomyl resistance. *FEMS Microbiology Lett* 60:261–265. <https://doi.org/10.1111/j.1574-6968.1989.tb03483.x>.
- Bilovol Y, Panaccione DG. 2016. Functional analysis of the gene controlling hydroxylation of festuclavine in the ergot alkaloid pathway of *Neosartorya fumigata*. *Curr Genet* 62:853–860. <https://doi.org/10.1007/s00294-016-0591-5>.
- Blakely RD, Edwards RH. 2012. Vesicular and plasma membrane transporters for neurotransmitters. *Cold Spring Harb Perspect Biol* 4:a005595. <https://doi.org/10.1101/cshperspect.a005595>.
- Blin K, Kim HU, Medema MH, Weber T. 2019. Recent development of antiSMASH and other computational approaches to mine secondary metabolite biosynthetic gene clusters. *Briefings in Bioinformatics* 20:1103–1113. <https://doi.org/10.1093/bib/bbx146>.
- Boenisch MJ, Broz KL, Purvine SO, Chrisler WB, Nicora CD, Connolly LR, Freitag M, Baker SE, Kistler HC. 2017. Structural reorganization of the fungal endoplasmic reticulum upon induction of mycotoxin biosynthesis. *Scientific Reports* 7:44296. <https://doi.org/10.1038/srep44296>.

- Bragg PE, Maust MD, Panaccione DG. 2017. Ergot alkaloid biosynthesis in the Maize (*Zea mays*) ergot fungus *Claviceps gigantea*. *J Agric Food Chem* 65:10703–10710. <https://doi.org/10.1021/acs.jafc.7b04272>.
- Britton K, Steen CR, Davis KA, Sampson JK, Panaccione DG. 2022. Contribution of a novel gene to lysergic acid amide synthesis in *Metarhizium brunneum*. *BMC Res Notes* 15:183. <https://doi.org/10.1186/s13104-022-06068-2>.
- Brown DW, Dyer RB, McCormick SP, Kendra DF, Plattner RD. 2004. Functional demarcation of the *Fusarium* core trichothecene gene cluster. *Fungal Genet Biology* 41:454–462. <https://doi.org/10.1016/j.fgb.2003.12.002>.
- Caceres I, Khoury AA, Khoury RE, Lorber S, Oswald IP, Khoury AE, Atoui A, Puel O, Bailly J-D. 2020. Aflatoxin biosynthesis and genetic regulation: a review. *Toxins* 12:150. <https://doi.org/10.3390/toxins12030150>.
- Castrillo LA, Griggs MH, Ranger CM, Reding ME, Vandenberg JD. 2011. Virulence of commercial strains of *Beauveria bassiana* and *Metarhizium brunneum* (Ascomycota: Hypocreales) against adult *Xylosandrus germanus* (Coleoptera: Curculionidae) and impact on brood. *Biological Control* 58:121–126. <https://doi.org/10.1016/j.biocontrol.2011.04.010>.
- Chanda A, Roze LV, Kang S, Artymovich KA, Hicks GR, Raikhel NV, Calvo AM, Linz JE. 2009. A key role for vesicles in fungal secondary metabolism. *PNAS* 106:19533–19538. <https://doi.org/10.1073/pnas.0907416106>.
- Chen J, Lai Y, Wang L, Zhai S, Zou G, Zhou Z, Cui C, Wang S. 2017. CRISPR/Cas9-mediated efficient genome editing via blastospore-based transformation in entomopathogenic fungus *Beauveria bassiana*. *Sci Rep* 8:45763. <https://doi.org/10.1038/srep45763f>.
- Chen Q, Lei L, Liu C, Zhang Y, Xu Q, Zhu J, Guo Z, Wang Y, Li Q, Li Y, Kong L, Jiang Y, Lan X, Wang J, Jiang Q, Chen G, Ma J, Wei Y, Zheng Y, Qi P. 2021. Major facilitator superfamily transporter gene *fgmfs1* is essential for *Fusarium graminearum* to deal with salicylic acid stress and for its pathogenicity towards wheat. *22:8497*. <https://doi.org/10.3390/ijms22168497>.
- Cheng JZ, Coyle CM, Panaccione DG, O'Connor SE. 2010. A role for old yellow enzyme in ergot alkaloid biosynthesis. *J Am Chem Soc* 132:1776–1777. <https://doi.org/10.1021/ja910193p>.
- Cheng JZ, Coyle CM, Panaccione DG, O'Connor SE. 2010. Controlling a structural branch point in ergot alkaloid biosynthesis. *J Am Chem Soc* 132:12835–12837. <https://doi.org/10.1021/ja105785p>.
- Chiang Y-M, Ahuja M, Oakley CE, Entwistle R, Asokan A, Zutz C, Wang CCC, Oakley BR. 2016. Development of genetic dereplication strains in *Aspergillus nidulans* results in the discovery of aspercryptin. *Angew Chem Int Ed* 55:1662–1665. <https://doi.org/10.1002/anie.201507097>.

- Correia T, Grammel N, Ortel I, Keller U, Tudzynski P. 2003. Molecular cloning and analysis of the ergopeptine assembly system in the ergot fungus *Claviceps purpurea*. *Chem Biol* 10:1281–1292. <https://doi.org/10.1016/j.chembiol.2003.11.013>.
- Cosson P, Perrin J, Bonifacino JS. 2013. Anchors aweigh: protein localization and transport mediated by transmembrane domains. *Trends in Cell Biology* 23:511–517. <https://doi.org/10.1016/j.tcb.2013.05.005>.
- Coyle CM, Cheng JZ, O'Connor SE, Panaccione DG. 2010. An old yellow enzyme gene controls the branch point between *Aspergillus fumigatus* and *Claviceps purpurea* ergot alkaloid pathways. *Appl Environ Microbiol* 76:3898–3903. <https://doi.org/10.1128/AEM.02914-09>.
- Coyle CM, Panaccione DG. 2005. An ergot alkaloid biosynthesis gene and clustered hypothetical genes from *Aspergillus fumigatus*. *Appl Environ Microbiol* 71:3112–3118. <https://doi.org/10.1128/AEM.71.6.3112-3118.2005>.
- Davis KA, Sampson JK, Panaccione DG. 2020. Genetic reprogramming of the ergot alkaloid pathway of *Metarhizium brunneum*. *Appl Environ Microbiol* 86:e01251-20. <https://doi.org/10.1128/AEM.01251-20>.
- Denning DW. 1998. Invasive aspergillosis. *Clin Infect Dis* 26:781–803. <https://doi.org/10.1086/513943>.
- Dogan YO, Hazir S, Yildiz A, Butt TM, Cakmak I. 2017. Evaluation of entomopathogenic fungi for the control of *Tetranychus urticae* (Acari: Tetranychidae) and the effect of *Metarhizium brunneum* on the predatory mites (Acari: Phytoseiidae). *Biological Control* 111:6–12. <https://doi.org/10.1016/j.biocontrol.2017.05.001>.
- Dorner JW, Cole RJ, Hill R, Wicklow D, Cox RH. 1980. *Penicillium rubrum* and *Penicillium biforme*, new sources of rugulovasines A and B. *Appl Environ Microbiol* 40:685–687. <https://doi.org/10.1128/aem.40.3.685-687.1980>.
- Du RH, Li EG, Cao Y, Song YC, Tan RX. 2011. Fumigaclavine C inhibits tumor necrosis factor α production via suppression of toll-like receptor 4 and nuclear factor κ B activation in macrophages. *Life Sciences* 89:235–240. <https://doi.org/10.1016/j.lfs.2011.06.015>.
- Eich E, Eichberg D, Schwarz G, Loos M. 1985. Antimicrobial activity of clavines. *Arzneimittelforschung* 35:1760–1762.
- Elleuche S, Pöggeler S. 2008. Visualization of peroxisomes via SKL-tagged DsRed protein in *Sordaria macrospora*. *Fungal Genet Rep* 55:9–12. <https://doi.org/10.4148/1941-4765.1083>.
- Fabian SJ, Maust MD, Panaccione DP. 2018. Ergot alkaloid synthesis capacity of *Penicillium camemberti*. *Appl Environ Microbiol* 84: e01583-18. <https://doi.org/10.1128/AEM.01583-18>.
- Fabian SJ. Ph.D. Thesis. West Virginia University; Morgantown, West Virginia: 2023. Extension of the Ergot Alkaloid Gene Cluster. Graduate Theses, Dissertations, and Problem Reports 11837. <https://doi.org/10.33915/etd.11837>.

- Fernández-Bodega Á, Álvarez-Álvarez R, Liras P, Martín JF. 2017. Silencing of a second dimethylallyltryptophan synthase of *Penicillium roqueforti* reveals a novel clavine alkaloid gene cluster. *Appl Microbiol Biotech* 101:6111–6121. <https://doi.org/10.1007/s00253-017-8366-6#Sec12>.
- Flieger M, Sedmera P, Vokoun J, Řičicová A, Řeháček Z. 1982. Separation of four isomers of lysergic acid α -hydroxyethylamide by liquid chromatography and their spectroscopic identification. *J Chromatogr* 236:441–452. [https://doi.org/10.1016/S0021-9673\(00\)84895-5](https://doi.org/10.1016/S0021-9673(00)84895-5).
- Florea S, Panaccione DG, Schardl CL. 2017. Ergot alkaloids of the family Clavicipitaceae. *Phytopathology* 107:504–518. <https://doi.org/10.1094/PHYTO-12-16-0435-RVW>.
- Flynn BL, Ranno AE. 1999. Pharmacologic management of alzheimer disease part II: antioxidants, antihypertensives, and ergoloid derivatives. *Geriatrics* 33:188–197. <https://doi.org/10.1345/aph.17172>.
- Frisvad JC, Hubka V, Ezekiel CN, Hong S-B, Nováková A, Chen AJ, Arzanlou M, Larsen TO, Sklenár F, Mahakarnchanakul W, Samson RA, Houbraken J. 2019. Taxonomy of *Aspergillus* section *Flavi* and their production of aflatoxins, ochratoxins and other mycotoxins. *Studies in Mycology* 93:1–63. <https://doi.org/10.1016/j.simyco.2018.06.001>.
- Furuta T, Koike M, Abe M. 1982. Isolation of cycloclavine from the culture broth of *Aspergillus japonicus* SAITO. *Agric Biol Chem* 46:1921–1922. <https://doi.org/10.1080/00021369.1982.10865353>.
- Gale LR, Bryant JD, Calvo S, Giese H, Katan T, O'Donnell K. 2005. Chromosome complement of the fungal plant pathogen *Fusarium graminearum* based on genetic and physical mapping and cytological observations. *Genetics* 171:985–1001. <https://doi.org/10.1534/genetics.105.044842>.
- Gerhards N, Neubauer L, Tudzynski P, Li SM. 2014. Biosynthetic pathways of ergot alkaloids. *Toxins (Basel)* 6:3281–3295. <https://doi.org/10.3390/toxins6123281>.
- Goettel MS, Leger RJ, Bhairi S, Jung MK, Oakley BR, Roberts DW, Staples RC. 1990. Pathogenicity and growth of *Metarhizium anisopliae* stably transformed to benomyl resistance. *Curr Genet* 17:129–132. <https://doi.org/10.1007/BF00312857>.
- Goetz KE, Coyle CM, Cheng JZ, O'Connor SE, Panaccione DG. 2011. Ergot cluster-encoded catalase is required for synthesis of chanoclavine-I in *Aspergillus fumigatus*. *Curr Genet* 57:201–211. <https://doi.org/10.1007/s00294-011-0336-4>.
- Grove JF. 2007. The trichothecenes and their biosynthesis. *Fortschr Chem Org Naturst* 88:63–130. https://doi.org/10.1007/978-3-211-49389-2_2.
- Guna A, Hegde RS. 2018. Transmembrane domain recognition during membrane protein biogenesis and quality control. *Curr Bio* 28: R498–R511. <https://doi.org/10.1016/j.cub.2018.02.004>.

- Guo L, Winzer T, Yang X, Li Y, Ning Z, He Z, Teodor R, Lu Y, Bowser TA, Graham IA, Ye K. 2018. The opium poppy genome and morphinan production. *Science* 362:343–347. <https://doi.org/10.1126/science.aat4096>.
- Haarmann T, Ortel I, Tudzynski P, Keller U. 2006. Identification of the cytochrome P450 monooxygenase that bridges the clavine and ergoline alkaloid pathways. *Chembiochem* 7:645–652. <https://doi.org/10.1002/cbic.200500487>.
- Haarmann T, Rolke Y, Giesbert S, Tudzynski P. 2009. Ergot: from witchcraft to biotechnology. *Molec Plant Pathol* 10:563–577. <https://doi.org/10.1111/J.1364-3703.2009.00548.X>.
- Han JO, Naeger NL, Hopkins BK, Sumerlin D, Stamets PE, Carris LM, Sheppard WS. 2021. Directed evolution of *Metarhizium* fungus improves its biocontrol efficacy against *Varroa* mites in honey bee colonies. *Sci Rep* 11:10582. <https://doi.org/10.1038/s41598-021-89811-2>.
- Havemann J, Vogel D, Loll B, Keller U. 2014. Cyclolization of D-lysergic acid alkaloid peptides. *Chem Biol* 21:146–155. <https://doi.org/10.1016/j.chembiol.2013.11.008>.
- Hofmann A. 1980. LSD—my problem child. McGraw-Hill, New York, NY.
- Hu S, Bidochka MJ. 2019. Root colonization by endophytic insect-pathogenic fungi. *J Appl Microbiol*. <https://doi.org/10.1111/jam.14503>.
- Iloff LD, Du Boulay GH, Marshall J, Ross Russell RW, Symon L. 1977. Effect of nicergoline on cerebral blood flow. *J Neurol Neurosurg Psychiatry* 40:746–747. <https://doi.org/10.1136/jnnp.40.8.746>.
- Itkin M, Heinig U, Tzfadia O, Bhide AJ, Shinde B, Cardenas PD, Bocobza SE, Unger T, Malitsky S, Finkers R, Tikunov Y, Bovy A, Chikate Y, Singh P, Rogachev I, Beekwilder J, Giri AP, Aharoni A. 2013. Biosynthesis of antinutritional alkaloids in solanaceous crops is mediated by clustered genes. *Science* 341:175–179. <https://doi.org/10.1126/science.1240230>.
- Jakubczyk D, Caputi L, Hatsch A, Nielsen CA, Diefenbacher M, Klein J, Molt A, Schröder H, Cheng JZ, Naesby M, O'Connor SE. 2015. Discovery and reconstitution of the cycloclavine biosynthetic pathway— enzymatic formation of a cyclopropyl group. *Angew Chem Int Ed Engl* 54:5117–5121. <https://doi.org/10.1002/anie.201410002>.
- Jakubczyk D, Caputi L, Stevenson CE, Lawson DM, O'Connor SE. 2016. Structural characterization of EasH (*Aspergillus japonicus*) – an oxidase involved in cycloclavine biosynthesis. *Chem Commun* 52:14306–14309. <https://doi.org/10.1039/C6CC08438A>.
- Jones AM, Panaccione DG. 2023. Ergot alkaloids contribute to the pathogenic potential of the fungus *Aspergillus leporis*. *Appl Environ Microbiol* 89:e0041523. <https://doi.org/10.1128/aem.00415-23>.
- Jones AM, Steen CR, Panaccione DP. 2021. Independent evolution of a lysergic acid amide in *Aspergillus* species. *Appl Environ Microbiol* 87:e01801-21. <https://doi.org/10.1128/AEM.01801-21>

- Kenne GJ, Chakraborty P, Chanda A. 2014. Modeling toxosome protrusions in filamentous fungi. *JSM Environ Sci Ecol* 2:1010.
- Keller NP. 2015. Translating biosynthetic gene clusters into fungal armor and weaponry. *Nat Chem Biol* 11:671–677. <https://doi.org/10.1038/nchembio.1897>.
- Kimura M, Matsumoto G, Shingu Y, Yoneyama K, Yamaguchi I. 1998. The mystery of the trichothecene 3-O-acetyltransferase gene. Analysis of the region around Tri101 and characterization of its homologue from *Fusarium sporotrichioides*. *FEBS Lett* 435:163–168. [https://doi.org/10.1016/s0014-5793\(98\)01061-8](https://doi.org/10.1016/s0014-5793(98)01061-8).
- Kistler HC, Broz K. 2015. Cellular compartmentalization of secondary metabolism. *Frontiers Microbiol* 6:68. <https://doi.org/10.3389/fmicb.2015.00068>.
- Krell V, Unger S, Jakobs-Schoenwandt D, Patel AV. 2018. Endophytic *Metarhizium brunneum* mitigates nutrient deficits in potato and improves plant productivity and vitality. *Fungal Ecology* 34:43–49. <https://doi.org/10.1016/j.funeco.2018.04.002>.
- Krogh A, Larsson B, von Heijne G, Sonnhammer ELL. 2001. Predicting transmembrane protein topology with a hidden Markov model: Application to complete genomes. *Journal of Molecular Biology* 305:567–580. <https://doi.org/10.1006/jmbi.2000.4315>.
- Körber K, Song D, Rheinheimer J, Kaiser F, Dickhaut J, Narine A, Culbertson DL, Thompson S, Rieder J. 2014. Cycloclavine and derivatives thereof for controlling invertebrate pests. WIPO WO2014096238A1.
- Kumar S, Stecher G, Tamura K. 2016. MEGA7: Molecular Evolutionary Genetics Analysis version 7.0 for bigger datasets. *Mol Biol Evol* 33:1870–1874. <https://doi.org/10.1093/molbev/msw054>.
- Kyte J, Doolittle RF. 1982. A simple method for displaying the hydropathic character of a protein. *Journal of Molecular Biology*. 157:105–32. [https://doi.org/10.1016/0022-2836\(82\)90515-0](https://doi.org/10.1016/0022-2836(82)90515-0).
- Le SQ, Gascuel O. 2008. An improved general amino acid replacement matrix. *Mol Biol Evol* 25:1307–1320. <https://doi.org/10.1093/molbev/msn067>.
- Leadmon CE, Sampson JK, Maust MD, Macias AM, Rehner SA, Kasson MT, Panaccione DG. 2020. Several *Metarhizium* species produce ergot alkaloids in a condition-specific manner. *Appl Environ Microbiol* 86:e00373-20. <https://doi.org/10.1128/AEM.00373-20>.
- Li Y-X, Himaya SWA, Dewapriya P, Zhang C, Kim S-K. 2013. Fumigaclavine C from a marine-derived fungus *Aspergillus Fumigatus* induces apoptosis in MCF-7 Breast Cancer Cells. *Mar Drugs* 11:5063–5086. <https://doi.org/10.3390/md11125063>.
- Liao X, O'Brien TR, Fang W, St Leger RJ. 2014. The plant beneficial effects of *Metarhizium* species correlate with their association with roots. *Appl Microbiol Biotechnol* 98:7089–7096. <https://doi.org/10.1007/s00253-014-5788-2>.

- Liu H, Jia Y. 2017. Ergot alkaloids: synthetic approaches to lysergic acid and clavine alkaloids. *Nat Prod Rep* 34:411–432. <https://doi.org/10.1039/c6np00110f>.
- Liu X, Homma A, Sayadi J, Yang S, Ohashi J, Takumi T. 2016. Sequence features associated with the cleavage efficiency of CRISPR/Cas9 system. *Sci Rep* 6:19675. <https://doi.org/10.1038/srep19675>.
- Liu X, Wang L, Steffan N, Yin W-B, Li S-M. 2009. Ergot alkaloid biosynthesis in *Aspergillus fumigatus*: FgaAT catalyses the acetylation of fumigaclavine B. *Chembiochem* 10:2325–2328. <https://doi.org/10.1002/cbic.200900395>.
- Lorenz N, Olšovská J, Šulc M, Tudzynski P. 2010. Alkaloid cluster gene *ccsA* of the ergot fungus *Claviceps purpurea* encodes chanoclavine I synthase, a flavin adenine dinucleotide-containing oxidoreductase mediating the transformation of N-methyl-dimethylallyltryptophan to chanoclavine I. *Appl Environ Microbiol* 76:1822–1830. <https://doi.org/10.1128/AEM.00737-09>.
- Lund BA, Leiros H-KS, Bjerga GEK. 2014. A high-throughput, restriction-free cloning and screening strategy based on *ccdB*-gene replacement. *Microbial Cell Factories* 13:38. <https://doi.org/10.1186/1475-2859-13-38>.
- Mantle PG, Waight ES. 1968. Dihydroergosine: a new naturally occurring alkaloid from the sclerotia of *Sphacelia sorghi* (McRae). *Nature* 218:581–582. <https://doi.org/10.1038/218581a0>.
- Martín JF, Álvarez-Álvarez R, Liras P. 2017. Clavine alkaloids gene clusters of *Penicillium* and related fungi: evolutionary combination of prenyltransferases, monooxygenases and dioxygenases. *Genes (Basel)* 8:E342. <https://doi.org/10.3390/genes8120342>.
- Matossian MK. 1989. *Poisons of the past: molds, epidemics, and history*. New Haven, CT: Yale University Press.
- Matuschek M, Wallwey C, Xie X-L, Li S-M. 2011. New insights into ergot alkaloid biosynthesis in *Claviceps purpurea*: an agroclavine synthase EasG catalyses, via a non-enzymatic adduct with reduced glutathione, the conversion of chanoclavine-I aldehyde to agroclavine. *Org Biomol Chem* 9:4328–4335. <https://doi.org/10.1039/c0ob01215g>.
- McCabe SR, Wipf P. 2016. Total synthesis, biosynthesis and biological profiles of clavine alkaloids. *Org Biomol Chem* 14:5894–5913. <https://doi.org/10.1039/c6ob00878j>.
- Menke J, Dong Y, Kistler HC. 2012. *Fusarium graminearum* Tri12p influences virulence to wheat and trichothecene accumulation. *Molec Plant-Microbe Interact* 25:1408–1418. <https://doi.org/10.1094/MPMI-04-12-0081-R>.
- Menke J, Weber J, Broz K, Kistler HC. 2013. Cellular development associated with induced mycotoxin synthesis in the filamentous fungus *Fusarium graminearum*. *PLoS ONE* 8:e63077. <https://doi.org/10.1371/journal.pone.0063077>.

- Merhej J, Richard-Forget F, Barreau C. 2011. Regulation of trichothecene biosynthesis in *Fusarium*: recent advances and new insights. *Appl Microbiol Biotechnol* 91:519–528. <https://doi.org/10.1007/s00253-011-3397-x>.
- Montastruc JL, Rascol O, Senard JM. 1993. Current status of dopamine agonists in Parkinson's disease management. *Drugs* 46:384–393. <https://doi.org/10.2165/00003495-199346030-00005>.
- Mulinti P, Allen NA, Coyle CM, Gravelat FN, Sheppard DC, and Panaccione DG. 2014. Accumulation of ergot alkaloids during conidiophore development in *Aspergillus fumigatus*. *Curr Microbiol* 68:1–5. <https://doi.org/10.1007/s00284-013-0434-2>.
- Nagaoka A, Kikuchi K, Nagawa Y. 1972. I. Pharmacological studies of new indole alkaloids, rugulovasine A and B hydrochloride. II. Hypotensive mechanism of both alkaloids in the anesthetized cats. *Arzneimittelforschung* 22:137–146.
- Nielsen CAF, Folly C, Hatsch A, Molt A, Schröder H, O'Connor SE, Naesby M. 2014. The important ergot alkaloid intermediate chanoclavine-I produced in the yeast *Saccharomyces cerevisiae* by the combined action of EasC and EasE from *Aspergillus japonicus*. *Microbial Cell Factories* 13:95. <https://doi.org/10.1186/s12934-014-0095-2>.
- Nishi O, Sato H. 2017. Species diversity of the entomopathogenic fungi *Metarhizium anisopliae* and *M. flavoviride* species complexes isolated from insects in Japan. *Mycoscience* 58: 472–479. <https://doi.org/10.1016/j.myc.2017.06.008>.
- Ortel I, Keller U. 2009. Combinatorial assembly of simple and complex D-lysergic acid alkaloid peptide classes in the ergot fungus *Claviceps purpurea*. *J Biol Chem* 284:6650–6660. <https://doi.org/10.1074/jbc.M807168200>.
- Østergaard JR, Mikkelsen E, Voldby B. 1981. Effects of 5-hydroxytryptamine and ergotamine on human superficial temporal artery. *Cephalalgia* 1:223–228. <https://doi.org/10.1046/j.1468-2982.1981.0104223.x>.
- Panaccione DG, Arnold SL. 2017. Ergot alkaloids contribute to virulence in an insect model of invasive aspergillosis. *Sci Rep* 7:8930. <https://doi.org/10.1038/s41598-017-09107-2>.
- Panaccione DG, Cipoletti JR, Sedlock AB, Blemings KP, Schardl CL, Machado C, Seidel GE. 2006. Effects of ergot alkaloids on food preference and satiety in rabbits, as assessed with gene-knockout endophytes in perennial ryegrass (*Lolium perenne*). *J Agric Food Chem* 54:4582–4587. <https://doi.org/10.1021/jf060626u>.
- Panaccione DG, Coyle CM. 2005. Abundant respirable ergot alkaloids from the common airborne fungus *Aspergillus fumigatus*. *Appl Environ Microbiol* 71:3106–11. <https://doi.org/10.1128/AEM.71.6.3106-3111.2005>.
- Panaccione DG, Ryan KL, Schardl CL, Florea S. 2012. Analysis and modification of ergot alkaloid profiles in fungi. *Methods Enzymol* 515:267–290. <https://doi.org/10.1016/B978-0-12-394290-6.00012-4>.

- Panaccione DG. 2023. Derivation of the multiply-branched ergot alkaloid pathway of fungi. *Microbial Biotechnology* 16:742-756. <https://doi.org/10.1111/1751-7915.14214>.
- Peplow AW, Meek IB, Wiles MC, Phillips TD, Beremand MN. 2003. Tri16 is required for esterification of position C-8 during trichothecene mycotoxin production by *Fusarium sporotrichioides*. *Appl Environ Microbiol* 69:5935–5940. <https://doi.org/10.1128/AEM.69.10.5935-5940.2003>.
- Pertz H, Eich E. 1999. Ergot alkaloids and their derivatives as ligands for serotonergic, dopaminergic, and adrenergic receptors. p. 411–440. In Kren V, Cvak L (ed), *Ergot: The Genus Claviceps*. Harwood Academic Publishers, Amsterdam, The Netherlands.
- Potter DA, Stokes JT, Redmond CT, Schardl CL, Panaccione DG. 2008. Contribution of ergot alkaloids to suppression of a grass-feeding caterpillar assessed with gene knockout endophytes in perennial ryegrass. *Entomol Experiment Appl* 126:138–147. <https://doi.org/10.1111/j.1570-7458.2007.00650.x>.
- Read ND. 2018. Fungal cell structure and organization. In: Kibbler CC, Barton R, Gow NAR, Howell S, MacCallum DM, Manuel RJ, editors. *Oxford Textbook of Medical Mycology*. Oxford University Press. <https://doi.org/10.1093/med/9780198755388.003.0004>.
- Rebek J, Shue Y-K, Tai DF. 1984. The rugulovasines: synthesis, structure, and interconversions. *J Org Chem* 49:3540–3545. <https://doi.org/10.1021/jo00193a018>.
- Reddy VS, Shlykov MA, Castillo R, Sun EI, Saler MH. 2012. The major facilitator superfamily (MFS) revisited. *FEBS* 279:2022–2035. <https://doi.org/10.1111/j.1742-4658.2012.08588.x>.
- Reddy GVP, Zhao Z, Humber RA. 2014. Laboratory and field efficacy of entomopathogenic fungi for the management of the sweetpotato weevil, *Cylas formicarius* (Coleoptera: Brentidae). *Journal of Invertebrate Pathology* 122:10–15. <https://doi.org/10.1016/j.jip.2014.07.009>.
- Riederer B, Han M, Keller U. 1996. D-Lysergyl peptide synthetase from the ergot fungus *Claviceps purpurea*. *J Biol Chem* 271:27524–27530. <https://doi.org/10.1074/jbc.271.44.27524>.
- Rigbers O, Li SM. 2008. Ergot alkaloid biosynthesis in *Aspergillus fumigatus* overproduction and biochemical characterization of a 4-dimethylallyltryptophan N-methyltransferase. *J Biol Chem* 283:26859–26868. <https://doi.org/10.1074/jbc.M804979200>.
- Robinson SL, Panaccione DG. 2014. Heterologous expression of lysergic acid and novel ergot alkaloids in *Aspergillus fumigatus*. *Appl Environ Microbiol* 80:6465–6472. <https://doi.org/10.1128/AEM.02137-14>.
- Robinson SL, Panaccione DG. 2015. Diversification of ergot alkaloids in natural and modified fungi. *Toxins (Basel)* 7:201–218. <https://doi.org/10.3390/toxins7010201>.
- Rothlin E. 1955. Historical development of the ergot therapy of migraine. *Allergy* 7:205–209. <https://doi.org/10.1159/000228229>.

- Roze LV, Chanda A, Linz JE. 2011. Compartmentalization and molecular traffic in secondary metabolism: a new understanding of established cellular processes. *Fungal Genet Biol* 48:35–48. <https://doi.org/10.1016/j.fgb.2010.05.006>.
- Russell CW, Uguine TA, Hajek AE. 2010. Interactions between imidacloprid and *Metarhizium brunneum* on adult Asian longhorned beetles (*Anoplophora glabripennis* (Motschulsky)(Coleoptera: Cerambycidae). *J Invert Pathol* 105:305–311. <https://doi.org/10.1016/j.jip.2010.08.009>.
- Ryan KL, Akhmedov NG, Panaccione DG. 2015. Identification and structural elucidation of ergotryptamine, a new ergot alkaloid produced by genetically modified *Aspergillus nidulans* and natural isolates of *Epichloë* species. *J Agric Food Chem* 63:61–67. <https://doi.org/10.1021/jf505718x>.
- Schardl CL, Panaccione DG, Tudzynski P. 2006. Ergot alkaloids biology and molecular biology. *Alkaloids* 63:45–86 [https://doi.org/10.1016/s1099-4831\(06\)63002-2](https://doi.org/10.1016/s1099-4831(06)63002-2).
- Schardl CL, Young CA, Hesse U, Amyotte SG, Andreeva K, Calie PJ, Fleetwood DJ, Haws DC, Moore N, Oeser B, Panaccione DG, Schweri KK, Voisey CR, Farman ML, Jaromczyk JW, Roe BA, O’Sullivan DM, Scott B, Tudzynski P, An Z, Arnaoudova EG, Bullock CT, Charlton ND, Chen L, Cox M, Dinkins RD, Florea S, Glenn AE, Gordon A, Güldener U, Harris DR, Hollin W, Jaromczyk J, Johnson RD, Khan AK, Leistner E, Leuchtman A, Li C, Liu JG, Liu J, Liu M, Mace W, Machado C, Nagabhyru P, Pan J, Schmid J, Sugawara K, Steiner U, Takach JE, Tanaka E, Webb JS, Wilson EV, Wiseman JL, Yoshida R, Zeng Z. 2013. Plant-symbiotic fungi as chemical engineers: multi-genome analysis of the Clavicipitaceae reveals dynamics of alkaloid loci. *PLoS Genet* 9:e1003323. <https://doi.org/10.1371/journal.pgen.1003323>.
- Schardl CL, Young CA, Pan J, Florea S, Takach JE, Panaccione DG, Farman ML, Webb JS, Jaromczyk J, Charlton ND, Nagabhyru P, Chen L, Shi C, Leuchymann A. 2013. Currencies of mutualisms: sources of alkaloid genes in vertically transmitted *Epichloae*. *Toxins* 5:1064–1088. <https://doi.org/10.3390/toxins5061064>.
- Schif PL. 2006. Ergot and its alkaloids. *American Journal of Pharmaceutical Education* 70:98. <https://doi.org/10.5688/aj700598>.
- Schultes RE, Hofmann A. 1973. *The botany and chemistry of hallucinogens*. Springfield: Charles C Thomas: 240–257.
- Shang Y, Ma Y, Zhou Y, Zhang H, Duan L, Chen H, Zeng J, Zhou Q, Wang S, Gu W, Liu M, Ren J, Gu X, Zhang S, Wang Y, Yasukawa K, Bouwmeester HJ, Qi X, Zhang Z, Lucas WJ, Huang S. 2014. Biosynthesis, regulation, and domestication of bitterness in cucumber. *Science* 341:175–179. <https://doi.org/10.1126/science.1259215>.
- Silar P. 1995. Two new easy to use vectors for transformations. *Fungal Genet Rep* 42:23. <https://doi.org/10.4148/1941-4765.1353>.

- States JS, Christensen M. 1966. *Aspergillus leporis*, a new species related to *A. flavus*. *Mycologia* 58:738–742. <https://doi.org/10.2307/3756848>.
- Stauffacher D, Niklaus P, Tschertter H, Weber HP, Hofmann A. 1969. Cycloclavin, ein neues alkaloid aus *Ipomoea hildebrandtii* vatke—71: Mutterkornalkaloide. *Tetrahedron* 25:5879–5887. [https://doi.org/10.1016/S0040-4020\(01\)83095-7](https://doi.org/10.1016/S0040-4020(01)83095-7).
- Steen CR, Sampson JK, Panaccione DG. 2021. A Baeyer-Villiger monooxygenase gene involved in the synthesis of lysergic acid amides affects the interaction of the fungus *Metarhizium brunneum* with insects. *Appl Environ Microbiol* 87:e00748-21. <https://doi.org/10.1128/AEM.00748-21>.
- Strickland D, Lin Y, Wagner E, Hope CM, Zayner J, Antoniou C, Sosnick TR, Weiss EL, Glotzer M. 2012. TULIPs: tunable, light-controlled interacting protein tags for cell biology. *Nat Methods* 4:379–384. <https://doi.org/10.1038/nmeth.1904>.
- Tasker NR, Wipf P. 2021. A short synthesis of ergot alkaloids and evaluation of the 5-HT_{1/2} receptor selectivity of lysergols and isolysergols. *Org Lett* 24:7255–7259. <https://doi.org/10.1021/acs.orglett.2c02569>.
- Tsai HF, Wang H, Gebler JC, Poulter CD, Scharidl CL. 1995. The *Claviceps purpurea* gene encoding dimethylallyltryptophan synthase, the committed step for ergot alkaloid biosynthesis. *Biochem Biophys Res Commun* 216:119–125. <https://doi.org/10.1006/bbrc.1995.2599>.
- Tudzynski P, Hölter K, Correia T, Arntz C, Grammel N, Keller U. 1999. Evidence for an ergot alkaloid gene cluster in *Claviceps purpurea*. *Mol Gen Genet* 261:133–141. <https://doi.org/10.1007/s004380050950>.
- Ulrich A, Andersen KR, Schwartz TU. 2012. Exponential megaprimer PCR (EMP) cloning—seamless DNA insertion into any target plasmid without sequence constraints. *PLoS ONE* 7:e53360. <https://doi.org/10.1371/journal.pone.0053360>.
- Unsöld IA, Li S-M. 2005. Overproduction, purification and characterization of FgaPT2, a dimethylallyltryptophan synthase from *Aspergillus fumigatus*. *Microbiology* 151:1499–1505. <https://doi.org/10.1099/mic.0.27759-0>.
- Unsöld IA, Li S-M. 2006. Reverse Prenyltransferase in the biosynthesis of fumigaclavine c in *Aspergillus fumigatus*: gene expression, purification, and characterization of fumigaclavine C synthase FGAPT1. *Chembiochem* 7:158–164. <https://doi.org/10.1002/cbic.200500318>.
- Unsöld IA. Ph.D. Thesis. Universität Tübingen; Tübingen, German: 2006. Molecular Biological and Biochemical Investigations on the Biosynthesis of Fumigaclavines in *Aspergillus fumigatus* AF 293/B 5233 and *Penicillium commune* NRRL2033.
- Vinokurova NG, Boichenko LV, Arinbasarov MU. 2003. Production of alkaloids by fungi of the genus *Penicillium* grown on wheat grain. *Appl Biochem Microbiol* 39:403–406. <https://doi.org/10.1023/A:1024576703367>.

- Wallwey C, Li S-M. 2011. Ergot alkaloids: structure diversity, biosynthetic gene clusters and functional proof of biosynthetic genes. *Nat Prod Rep* 28:496–510. <https://doi.org/10.1039/c0np00060d>.
- Wallwey C, Matuschek M, Li S-M. 2010. Ergot alkaloid biosynthesis in *Aspergillus fumigatus*: conversion of chanoclavine-I to chanoclavine-I aldehyde catalyzed by a short-chain alcohol dehydrogenase FgaDH. *Arch Microbiol* 92:127–134. <https://doi.org/10.1007/s00203-009-0536-1>.
- Wallwey C, Matuschek M, Xie X-L, Li S-M. 2010. Ergot alkaloid biosynthesis in *Aspergillus fumigatus*: conversion of chanoclavine-I aldehyde to festuclavine by the festuclavine synthase FgaFS in the presence of the old yellow enzyme FgaOx3. *Org Biomol Chem* 8:3500–3508. <https://doi.org/10.1039/c003823g>.
- Wu X-F, Fei M-J, Shu R-G, Tan R-X, Xu Q. 2005. Fumigaclavine C, an fungal metabolite, improves experimental colitis in mice via downregulating Th1 cytokine production and matrix metalloproteinase activity. *International Immunopharmacology* 5:1543–1553. <https://doi.org/10.1016/j.intimp.2005.04.014>.
- Yao Y, An C, Evans D, Liu W, Wang W, Wei G, Ding N, Houk KN, Gao S-S. 2021. Catalase involved in oxidative cyclization of the tetracyclic ergoline of fungal ergot alkaloids. *J Am Chem Soc* 141:17517–17521. <https://doi.org/10.1021/jacs.9b10217>.
- Young CA, Schardl CL, Panaccione DG, Florea S, Takach JE, Charlton ND, Moore N, Webb JS, Jaromczyk J. 2015. Genetics, genomics and evolution of ergot alkaloid diversity. *Toxins* 7:1273–1302. <https://doi.org/10.3390/toxins7041273>.
- Zhao Y, Liu J, Wang J, Wang L, Yin H, Tan R, Xu Q. 2010. Fumigaclavine C improves concanavalin A-induced liver injury in mice mainly via inhibiting TNF- α production and lymphocyte adhesion to extracellular matrices. *Journal of Pharmacy and Pharmacology* 56:775–782. <https://doi.org/10.1211/0022357023592>.